

THE EFFECTS OF NICKEL ON ORGANIC REMOVAL AND
NITRIFICATION IN THE COMPLETELY MIXED
ACTIVATED SLUDGE PROCESS

by

Debra A. Smith

Thesis submitted to the Faculty of the
Virginia Polytechnic Institute and State University
in partial fulfillment of the requirements for a degree of

MASTER OF SCIENCE

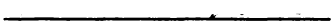
in

Sanitary Engineering

APPROVED:

 J. H. Sherrard, Chairman


C. W. Randall


R. C. Hoehn

July, 1982

Blacksburg, Virginia.

DEDICATION

To My Parents Kenneth J. Smith and Jean Smith
for Their Confidence and Encouragement

ACKNOWLEDGEMENTS

The author would like to express her sincere appreciation to the following persons for their help in completing this research.

Dr. Joseph A. Sherrard for acting as chairman of the author's graduate committee and for guiding and encouraging the author in her research.

Dr. Clifford W. Randall and Dr. Robert C. Hoehn for serving on the author's graduate committee.

Dr. John Novak for his assistance to the author during her data analysis.

Marilyn Grender for performing the nickel analyses.

Mr E. G. Williard for his laboratory assistance.

Carmella Page for typing the author's thesis.

Mr. David Miles for drawing the graphs depicted in the literature review.

Robin Byrd for assisting the author in proofreading and preparing the final copy of this thesis.

Mr. Dave Buth for all his assistance and advice throughout the author's laboratory research.

Mr. Kip Foster for his moral support during the author's graduate studies.

Ms. Deb Manning and Mr. Bob Adam for their babysitting services when the author was away from the lab.

Robin Byrd, Joan Lupashunski, Susan Messick, Diane Paul, and all graduate students in Sanitary Engineering and Environmental Sciences and Engineering for their friendship and encouragement.

The entire Smith family for their love and support, especially while the author was writing her thesis.

The Environmental Protection Agency for providing financial assistance.

TABLE OF CONTENTS

<u>Chapter</u>	<u>Page</u>
Dedication	ii
Acknowledgements	iii
List of Tables	vii
List of Figures	ix
I. INTRODUCTION	1
II. LITERATURE REVIEW	2
Properties of Nickel	2
Chemistry of Nickel	2
Complexation	3
Nickel-Amine Complexation	4
Nickel-Hydroxide Complexation	9
Precipitation of Nickel	13
Adsorption of Nickel	16
Activated Sludge	19
Microbial Growth	20
Microbial Growth Kinetics	20
Kinetics of the Activated Sludge Process	24
Stoichiometry of the Activated Sludge Process	29
Nitrification	30
Heavy Metals and Biological Wastewater Treatment	37
Microbial Enzymes	38
Effects of Heavy Metals on Biological Treatment Processes	39
Heavy Metal Removal in the Activated Sludge Process	49
Influence of Various Factors on the Removal of Heavy Metals in Biological Treatment	50
III. MATERIALS AND METHODS	53
Laboratory Apparatus	53
Feed Solution	55

Table of Contents (continued)
Page 2 of 3

	<u>Page</u>
System Startup	57
Daily Protocol	57
Sampling Procedure	58
Analytical Techniques	60
Data Analysis	61
IV. RESULTS AND DISCUSSION	68
Results	69
Control	69
COD:TKN=1.03:1, COD=400 mg/l, Ni(II)=0.77 mg/l	72
COD:TKN=0.54:1, COD=400 mg/l, Ni(II)=0.77 mg/l	75
Discussion	79
COD Removal	79
Total Reactor Microorganisms Concentration	79
Specific Utilization Rate	82
Biokinetic Coefficients	85
Observed Yield	87
Nickel Removal Efficiency	91
Effluent Nitrate Concentration	93
Percent Distribution of Effluent and Wasted Nitrogen	95
Effluent pH	100
Nitrification in Relation to MLSS:Ni(II)	102
V. CONCLUSIONS	104
RECOMMENDATION FOR FUTURE STUDY	107
REFERENCES	108
 <u>APPENDIX</u>	
Appendix A Calculations for Log - Concentration Diagram of Nickel-Amine Complexes	112
Appendix B Calculation for Distribution Diagram of Nickel-Amine Complexes	115

Table of Contents (continued)
Page 3 of 3

	<u>Page</u>
Appendix C Calculation for Distribution Diagram of Nickel Hydroxide Complexes	121
Appendix D Calculations for Theoretical Nickel Hydroxide Solubility Diagram	124
Appendix E Calculations for the Biokinetic Coefficients Pertaining to Other Nickel Toxicity Studies (34, 40, 47)	127
Appendix F Raw Data for the Steady State Runs of the Completely Mixed Activated Sludge Units	130
VITA	143
ABSTRACT	

LIST OF TABLES

<u>Table</u>	<u>Page</u>
I. Composition of Wastewater Feed Solution	56
II. Parameters Monitored Daily During Steady State Periods	59
III. Summary of Steady State Data Control Reactor, COD:TKN = 3.71:1	70
IV. Summary of Steady State Data, COD:TKN = 1.03:1, Ni(II) = 0.77 mg/l	73
V. Summary of Steady State Data, COD:TKN = 0.54:1, Ni(II) = 0.77 mg/l	76

Appendix

F-I Raw Data for Control Reactor - COD = 386 mg/l, $\theta_c = 5.8$ days	131
F-II Raw Data For Control Reactor - COD = 405 mg/l, $\theta_c = 11.5$ days	132
F-III Raw Data for Control Reactor - COD = 390 mg/l, $\theta_c = 12.3$ days	133
F-IV Raw Data for Control Reactor - COD = 396 mg/l, $\theta_c = 16.4$ days	134
F-V Raw Data for COD:TKN = 1.06:1 - Ni(II) = 0.75 mg/l, $\theta_c = 3.0$ days	135
F-V Raw Data for COD:TKN = 1.02:1 - Ni(II) = 0.77 mg/l, $\theta_c = 6.5$ days	136
F-VI Raw Data for COD:TKN = 1.02:1 - Ni(II) = 0.77 mg/l, $\theta_c = 13.6$ days	137
F-VII Raw Data for COD:TKN = 1.02:1 - Ni(II) = 0.77 mg/l, $\theta_c = 20.0$ days	138
F-VIII Raw Data for COD:TKN = 0.55:1 - Ni(II) = 0.79 mg/l, $\theta_c = 3.0$ days	139
F-IX Raw Data for COD:TKN = 0.52:1 - Ni(II) = 0.76 mg/l, $\theta_c = 6.1$ days	140

List of Tables (continued)
Page 2 of 2

<u>Appendix</u>		<u>Page</u>
F-X	Raw Data for COD:TKN = 0.57:1 - Ni(II) = 0.73 mg/l, $\theta_c = 14.0$ days	141
F-XI	Raw Data for COD:TKN = 0.53:1 - Ni(II) = 0.79 mg/l, $\theta_c = 17.8$ days	142

LIST OF FIGURES

		<u>Page</u>
Figure 1	Log Concentration Diagram for Nickel-Amine Complexes ($[Ni^{2+}] = 10^{-4.89} M$)	8
Figure 2	Distribution Diagram for Nickel-Amine Complexes	10
Figure 3	Distribution Diagram for Nickel-Hydroxide Complexes	12
Figure 4	Comparison of Nickel-Carbonate Solubility Data with Theoretical Phase Diagram for Nickel-Hydroxide and Nickel-Carbonate	14
Figure 5	Comparison of Nickel-Hydroxide and Nickel-Carbonate Data with Theoretical Hydroxide Solubility Curve	15
Figure 6	Theoretical Solubility Diagram for Nickel-Hydroxide	17
Figure 7	General Microorganism Growth Pattern in a Batch System	21
Figure 8	Plot of Specific Growth Rate Versus Specific Utilization Rate	23
Figure 9	Flow Scheme for the Completely Mixed Activated Sludge Process	25
Figure 10	Percent of Maximum Rate of Nitrification at Constant Temperature Versus pH	33
Figure 11	Comparison of Theoretical Alkalinity Change and Measured Alkalinity Change	35
Figure 12	Patterns of Performance Depreciation in Sewage Treatment Processes	42
Figure 13	Response of the Activated Sludge System to Metal Doses	44
Figure 14	General Effects of Salts or Other Materials on Biological Reactions	46

List of Figures (continued)
Page 2 of 3

	<u>Page</u>
Figure 15	Schematic Diagram of Laboratory Apparatus 54
Figure 16	Effect of Nickel on COD Removal Efficiency at Different Mean Cell Residence Times 80
Figure 17	Effect of Nickel on Heterotrophic Mixed Liquor Suspended Solids at Different Mean Cell Residence Times 81
Figure 18	Effect of Nickel on Specific Utilization Rate of Heterotrophic Mixed Liquor Suspended Solids as a Function of Mean Cell Residence Time 83
Figure 19	Effect of Nickel on the Biokinetic Coefficients of Heterotrophic Microorganisms 86
Figure 20	Effect of Nickel on Maximum Yield Coefficient of Heterotrophic MLSS 88
Figure 21	Effect of Nickel on Microbial Decay Coefficient of Heterotrophic MLSS 89
Figure 22	Effect of Nickel on the Observed Yield Coefficient as a Function of Mean Cell Residence Time 90
Figure 23	Nickel Removal Efficiency at Different Mean Cell Residence Times 92
Figure 24	Effect of Nickel on Nitrification at Different Mean Cell Residence Times 94
Figure 25	Percent Distribution of Effluent and Wasted Nitrogen as a Function of Mean Cell Residence Time - Control, COD:TKN = 3.71:1 96
Figure 26	Percent Distribution of Effluent and Wasted Nitrogen as a Function of Mean Cell Residence Time - Ni(II) = 0.77 mg/l, COD:TKN = 1.03:1 97
Figure 27	Percent Distribution of Effluent and Wasted Nitrogen as a Function of Mean Cell Residence Time - Ni(II) = 0.77 mg/l, COD:TKN = 0.54:1 98

List of Figures (continued)
Page 3 of 3

	<u>Page</u>
Figure 28	Change in Effluent pH as a Function of Mean Cell Residence Time 101
Figure 29	Effect of the MLSS:Ni Ratio on Nitrification 103

I. INTRODUCTION

Advanced technology has provided mankind with the opportunity to make use of many of his natural resources in developing and manufacturing new products. Unfortunately, this surge in industrialization has been accompanied by an increase in the discharge of wastes to the environment. A high percentage of this industrial pollution is attributed to metal production and electroplating operations. Certain processes of these industries emit large concentrations of heavy metals into their waste streams. These wastewaters are often discharged directly into municipal sewer systems and subsequently reach municipal wastewater treatment plants.

The recent discoveries of the detrimental effects of heavy metals on the environment has led to increasingly stringent effluent regulations and a need to assess the fate of these pollutants in wastewater treatment processes. Recently, many investigations have been conducted to determine the feasibility of using the aerobic, completely-mixed activated sludge process as a means of reducing metal concentrations in wastewaters. While some reports indicate the ability of the aerobic processes to operate while removing heavy metals, other studies have shown a marked decrease in process efficiency.

The purpose of this research was to conduct a laboratory study to determine the effects of nickel on the completely-mixed activated sludge system. Continuous-flow bench-scale reactors were operated at low chemical oxygen demand to total Kjeldahl nitrogen ratios, COD:TKN, and fed a fixed concentration of nickel. The mean cell residence time, θ_c , was used as the operational parameter to assess the effects of nickel on organic removal efficiency, on the degree of nitrification, and on the maximum yield and the microbial maintenance energy coefficients, Y_{max} and k_d .

II. LITERATURE REVIEW

Properties of Nickel

Nickel is a silvery-white metal that is very ductile, tenacious and malleable. As a member of the first series of the transition elements in the periodic table, nickel has an atomic number of 28 and an atomic weight of 58.71. Other characteristics of nickel include a boiling temperature of 2732 °C, a melting temperature of 1453 °C, and a specific gravity of 8.9.

Approximately 0.018 percent of the earth's crust is composed of nickel (1). Most of this is contained in the ores of igneous rocks, while small percentages are found in petroleum and coal. Low concentrations of nickel are also present in surface and groundwaters due to the weathering processes of the lithosphere.

In 1972, the United States' consumption of nickel, excluding scrap, was estimated to be 160,000 tons, which consisted mainly of pure nickel (1). Greater than one third of the commercially pure nickel is used in the manufacture of stainless steel, while the electroplating industry, in enhancing the appearance and corrosion resistance of metal, utilizes approximately 16 percent of the total nickel consumption. Other uses of nickel include the manufacture of nickel alloys, nickel powders, and nickel salts, along with ferrous casting and electronic applications.

Chemistry of Nickel

The soluble species of a metal is mainly responsible for interferences with the biological oxidation of recipient organisms (2, 3, 4). Thus, an assessment of nickel-bearing wastewaters on biological treatment requires chemical analysis of metals and their related compounds and their solubility equilibria in solution.

Although natural waters are too complex to fully describe, useful insights into their chemistry can be gained through the application of equilibrium models to simple, natural aquatic systems.

Parameters controlling the solubility of the mineral phases are the pH of the solution, the type and concentration of complexing inorganic and organic ligands and chelating agents, the oxidation state of the mineral components, and the environment of the system(s). If the conditions existing in a wastewater are such to cause complexation, precipitation, or adsorption of a metal, thereby reducing the soluble metal content, then its severity will be reduced.

Complexation

A complex ion or complex compound consists of one or more central metal cations to which are bound several anions or molecules, called ligands. The ligands are directly attached to the central species by coordinated covalent bonds in which the metal ion acts as an electron acceptor and the ligands act as electron donors. Certain ligands, including anions and molecules, such as OH^- , CN^- , Cl^- , NH_3 and H_2O , donate only one pair of electrons to a complex, and are referred to as monodentate. Ligands that donate two or more electron pairs, such as the carbonate ion, CO_3^{2-} , are known as multidentate ligands or chelating agents. In general, the chelates are more stable than complexes containing only monodentate ligands and are thereby capable of drastically reducing the concentration of free metal ions in solution (6).

The number of bonded positions of a central metal ion determines its coordination number. Generally, each metal exhibits more than one coordination number and geometry in its complexes depending upon the nature of the attached ligands

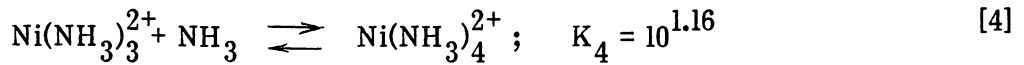
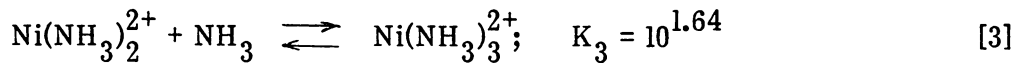
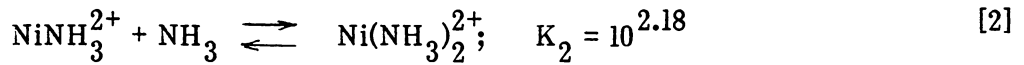
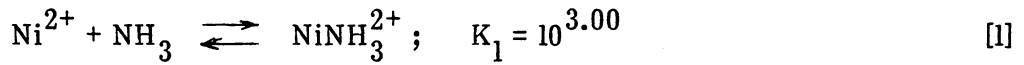
and the equilibrium conditions existing in solution (7). For example, Ni(II) has a coordination number of two in its complex with carbonate, NiCO_3 , while in combination with carbonyl, $\text{Ni}(\text{CO})_4$, its coordination number is four.

Metal ions in a simple solution are never in the uncomplexed state but are always bound with solvent molecules. For example, nickel would exist in solution as $\text{Ni}(\text{H}_2\text{O})_6^{2+}$, not as the Ni^{2+} ion. In wastewaters, however, the heavy metals rarely remain as simple hydrated compounds. Concentrations of anionic species, such as hydroxides, carbonates, chlorides, organic acids and amino acids, are sufficient to complex with the metal ions by replacing the coordinated water. These complexes generally reduce the free metal ion concentration and, in turn, modify the solubility, toxicity, and adsorption properties of the metal species. The fraction of soluble and insoluble complexed metal species in a solution is a function of metal concentration, ligand concentration and pH (5). Thus, an understanding of the equilibrium relationships for these complexes is essential in the design and operation of biological wastewater treatment processes.

Nickel-Amine Complexation

Metal-amine complexation is common in wastewaters, especially those high in ammonia-nitrogen concentration. The transition metal ions including, Cr^{2+} , Cr^{3+} , Fe^{2+} and Ni^{2+} , have a strong tendency to form complexes with ammonia and they react within seconds to minutes of contact. The presence of these complexes is significant in biological wastewater treatment due to their interference in the the nitrification process and their alteration of the metal ion toxicity.

Equilibria of the nickel-amine complexes can be expressed as the following stepwise formation (8):



where K_n is the stepwise formation constant which satisfies the following equilibrium relationships:

$$\frac{[\text{NiNH}_3^{2+}]}{[\text{Ni}^{2+}] [\text{NH}_3]} = K_1 \quad [5]$$

$$\frac{[\text{Ni}(\text{NH}_3)_2^{2+}]}{[\text{NiNH}_3^{2+}] [\text{NH}_3]} = K_2 \quad [6]$$

$$\frac{[\text{Ni}(\text{NH}_3)_3^{2+}]}{[\text{Ni}(\text{NH}_3)_2^{2+}] [\text{NH}_3]} = K_3 \quad [7]$$

$$\frac{[\text{Ni}(\text{NH}_3)_4^{2+}]}{[\text{Ni}(\text{NH}_3)_3^{2+}] [\text{NH}_3]} = K_4 \quad [8]$$

For ease in calculations, the stepwise formation constants can be represented by overall formation constants, β_n where:

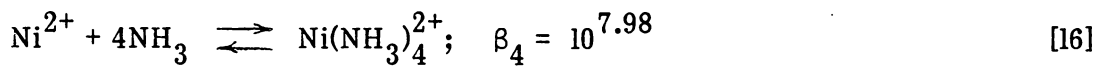
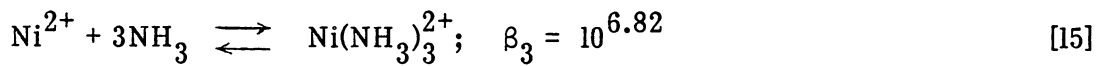
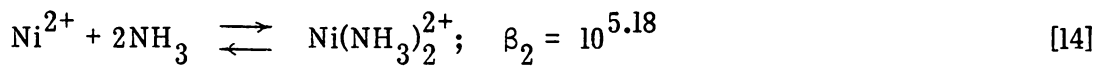
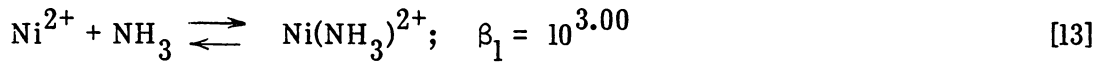
$$\beta_1 = K_1 \quad [9]$$

$$\beta_2 = K_1 \times K_2 \quad [10]$$

$$\beta_3 = K_1 \times K_2 \times K_3 \quad [11]$$

$$\beta_4 = K_1 \times K_2 \times K_3 \times K_4 \quad [12]$$

The overall equilibrium can then be expressed as:



where,

$$\frac{[\text{Ni}(\text{NH}_3)^{2+}]}{[\text{Ni}^{2+}] [\text{NH}_3]} = \beta_1 \quad [17]$$

$$\frac{[\text{Ni}(\text{NH}_3)_2^{2+}]}{[\text{Ni}^{2+}] [\text{NH}_3]^2} = \beta_2 \quad [18]$$

$$\frac{[\text{Ni}(\text{NH}_3)_3^{2+}]}{[\text{Ni}^{2+}] [\text{NH}_3]^3} = \beta_3 \quad [19]$$

$$\frac{[\text{Ni}(\text{NH}_3)_4^{2+}]}{[\text{Ni}^{2+}] [\text{NH}_3]^4} = \beta_4 \quad [20]$$

The above equilibrium relationships expressed in logarithmic form are:

$$\log[\text{Ni}(\text{NH}_3)^{2+}] = \log\beta_1 + \log[\text{Ni}^{2+}] + \log[\text{NH}_3] \quad [21]$$

$$\log[\text{Ni}(\text{NH}_3)_2^{2+}] = \log\beta_2 + \log[\text{Ni}^{2+}] + 2\log[\text{NH}_3] \quad [22]$$

$$\log[\text{Ni}(\text{NH}_3)_3^{2+}] = \log\beta_3 + \log[\text{Ni}^{2+}] + 3\log[\text{NH}_3] \quad [23]$$

$$\log[\text{Ni}(\text{NH}_3)_4^{2+}] = \log\beta_4 + \log[\text{Ni}^{2+}] + 4\log[\text{NH}_3] \quad [24]$$

Figure 1 shows a log-concentration diagram for the nickel-amine complexes.

(See Appendix A for detailed calculations).

A mass balance for the total soluble nickel species, assuming only ammonia complexation, is:

$$C = [\text{Ni}^{2+}] + [\text{Ni}(\text{NH}_3)^{2+}] + [\text{Ni}(\text{NH}_3)_2^{2+}] + [\text{Ni}(\text{NH}_3)_3^{2+}] + [\text{Ni}(\text{NH}_3)_4^{2+}] \quad [25]$$

where C equals the total nickel concentration in moles/liter.

Substituting from the equilibrium relationships:

$$C = [\text{Ni}^{2+}] (1 + \beta_1[\text{NH}_3] + \beta_2[\text{NH}_3]_2 + \beta_3[\text{NH}_3]_3 + \beta_4[\text{NH}_3]_4) \quad [26]$$

Given a certain ammonia concentration, then, the fraction of a particular species, relative to the total analytic concentration, can be calculated as follows:

$$\alpha_o = \frac{[\text{Ni}^{2+}]}{C} = \frac{1}{[1 + \beta_1(\text{NH}_3) + \beta_2(\text{NH}_3)^2 + \beta_3(\text{NH}_3)^3 + \beta_4(\text{NH}_3)^4]} \quad [27]$$

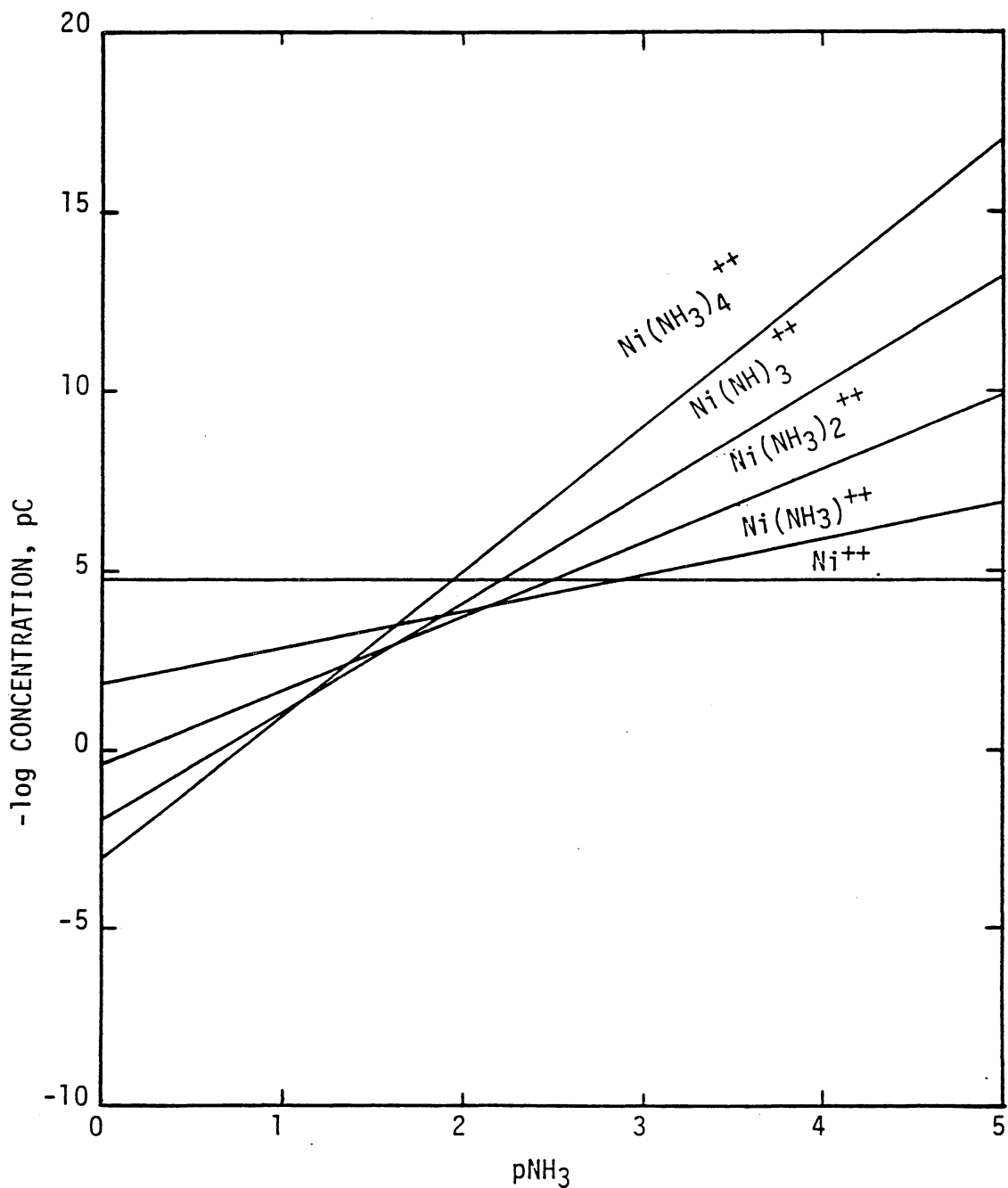


Figure 1. Log Concentration Diagram For Nickel Amine Complexes (Ni(II) = 0.77 mg/l)
(See Appendix A)

$$\alpha_1 = \frac{[\text{Ni}(\text{NH}_3)^{2+}]}{C} = \beta_1[\text{NH}_3] \alpha_0 \quad [28]$$

$$\alpha_2 = \frac{[\text{Ni}(\text{NH}_3)_2^{2+}]}{C} = \beta_2[\text{NH}_3]^2 \alpha_0 \quad [29]$$

$$\alpha_3 = \frac{[\text{Ni}(\text{NH}_3)_3^{2+}]}{C} = \beta_3[\text{NH}_3]^3 \alpha_0 \quad [30]$$

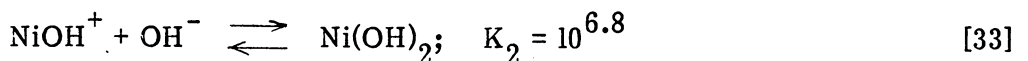
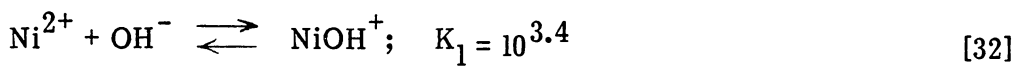
$$\alpha_4 = \frac{[\text{Ni}(\text{NH}_3)_4^{2+}]}{C} = \beta_4[\text{NH}_3]^4 \alpha_0 \quad [31]$$

Figure 2 shows the distribution for each of these nickel-amine complexes as a function of ammonia concentration. (See Appendix B for calculations pertinent to this research.)

Nickel-Hydroxide Complexation

The complexation of a metal species with hydroxide involves the abstraction of H^+ ions from the coordinated water bound to the metal to form a water molecule in solution (5). This process is commonly referred to as hydrolysis. In general, the percentage of the hydrolyzed metal species in solution increases with increasing pH. Highly charged metal ions, such as Fe^{3+} and Cr^{2+} , are strongly hydrolyzed in aqueous solutions and will complex with OH^- at low pH conditions. Divalent metals, such as Ni^{2+} and Cr^{2+} , hydrolyze in the pH of natural waters.

The equilibria of the hydroxy complexes for nickel is expressed as the following stepwise formation (5):



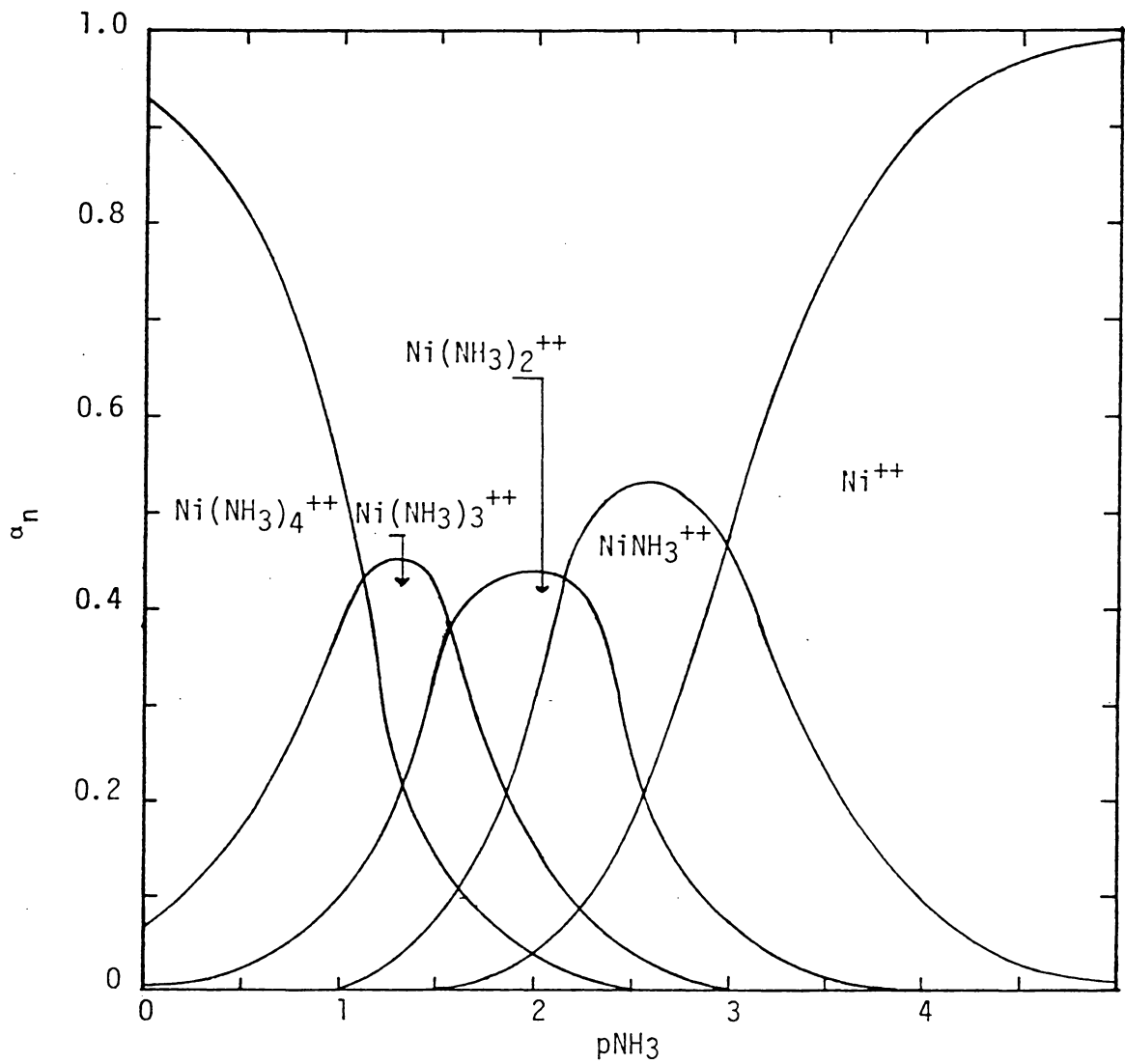
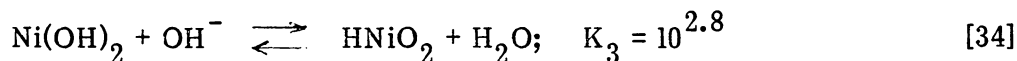


Figure 2. Distribution Diagram for Nickel Amine Complexes.
(See Appendix B)



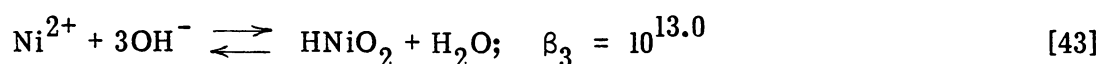
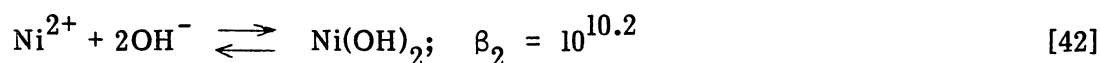
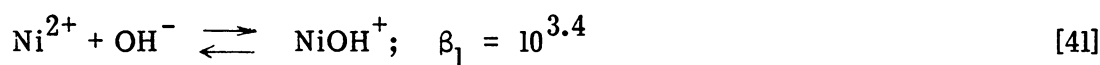
where K_1 , K_2 , and K_3 are the stepwise formation constants which satisfy the following equilibrium relationships:

$$\frac{[\text{NiOH}^+]}{[\text{Ni}^{2+}] [\text{OH}^-]} = K_1 \quad [35]$$

$$\frac{[\text{Ni(OH)}_2]}{[\text{NiOH}^+] [\text{OH}^-]} = K_2 \quad [36]$$

$$\frac{[\text{HNiO}_2]}{[\text{NiOH}_2] [\text{OH}^-]} = K_3 \quad [37]$$

The overall equilibrium can be expressed as:



A mass balance on the total soluble nickel species, gives:

$$C = [\text{Ni}^{2+}] + [\text{NiOH}^+] + [\text{Ni(OH)}_2] + [\text{HNiO}_2^-] \quad [44]$$

$$\text{or: } C = [\text{Ni}^{2+}] (1 + B_1[\text{OH}^-] + B_2[\text{OH}^-]^2 + B_3[\text{OH}^-]^3) \quad [45]$$

The fraction of a certain nickel-hydroxide species can then be calculated according to the same method used for the nickel-amine complexes. (See Appendix C). Figure 3 depicts the distribution of the nickel-hydroxy complexes as a function of pH.

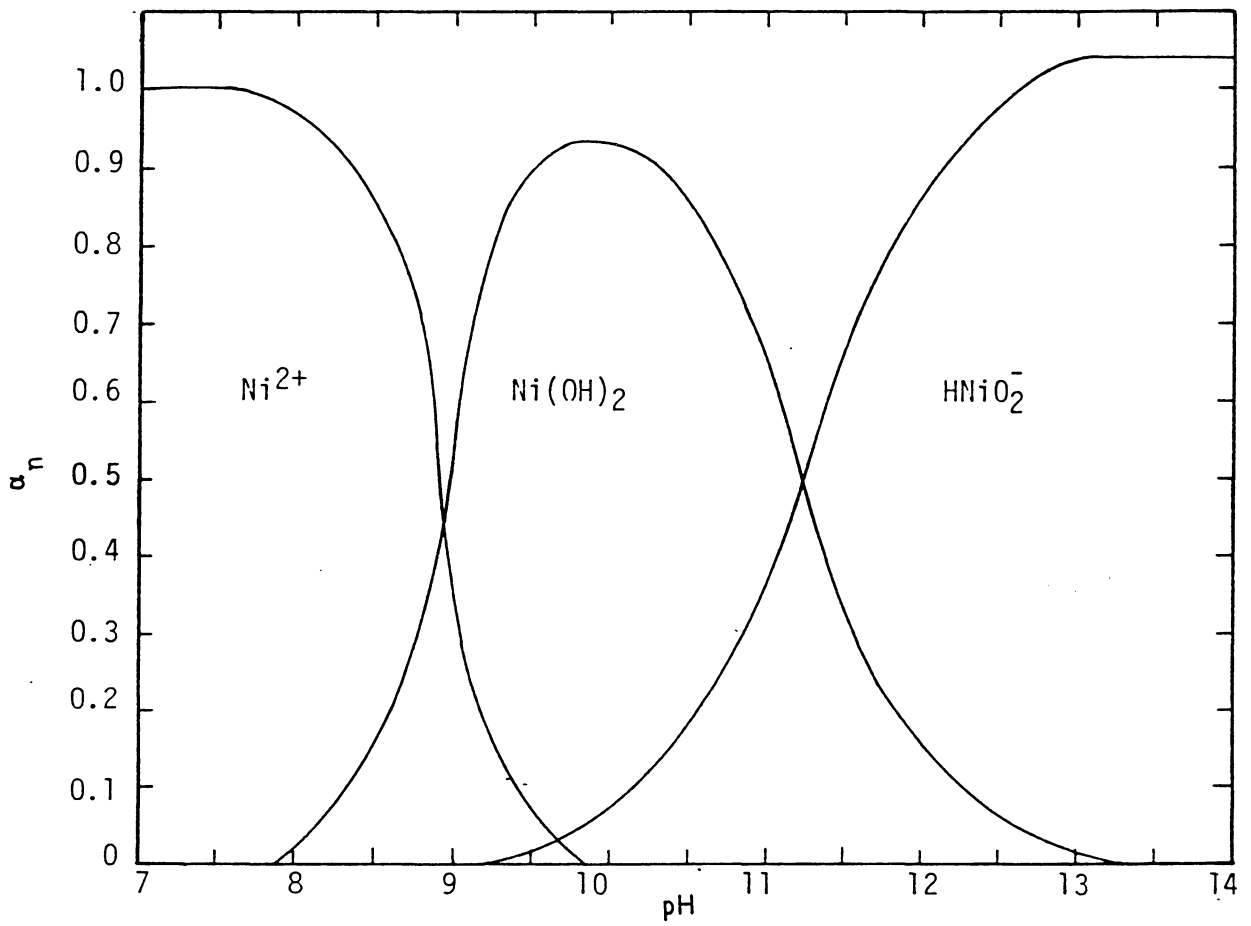


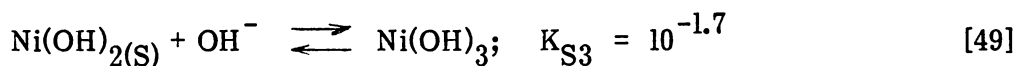
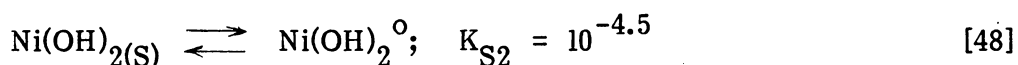
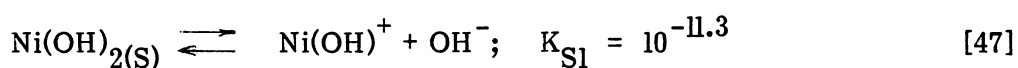
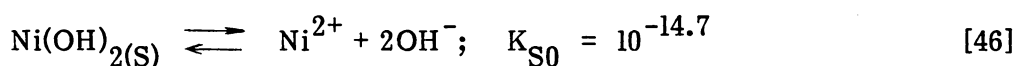
Figure 3. Distribution Diagram for Nickel Hydroxide Complexes (34).
(See Appendix C)

Precipitation of Nickel

The most common treatment method for the removal of heavy metals is hydroxide precipitation, where lime or caustic is added to adjust the wastewater to an alkaline pH, followed by precipitation and settling. Although this form of treatment has proven effective, it contains several drawbacks, including poor sludge filterability, the generation of large volumes of sludge, and fairly high costs.

Patterson et al. (9) investigated the carbonate system to determine whether carbonate precipitation offered any advantage in reducing the soluble metal concentration when compared to the hydroxide system. These authors compared their nickel-carbonate experimental results, at a total carbonate concentration of $10^{-1.2}$ moles/liter, to the theoretical phase diagram for nickel-hydroxide and nickel-carbonate at the same total carbonate concentration (See Figure 4). The solubility data for the nickel-carbonate system were identical to the nickel-hydroxide results as shown in Figure 5, indicating that precipitation in the nickel-carbonate system is controlled by hydroxide solubility.

In the absence of carbonate, the solubility of nickel-hydroxide is expressed as (9):



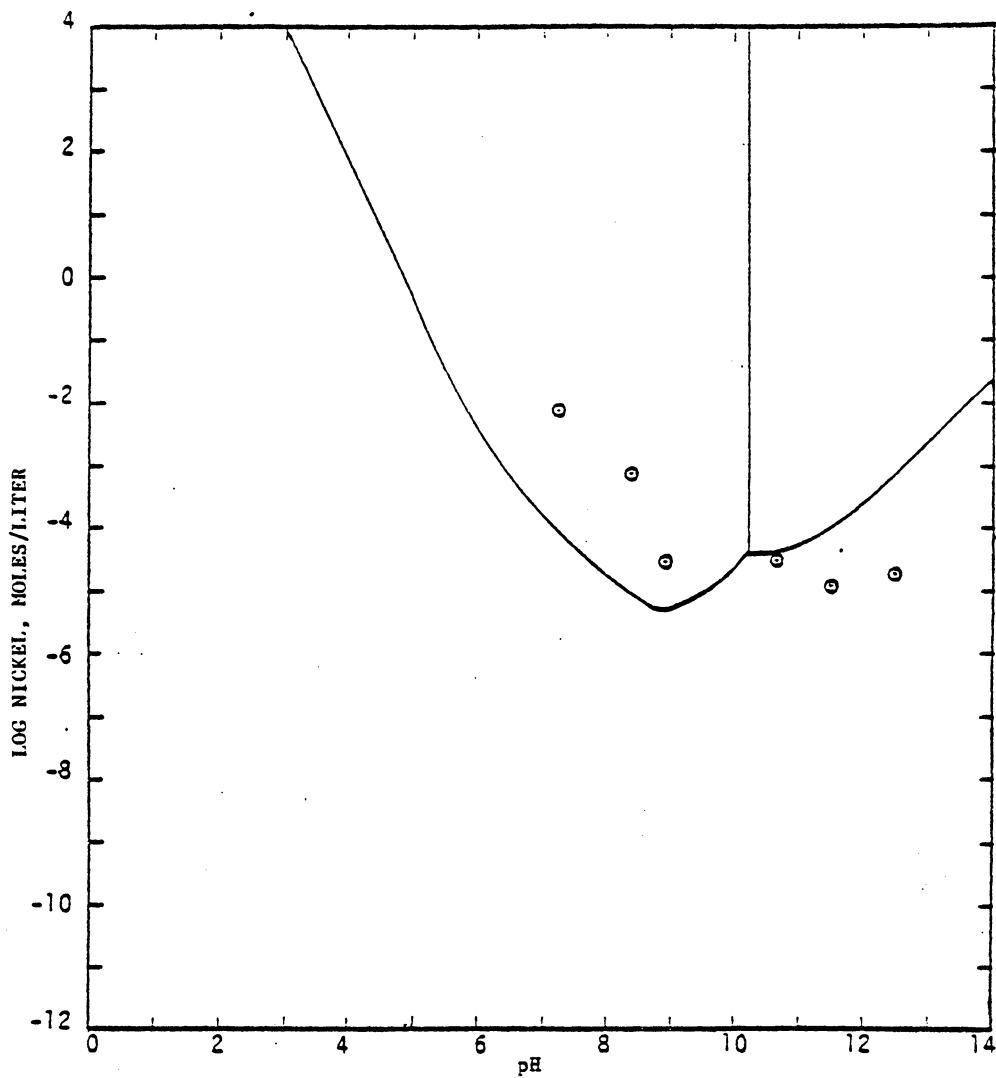


Figure 4. Comparison of Nickel Carbonate Solubility Data With Theoretical Phase Diagram.

$$C_T = 10^{-1.2} \text{ moles/liter (9).}$$

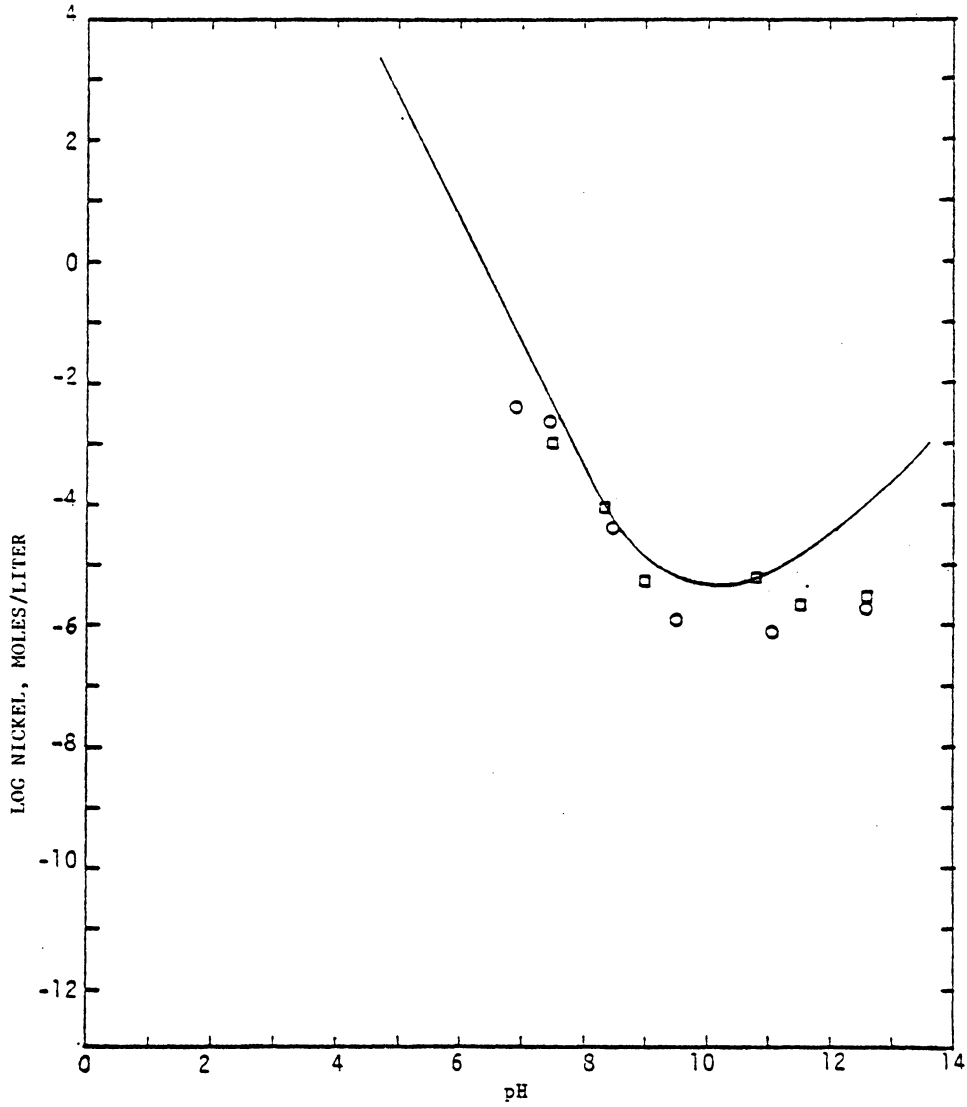


Figure 5. Comparison of Nickel Hydroxide and Nickel Carbonate Data With Theoretical Hydroxide Solubility Curve (9).

where K_S is the solubility product which determines the equilibrium for the hydroxides as follows:

$$K_{S0} = [\text{Ni}^{2+}] [\text{OH}^-]^2 \quad [50]$$

$$K_{S1} = [\text{Ni}(\text{OH})^+] [\text{OH}^-] \quad [51]$$

$$K_{S2} = [\text{Ni}(\text{OH})_2^0] \quad [52]$$

$$K_3 = \frac{[\text{Ni}(\text{OH})_3^-]}{[\text{OH}^-]} \quad [53]$$

For a given pH value, the concentration of each nickel-hydroxide species can be calculated from the above equations. The solubility curve for the nickel-hydroxides is shown in Figure 6. (See Appendix D for calculations.) Deviations from this curve occur at pH values above 8.5, where the solubility of nickel is affected by nickel-hydroxide complexation.

Adsorption of Nickel

When solutions of trace metals or other dilute solutes come in contact with solid phases, the concentration of the metal, or solute, usually decreases through its association with the solid phase (5). The reduction of aqueous metal ions in wastewaters has generally been attributed to this adsorption phenomenon. Most reduction of the dissolved metal species has been found to occur in the aeration tank by adsorption onto biological floc (10).

Brown and Lester (11) concluded from their research that bacterial cell flocs both in pure cultures and in complex activated sludge systems adsorb large quantities of metal ions from solution. Microorganisms are known to produce large

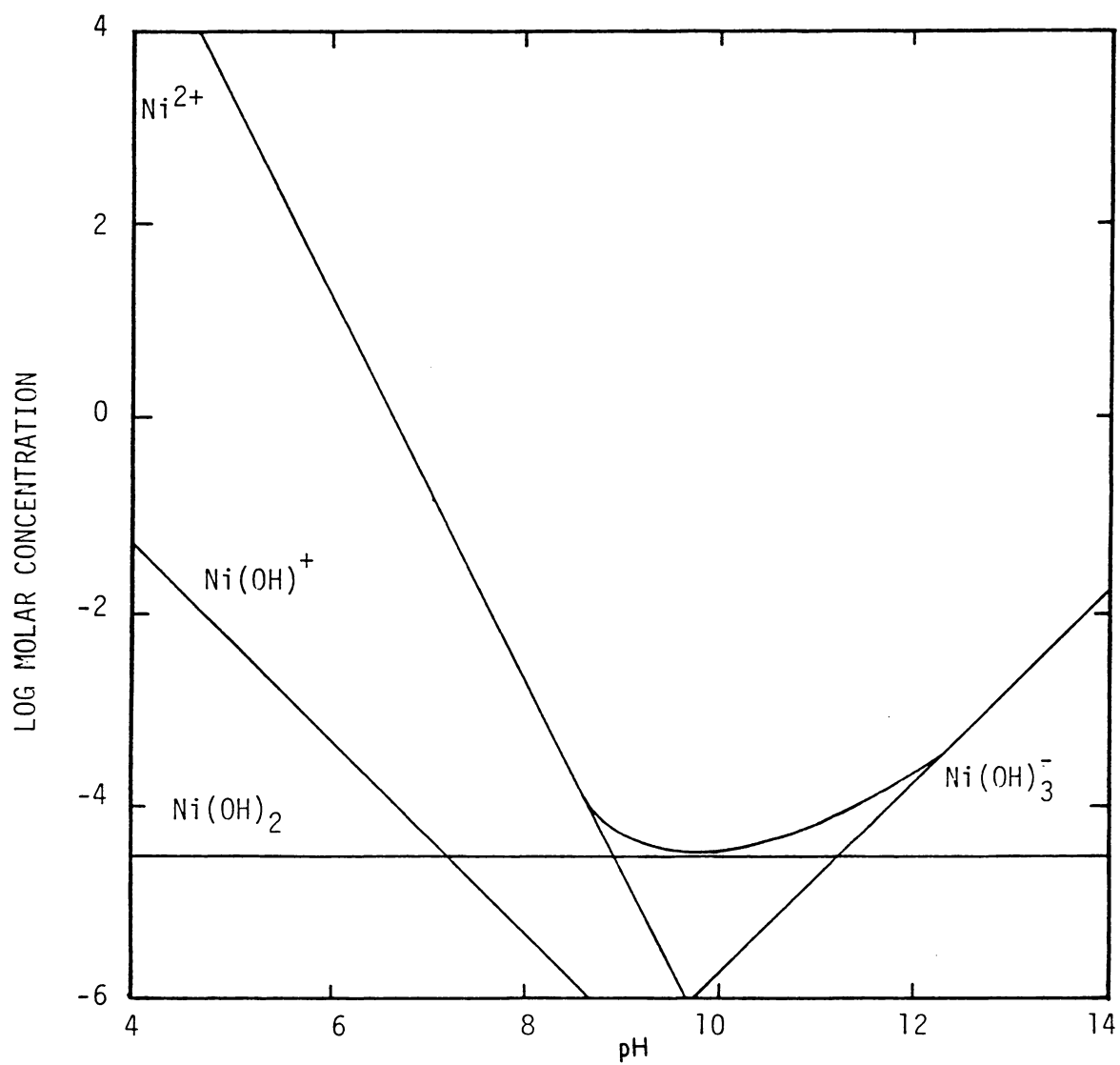


Figure 6. Theoretical Solubility Diagram for Nickel Hydroxide (34). (See Appendix D)

quantities of extracellular polysaccharides which are organized in well-defined capsules around the cells or are excreted as loose material into the growth medium (11, 12). Many of these polysaccharides possess negatively charged groups, giving the floc surfaces an overall negative charge. The degree to which the positively charged metals associate with the sludge affects the extent reduction of a soluble metal species in a biological process. A strong affinity between the metal and the sludge will result in low metal concentrations in wastewater effluents. Unfortunately, this strong affinity may also result in a toxic effect on the microorganisms, and, in turn, cause process failure.

Friedman and Dugan (13) studied the concentration and assimilation of heavy metals by a pure culture of the bacterium zoogloea. *Zoogloea ramigera* 115 is a capsular, matrix-producing pseudomonad which contributes to the successful function of aerobic treatment by removing organic matter in wastewaters (14). These bacteria have the capacity to produce large quantities of extracellular polymer which can adsorb metal ions, organics, or both from solution and can, in turn, be removed from a wastewater by flocculation and settling processes. Friedman and Dugan (13) added heavy metals to a culture of zoogloea during various cell growth cycles. Metal removal was found to vary with the physiological state of the organisms and proved to be greatest at high growth rates. The total uptake of the metal ions by the zoogloea bacteria was contributed to the combined influence of the cell and its surrounding matrix.

Similarly, Cheng et al. (15) investigated the ability of sludge to remove soluble metal species from wastewaters and the affinity of a biological mass for selected heavy metals. His kinetics studies revealed a rapid initial uptake of metals by sludge followed by a long-term slower rate of uptake. The affinity of

the sludge for metals was found to be in the order of lead→cadmium→nickel, as measured on a molar basis. Total metal removal was found to be a function of pH, the concentration of sludge, the soluble organic matter content, and the metal ion concentration.

Activated Sludge

The activated sludge process was developed in England, during 1914, by Arden and Lockett (16) and was so named because it involved the stabilization of wastes by an active mass of microorganisms. Today, the activated sludge process is utilized for both secondary biological treatment and complete aerobic treatment with no primary sedimentation.

In activated sludge process, wastewater is fed continuously to an aerated tank where a diverse group of microorganisms remove the soluble and colloidal organic material from solution. A large fraction of the organic wastes is used by aerobic and facultative bacteria for the synthesis of cellular material, while the remainder is converted to more stable inorganic forms, including carbon dioxide and water. Inorganic constituents present in the wastewater, such as nitrogen, phosphorous, potassium and sodium, are removed along with the organics and incorporated into the tissues of microbial cells.

After a certain aeration period, the biomass is separated from the treated wastewater by sedimentation. A portion of the settled biomass, or activated sludge, is returned to the aeration tank, while the remainder is removed from the process.

Microbial Growth

A small number of microorganisms placed in a batch system with an unlimited food supply and a suitable environment exhibit unrestricted growth (17). After some time, however, limiting conditions will be reached and the growth may follow a pattern as shown in Figure 7. This curve depicts the five main phases of microbial growth: the lag phase, microbial adaptation to a new environment; the exponential phase, minimal generation time and maximum specific growth rate; the declining growth phase, increasing generation time and decreasing specific growth rate due to a gradual decrease in substrate concentration; the stationary phase, exhaustion of nutrients and a balance between growth and death; and the death phase, endogenous metabolism and cell lysis. Of these periods of growth, the declining growth phase is normally encountered in conventional activated sludge treatment where continuous flow processes are employed.

Microbial Growth Kinetics

The removal of organic and inorganic material in the activated sludge process is accomplished by a heterogeneous culture of microorganisms and is thus dependent upon their behavior. Lawrence and McCarty (18) have developed a unified method for the design and operation of biological waste treatment based upon the microbial culture theory. According to these authors, biological growth and substrate utilization can be described by the following equation:

$$\frac{dX}{dt} = Y_{\max} \frac{dF}{dt} - k_d X \quad [54]$$

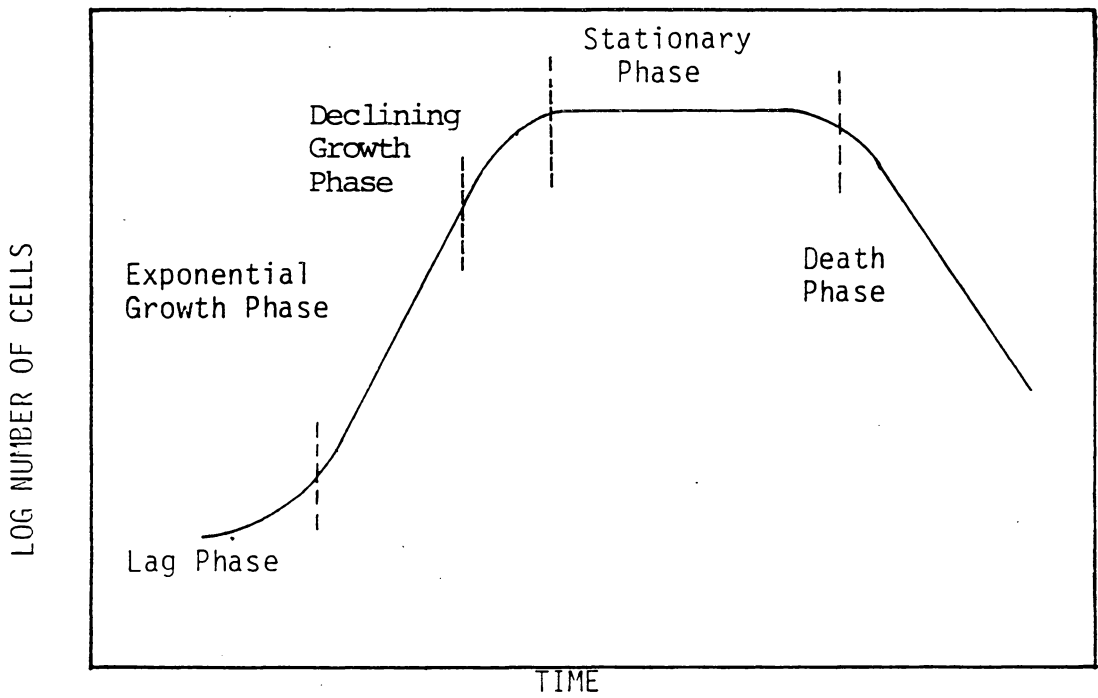


Figure 7. General Microorganism Growth Pattern in a Batch System (17).

where, $\frac{dX}{dt}$ = net growth rate of organisms per unit volume of reactor,
mass/volume - time,

Y_{\max} = maximum microbial growth yield coefficient, mass of micro-organisms/mass of substrate utilized,

$\frac{dF}{dt}$ = rate of substrate utilization, mass/unit volume,

k_d = microbial decay coefficient (or auto-oxidation of microbial mass in the absence of substrate), time⁻¹, and

X = microbial mass concentration, mass/unit volume.

Dividing both sides of equation [5] through by the microbial mass concentration, X , gives a linear equation in the form of:

$$\frac{\frac{dX}{dt}}{X} = Y_{\max} \frac{\frac{dF}{dt}}{X} - k_d \quad [55]$$

A plot of equation [55] yields a graph similar to that shown in Figure 8. The values of Y_{\max} and k_d can be obtained from the slope and intercept of the line, respectively. These values are typically employed in the evaluation of activated sludge process performance.

Sherrard and Shroeder (19) found that for a continuous-flow system, the auto-oxidation of cell mass may not occur. These authors have shown that an equation in the form of:

$$\frac{dX}{dt} = Y_{\text{obs}} \frac{dF}{dt} \quad [56]$$

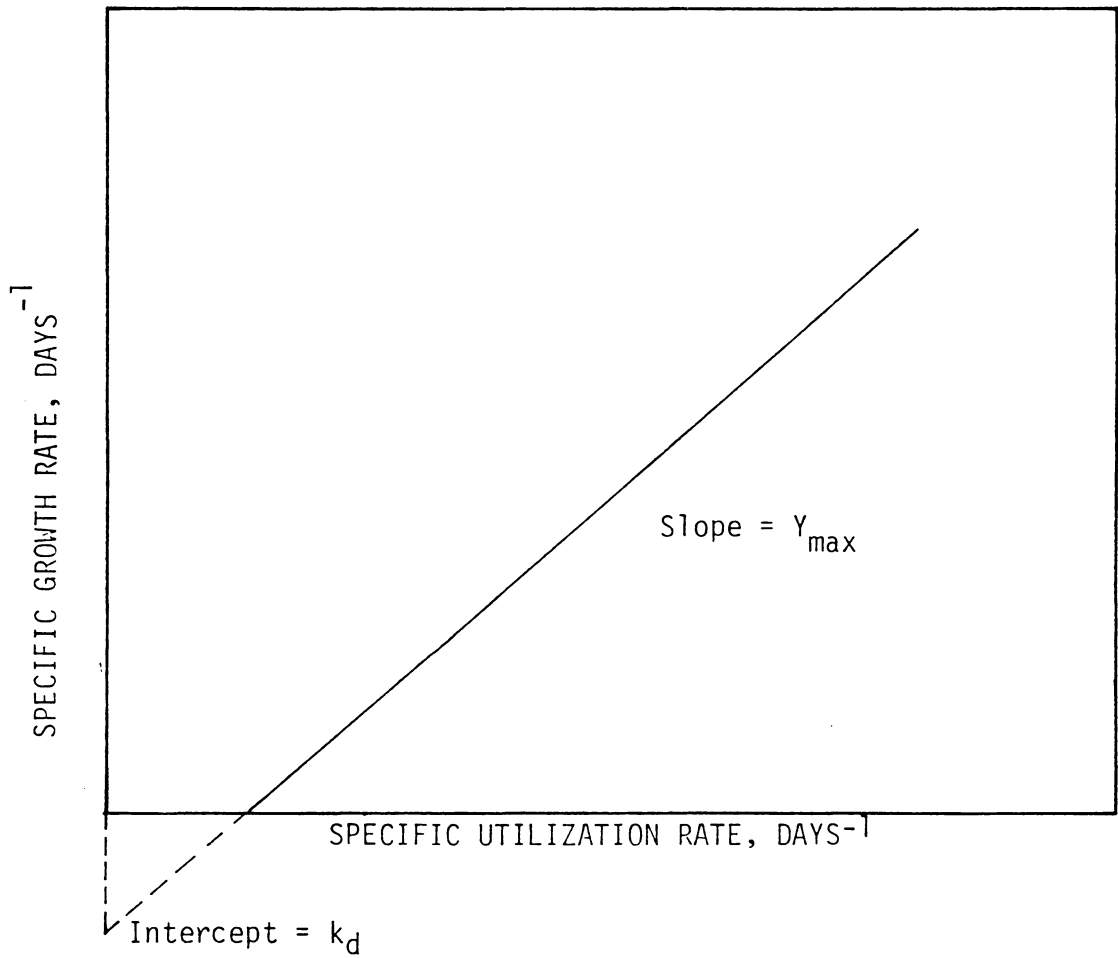


Figure 8. Biokinetic Coefficients From Specific Growth Versus Specific Utilization Rate.

where, Y_{obs} , the observed yield coefficient, more accurately describes the net growth rate and should be used in process evaluation. In this equation, Y_{obs} incorporates any decay of the microorganisms and depends upon the conditions of process operations. At low microbial growth rates, the observed yield is minimized due to increased maintenance energy requirements and predator activities. At high microbial growth rates, however, the observed yield is maximized because a greater portion of energy is utilized for growth rather than for maintenance.

Kinetics of the Activated Sludge Process

A typical flow scheme for the completely mixed activated sludge process is depicted in Figure 9 (17), where:

Q = the rate of raw wastewater entering the aeration tank,
volume/time,

S_o = the substrate concentration in the raw wastewater,
mass/volume,

V = the volume of the aeration tank, volume,

X = the biomass concentration in the aeration tank and the effluent
from the aeration tank (often referred to as mixed liquor
suspended solids, MLSS), mass/volume,

S_e = the steady-state substrate concentration after treatment,
mass/volume,

Q_r = the rate of sludge recycle, volume/time,

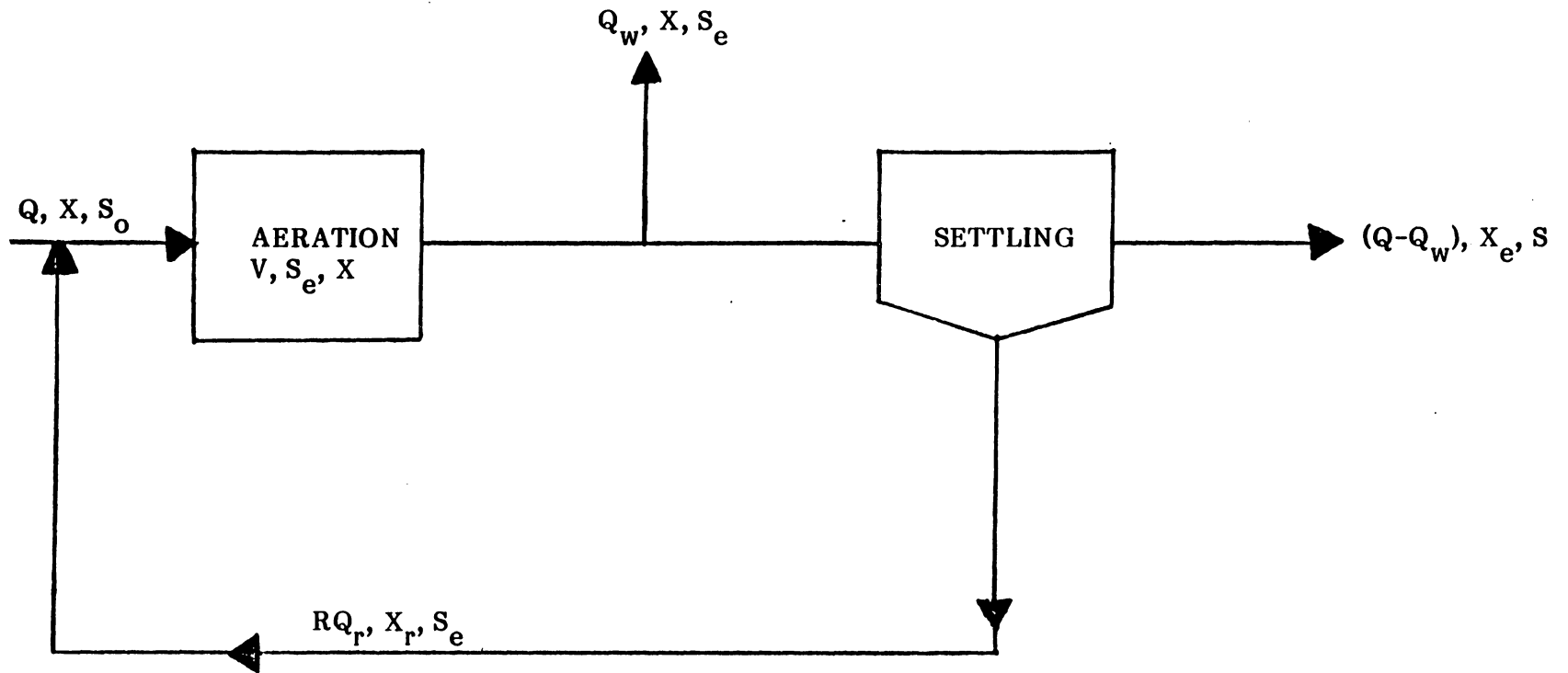


Figure 9. Completely Mixed Activated Sludge Process (17).

R = the sludge recycle ratio, Q_r/Q ,

Q_w = the rate of sludge wasting, volume/time, and

X_r = the biomass concentration in the underflow from the secondary clarifier, mass/volume.

The mathematical models which describe this activated sludge process have been developed from the microbial growth kinetics theory, and are based on the following assumptions:

1. All waste stabilization takes place in the biological reactor.
2. The total biological mass in the system equals the biological mass in the reactor.
3. Sludge is wasted from the aeration tank, not from the clarifier.

A materials-balance equation surrounding the entire activated sludge system shown in Figure 9, gives:

Net rate of change in amount of biomass within system	=	Rate at which biomass appears in system	-	Rate at which biomass leaves system
---	---	---	---	---

or:
$$\frac{(dX)V}{dt} = QX_o + \frac{(dX)V}{dtg} - [Q_w X + (Q - Q_w)X_e]$$
 [57]

Assuming that no microorganisms are present in the influent, $X_o = 0$, and the system is at "steady state," where the rate at which biomass enters the system equals the rate at which biomass leaves the system, $\frac{dX}{dt} = 0$, equation [57] can be arranged to yield:

$$\frac{\frac{(dX)}{(dt)g}}{X} = \frac{[Q_w X + (Q - Q_w) X_e]}{VX} \quad [58]$$

where, $\frac{(dx)}{(dt)g} =$ the specific microbial growth rate, days⁻¹

Substituting equation [55], which describes the specific microbial growth rate, into equation [58], yields:

$$Y_{\max} \frac{\frac{dF}{dt}}{X} - k_d = \frac{[Q_w X + (Q - Q_w) X_e]}{VX} \quad [59]$$

An operational parameter, θ_c , or mean cell residence time, is typically employed to control biological wastewater treatment. The mathematical concept was first introduced by Lawrence and McCarty (18), and is defined as:

$$\theta_c = \frac{VX}{Q_w X + (Q - Q_w) X_e} \quad [60]$$

Substituting equation [60] into equation [59] yields:

$$\frac{1}{\theta_c} = Y_{\max} \frac{\frac{dF}{dt}}{X} - k_d \quad [61]$$

The term $(dF/dt/X)$, referred to as the specific utilization rate, is represented by the parameter, U , which is defined as:

$$U = \frac{S_o - S_e}{\theta X} \quad [62]$$

where, U = specific utilization rate, time^{-1} , and

θ = hydraulic detention time, volume of total reactor divided by the influent flow rate to the reactor.

Prior to the introduction of the mean cell residence time, θ_c , as a control parameter for the activated sludge process, the specific utilization rate governed the operation of most biological treatment facilities. Both of these control parameters can be related by the following equation which describes microbial growth:

$$\frac{1}{\theta_c} = YU - k_d \quad [63]$$

Lawrence and McCarty (18) demonstrated that the operational parameters for each activated sludge system can, in turn, be used to determine other important process parameters. At each mean cell residence time, the effluent substrate concentration, waste sludge production, mixed liquor suspended solids concentration, and observed yield can be obtained through the following relationships:

$$S_e = \frac{K_s(1 + k_d\theta_c)}{\theta_c(Yk - k_d) - 1} \quad [64]$$

where, S_e = the effluent substrate concentration, mass/volume,

k = the maximum rate of substrate utilization per unit weight of microorganisms, time^{-1} ,

K_s = substrate concentration at one-half the maximum rate of substrate utilization per unit weight of microorganisms, mass/volume.

The waste sludge production can be described as:

$$P_x = \frac{YQ(S_o - S_e)}{1 + k_d \theta_c} \quad [65]$$

where, P_x = waste sludge production per unit time.

The estimated reactor mixed liquor suspended solids concentration can be calculated as following:

$$X = \frac{Y(S_o - S_e)\theta_c}{1 + k_d \theta_c} \quad [66]$$

where, X = biomass concentration, MLSS, in the total biological reactor, mass/volume.

The observed yield coefficient, as introduced by Sherrard and Shroeder [19], is determined by:

$$Y_{obs} = \frac{P_x}{Q(S_o - S_e)} \quad [67]$$

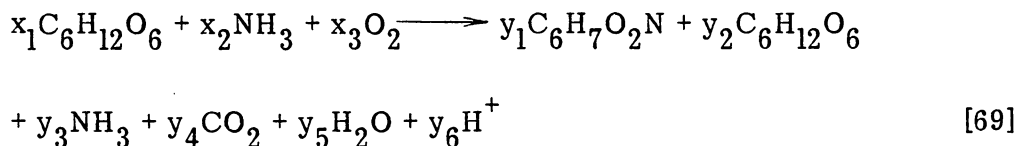
where, Y_{obs} = variable microorganism yield coefficient, mass/mass.

Stoichiometry of the Activated Sludge Process

Sherrard (20) has described the aerobic treatment process through the integration of mathematical models and chemical stoichiometric equations. The bio-oxidation of organic material can be represented as:



For an organic wastewater containing glucose, alone, equation [68] can be quantified as:



where, x_n = influent substrate concentration to the reactor, moles/liter,

y_n = effluent concentration from reactor, moles/liter,

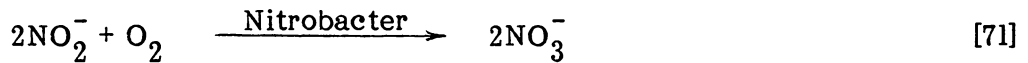
$C_6 H_{12} O_6$ = glucose,

$C_5 H_7 O_2 N$ = bacterial cells.

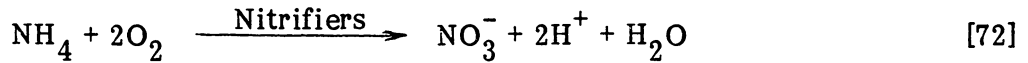
For a given activated sludge system with a known influent substrate concentration, equations [64] through [67] can be used to predict the microbial yields and effluent substrate concentrations at various θ_c values. The stoichiometric equation can then be balanced with respect to other influent and effluent constituents.

Nitrification

The discharge of nitrogen compounds from wastewater treatment plants has recently received considerable attention. In rivers and streams, any nitrogen tied up in organic compounds is readily converted to ammonia, and under certain environmental conditions, the ammonia is readily oxidized to nitrate-nitrogen. This process, known as nitrification, is accomplished by chemoautotrophic bacteria as illustrated in the following two-step reaction:



The overall reaction can be expressed as follows:



As shown, the Nitrosomonas are responsible for the oxidation of ammonia to nitrite, NO_2^- , while the Nitrobacter convert nitrite to nitrate, NO_3^- . Most of the nitrogen removed in this process serves as an energy source for the microorganisms, while a small fraction is utilized, along with inorganic carbon, for the synthesis of new cells.

As shown in equation [72], the overall nitrification process consumes two moles of oxygen for each mole of ammonia oxidized. If this reaction takes place in rivers and streams, large quantities of oxygen may be depleted and result in detrimental effects on most of the aquatic life. Thus, the removal of nitrogen from a wastewater prior to its discharge from a wastewater treatment plant is imperative and has become a common practice in most biological treatment systems. The activated sludge process has been found to be effective in achieving nitrification by providing an artificial aerobic setting for the bacteria to oxidize ammonia-nitrogen to nitrate-nitrogen. Typically, activated sludge plants have combined nitrification with existing organic removal processes.

Nitrification process efficiency in activated sludge treatment depends upon the environmental conditions in a wastewater including, temperature, pH, alkalinity, mean cell residence time, ammonia concentration and COD:TKN ratio. These parameters are discussed in the following paragraphs.

Wild et al. (21) investigated the effects of temperature and pH on nitrification kinetics. Results of their temperature study showed that nitrification was able to occur at temperature ranging from 5-30°C and that nitrifying activity increased with temperature over the range studied. From their pH study, the authors developed a percent nitrification curve for varying pH values. As shown in Figure 10, the optimum pH for nitrification lies in the range of 7.0 to 9.8. Metcalf and Eddy (16) recommend a temperature in the range of 20-30°C and a wastewater pH between 6.5 and 7.5 for the most efficient nitrogen removal.

During the nitrification process, two moles of hydrogen ions are released per mole of ammonia-nitrogen oxidized. To maintain the optimum pH for the nitrifiers in an activated sludge process, then, the alkalinity in a wastewater must be sufficient to buffer against a large pH depression. Theoretical calculations have been developed to predict the alkalinity destruction during nitrification. According to the nitrification equations [70] through [72], approximately 7.14 mg/l alkalinity as CaCO₃ is destroyed per mg/l NO₃-N formed (or mg/l NH₄⁺-N oxidized). Searce et al. (22) and Sherrard et al. (23), however, observed that the alkalinity destruction was less than that predicted theoretically and it varied with the age of the microorganisms. Through batch and continuous studies, these authors found that the mineralization of 1 mg/l organic nitrogen to ammonia-nitrogen imparted approximately 3.57 mg/l alkalinity as CaCO₃ to a wastewater. Any ammonia subsequently incorporated into microbial mass would cause the removal of 3.57 mg/l alkalinity. The overall change in alkalinity can be represented as:

$$\Delta \text{ Alkalinity} = 3.57[(\Delta \text{ filtrate organic N}) - \text{synthesized N}] - 7.14(\Delta \text{ NO}_3 - \text{N}) \quad [73]$$

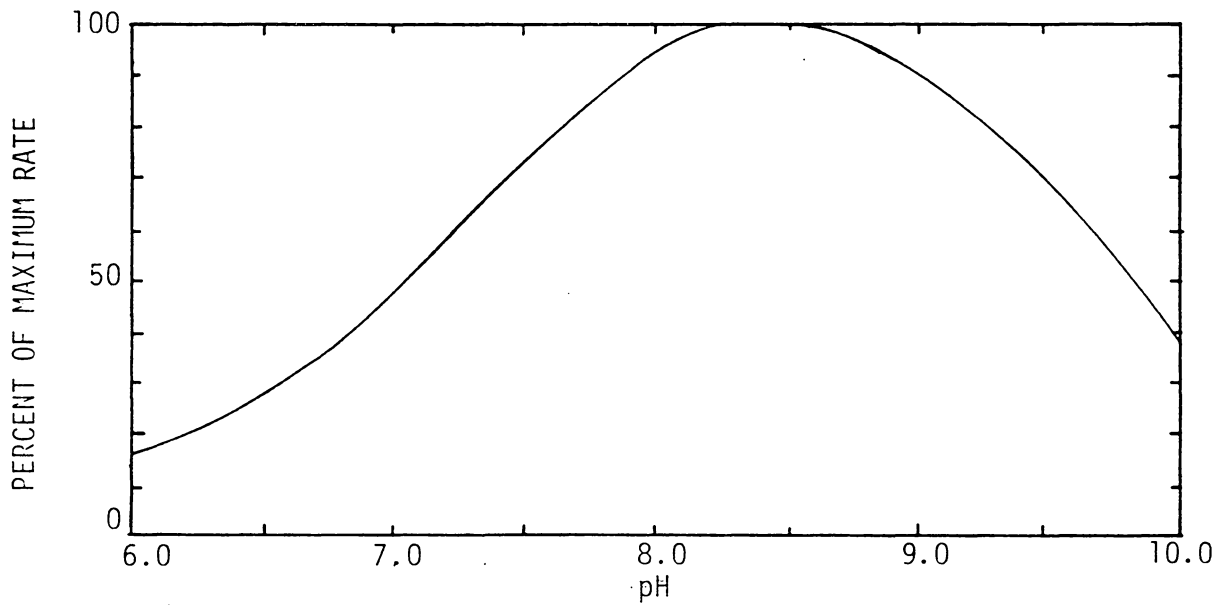


Figure 10. Percent of Maximum Rate of Nitrification at Constant Temperature Versus pH (20).

The observed alkalinity versus the theoretical alkalinity as predicted by equation [73] is shown in Figure 11.

To maintain nitrification in the activated sludge process, sewage must be retained in the aeration units in excess of a critical period which depends upon the mixed liquor suspended solids concentration, and the growth rate of nitrifying bacteria. Because the nitrifying organisms are slow growers and are very sensitive to environmental conditions, they cannot compete with the heterotrophs for ammonia nitrogen. Stover and Kincannon (24) found that the heterotrophic organisms actually "crowd out" the autotrophic nitrifiers. Based upon his studies, Sherrard (20) noted that nitrification did not occur until a θ_c of approximately 3 days. As θ_c increased, so did nitrification due to less sludge production and less incorporation of nitrogen into heterotrophic cellular material. Stover and Kincannon (24) observed that at a θ_c greater than 10 days, essentially complete nitrification was obtained by all reactors in their study. Nitrification decreased with decreasing sludge age and was essentially stopped at a θ_c equal to 3 days. Jenkins and Garrison (25) studied data from various activated sludge treatment plants with combined organic removal nitrification processes and found that at a θ_c equal to 5 days, nitrification was barely possible, while at a θ_c equal to 10 days, nitrification was practically complete. The organic removal efficiency, however, was essentially constant for a θ_c value greater than 2 days. Other studies (24, 26) on combined organic removal nitrification systems also show that biological nitrification does not affect the activity of heterotrophic organisms.

Ammonia-nitrogen exists in aqueous solutions as unionized ammonia and as the ammonium ion, depending upon the equilibrium position of the following reaction:

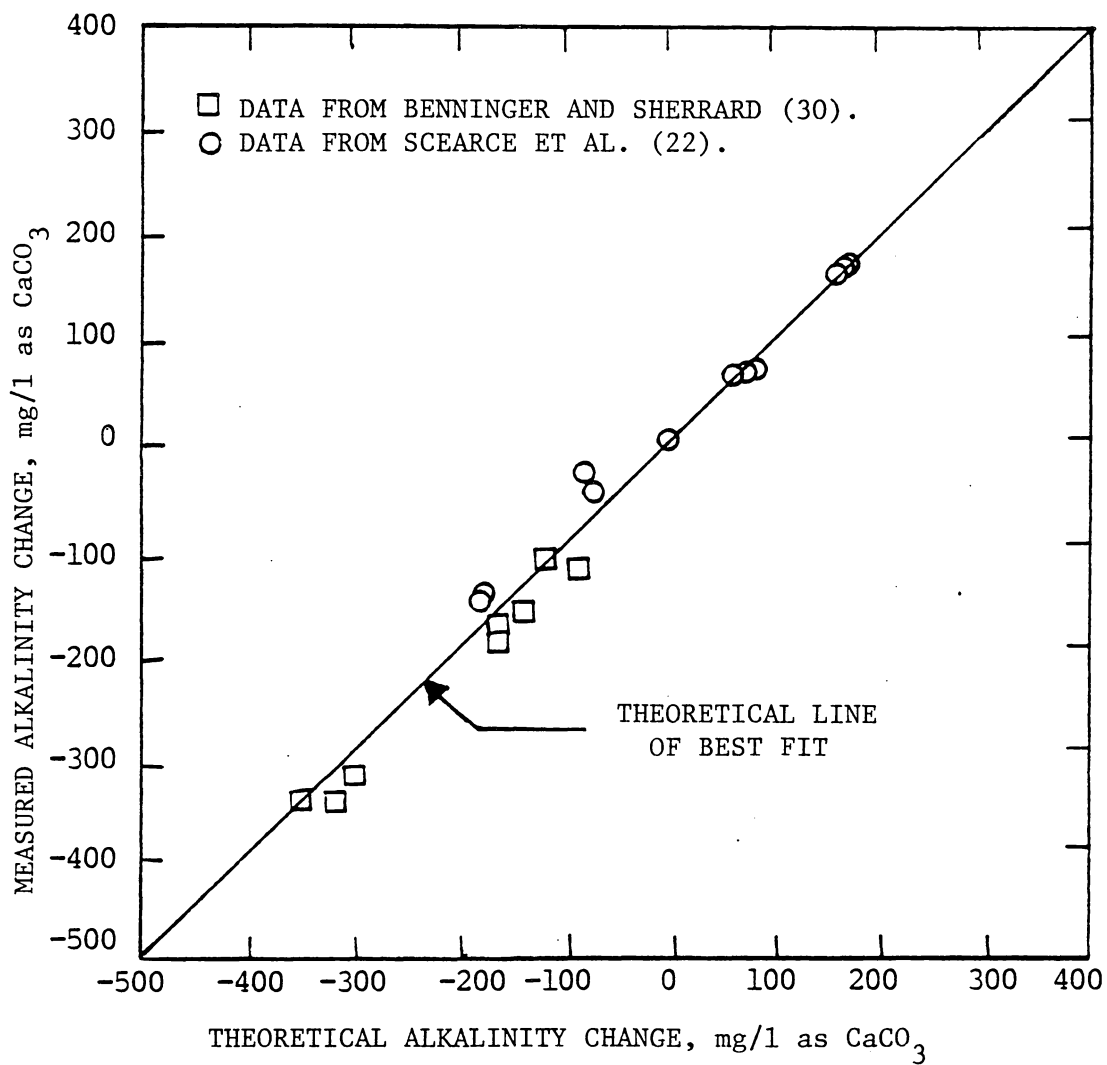


Figure 11. Comparison of Theoretical Alkalinity Change and Measured Alkalinity Change.



Under high pH, or alkaline conditions, the NH_3 form of nitrogen predominates, while under acidic conditions the ammonium form predominates. Studies (27, 28, 29) have shown that high concentrations of unionized ammonia can be toxic to the nitrification process. Neufeld et al. (27) noted from their fill and draw bench scale studies that nitrification process instability can be caused by the interaction of organics via a substrate inhibition mechanism at high levels of unionized ammonia. Unionized ammonia began to inhibit nitrification at concentrations of 10 mg/l. Ford et al. (28) conducted bench-scale treatability studies to investigate factors affecting biological nitrification. Results showed that free ammonia concentrations of 30 mg/l inhibited *Nitrosomonas*. Anthonisen et al. (29) also suggested that the nitrification process efficiency depends on the concentration of free ammonia in solution, not on the total ammonia concentration. In bench-scale studies, *Nitrosomonas* and *Nitrobacter* were inhibited by free ammonia concentrations of 10-150 mg/l and 0.1-1.0 mg/l, respectively. The sensitivity of *Nitrobacter* to the free ammonia resulted in an accumulation of nitrite-nitrogen without subsequent oxidation to nitrate-nitrogen.

Recent investigations have shown that for the combined organic removal nitrification process, the degree of nitrification depends not on the amount of ammonia in the wastewater, but on the carbon to total Kjeldahl nitrogen (ammonia-nitrogen + organic nitrogen) ratio, COD:TKN. According to Sherrard et al. (23), the heterotrophic biomass removes organic and ammonia nitrogen in proportion to organic carbon for the synthesis of new cells. Only that fraction of nitrogen remaining in solution is available for nitrification. Therefore, low

COD:TKN ratios will exhibit a larger extent of nitrification due to less accumulation of nitrogen by the bacteria.

Stover and Kincannon (24) operated one-stage activated sludge pilot plants at COD:NH₃-N ratios of 2:1, 10:1, and 20:1, utilizing θ_c as the operational variable. The actual limiting sludge age for nitrification was found to depend upon the COD:NH₃-N ratio. At a θ_c approximately equal to 10 days, the ammonia nitrogen removal was essentially complete for all three pilot plants. However, the amount of the removed ammonia that was subsequently oxidized to nitrate decreased with increasing COD:NH₃-N ratios. This observance was attributed to the dominance of cellular synthesis over oxidation in nitrogen removal.

Benninger and Sherrard (30) found that for a continuous flow process, a larger COD:TKN ratio resulted in higher organic nitrogen and ammonia-nitrogen removal efficiencies with large percentages of nitrogen in the waste sludge. In addition, decreased concentrations of TKN and nitrate were present in the effluent.

Heavy Metals and Biological Wastewater Treatment

Since its discovery in 1914, the activated sludge process has become the most widely used biological wastewater treatment process for both organic removal and nitrification. Experience with this process has shown that environmental control must be practiced in order to obtain optimum performance of biological waste treatment systems. The variables of concern, in each wastewater treated by this process, include temperature, pH, dissolved oxygen, BOD, TKN and the presence of inhibitory or toxic materials.

The recent surge in technology and production has led to an increase in the generation of industrial wastes and to an increased concern for the effects of these wastes on the environment. Heavy metals, associated with the electroplating

industry have received the most attention since these industries tend to discharge into municipal sewer systems. Studies have shown that the transition metals including mercury, cadmium, copper, nickel and zinc, can adversely affect the environment at relatively low concentrations. Subsequent to this discovery, many investigations have been conducted to determine the effects of the heavy metals on the completely-mixed activated sludge system and the feasibility of utilizing this process to reduce metal concentrations in wastewaters.

Microbial Enzymes

The activated sludge process is carried out by a diverse group of microorganisms and depends upon all their life functions. The process by which the microorganisms grow and obtain energy from their utilization of food involves many pathways and cycles (16). Essential to the reactions that occur along the pathways are the actions of enzymes, the organic catalysts produced by a cell. Enzymes are responsible for every reaction that occurs in a cell and act to accelerate a complex network of biological reactions in aqueous solutions.

Enzyme-catalyzed reactions involve the reversible formation of an enzyme-substrate complex and the irreversible decomposition of the complex to form a free enzyme and a reaction product [17].



where, K_n is the reaction constant.

Enzymes are substrate specific, therefore, the cell must produce a different enzyme for each type of substrate it utilizes. In a metabolic chain, the product from the enzymatic reaction with one substrate serves as substrate for another

reaction. A sequence of reactions is often required to convert the original substrate to a final end product.

The activity and velocity of each enzymatic reaction is controlled by enzyme concentration, substrate concentration, pH, temperature and the presence of activators or inhibitors. The poisoning of any single enzyme in the metabolic chain will inoperate the entire chain and have a fatal effect on the microorganism. Adams et al. (31) concluded from their investigations that heavy metals in a wastewater treatment process tend to form metal-enzyme complexes with certain essential extracellular constituents of a biomass. Normal biological activities are often inhibited, thereby causing process failure. An increase in MLSS or a decrease in metal concentration decreases the proportion of metal-enzyme complexes and reduces the inhibitory effects of metals to the biomass. Barth (32) discovered that the transitional metals also form stable complexes with the intracellular functional groups of a cell. These functional groups are present as polysaccharides, lipids and nucleic acids in the biological protoplasm. Metals block the active sites of these groups by forming stable complexes.

Effects of Heavy Metals on Biological Treatment Processes

Toxicity studies involving heavy metals in biological treatment processes deal with low concentrations of heavy metals in heterogeneous biological systems. A true assessment of the inhibitory effects of these metals on microbial species requires very long, controlled observations. Tomlinson et al. (33) concluded from their studies that short-term effects of inhibition are not accurate guides when applied to full-scale continuous-flow activated sludge plants. In some biological processes the long-term effects of heavy metals are more severe than the short-term effects due to the limited adsorptive or complexing capacity of organic

matter in sludge. In other systems, however, the long-term effects may be insignificant. Barth (32) attributed this phenomena to the acclimation of microorganisms to heavy metals. Initial doses of a metal to a biological system may cause detrimental effects on its treatment efficiency. With time, however, the metal content of the sludge may build up to a condition of operating equilibrium and the process may return to normal operation. Sujarittanonta (34) examined the influence of nickel on completely-mixed batch activated sludge units. Unacclimated batch reactors receiving Ni(II) doses of 1, 5 and 10 mg/l exhibited decreased COD removal efficiencies of 2, 8 and 11 percent, respectively, while acclimated batch reactors showed negligible effects when administered the same metal doses. The adverse effect on the unacclimated reactors was attributed to the inhibitory effects of nickel on the microbial utilization of substrate. Sujarittanonta also noted a rapid uptake of nickel in the unacclimated reactors during the first 90 minutes after dosing, followed by a declining rate of uptake. The acclimated reactors, on the other hand, exhibited a gradual uptake of nickel after dosing, which began to decrease after three hours of aeration.

According to Neufeld and Hermann (35), a true assessment of the effects and removal of metals in biological treatment processes must include a study of the kinetics of the microbial system as well as an evaluation of process performance. In biological treatment, however, toxicity studies must deal with diverse groups of life forms, and must encompass group reactions (32). Several species of organisms may be adversely affected by a toxic material with no total effect realized. Tomlinson et al. (33) investigated the inhibition of nitrification by the heavy metals, copper, mercury and chromium, in both pure cultures of N. europaea and in mixtured cultures of activated sludge and sewage. Results showed that the growth of the N. europaea was inhibited at metal concentrations less than 1 mg/l, while,

much larger metal doses were required to reduce the nitrifying capacity of the activated sludge to the same extent. The authors attributed this observation to the formation of chemical complexes and organic matter in the sewage or activated sludge. Poon and Bhayani (36) employed a Michaelis-Menton model of inhibition to assess the toxicity of heavy metals to both pure and mixed cultures of bacteria. Results showed a different toxic effect of metals on each of the species of organisms studied. The authors concluded that application of microbial growth models to evaluate metal toxicity in biological treatment, can only estimate, at best, the overall kinetics of a mixed culture system.

Various dose-response relationships have been developed to describe the effects of heavy metals on biological treatment. Barth (32) studied the response of the aerobic and anaerobic biological treatment processes to the continuous addition of heavy metals. From data, he developed a dose-response curve for each process, as depicted in Figure 12. The aerobic process exhibited a threshold effect at low metal concentrations, approximately 1-2 mg/l, but was not seriously affected until exposed to metal concentrations several orders of magnitude beyond the threshold dose. The anaerobic process, on the other hand, followed an "all or nothing" pattern of behavior and would not tolerate a wide range of metal concentrations. Barth attributed his observations of system performance to the diverse life forms present in aerobic processes as compared to the narrow life forms present in anaerobic processes. In aerobic biological treatment, some species may be adversely affected by toxic substances, while the overall system may show no loss in treatment efficiency.

Barth et al. (37) published a summary report on the effects of heavy metals in the biological treatment process, based upon investigations of several activated

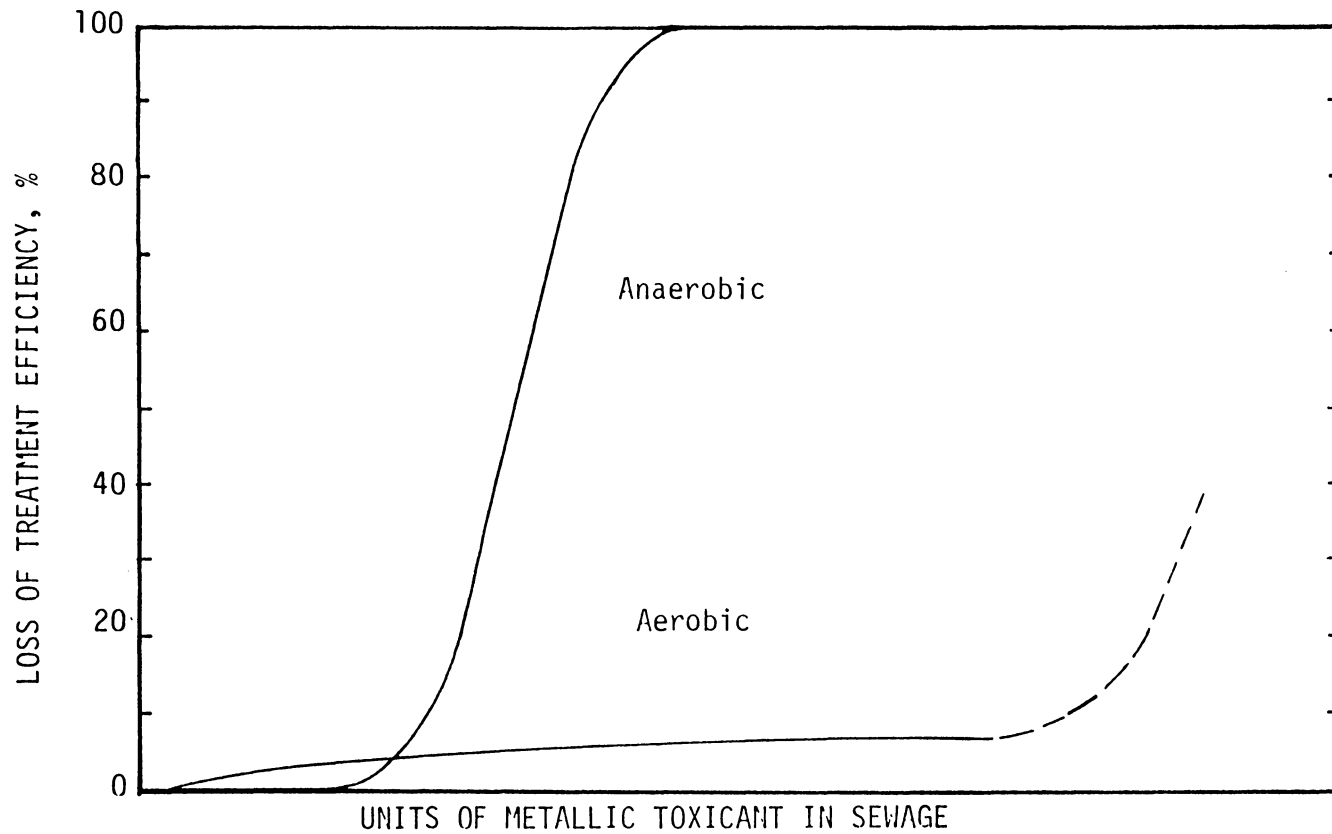


Figure 12. Patterns of Performance Depreciation in Sewage Treatment Processes (32).

sludge pilot plants. For each metal studied, the activated sludge process exhibited a plateau-type dose-response reaction, as shown in Figure 13. A small dose of metal to a process resulted in a significant reduction in treatment efficiency, while substantially larger doses could be introduced to the system without any further decrease in process performance. Complete failure of a system occurred only at continuous metal doses much greater than the threshold limit. Data showed that the aerobic biological treatment process can tolerate continuous influent doses of chromium, copper, nickel and zinc up to a total metal concentration of 10 mg/l, with only a 5 percent reduction in COD removal efficiency. The nitrification process, however, was severely inhibited by metal doses of 5 mg/l. The threshold level for slug doses of various metals to the biological process, as determined by COD removal efficiency, ranged from 50-500 mg/l.

McDermott et al. (3) conducted a treatability study on three replicate pilot plants to determine the threshold limit of nickel in biological treatment processes. Results, similar to those of Barth et al. (37), demonstrated that the effects of nickel on activated sludge are not linear with concentration but display a decreasing response to increasing concentrations. Based upon BOD and COD data, nickel doses between 1 and 2.5 mg/l had essentially no effect on activated sludge. Nickel doses ranging from 2.5 to 10 mg/l reduced BOD removal efficiency a maximum of 5 percent and increased turbidity in the final effluent. The overall effects on the system from the 10 mg/l dose were about the same as those for the 2.5 mg/l dose. Slug doses of nickel less than 200 mg/l did not seriously upset the activated sludge system and only temporarily decreased effluent quality. The system returned to normal at the end of 40 hours. In a similar treatability study, McDermott et al. (39) found that the maximum concentration of copper that can be

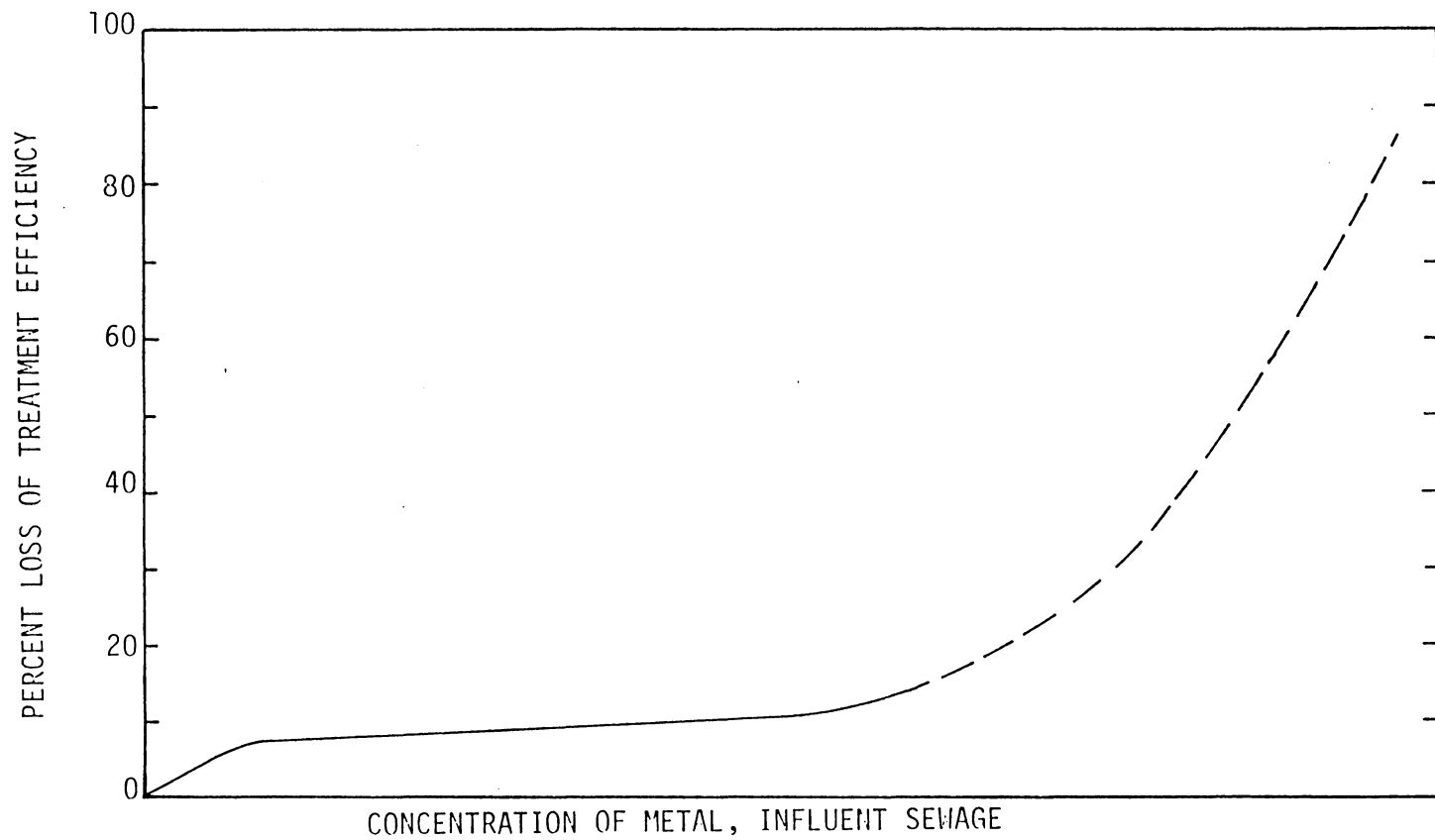


Figure 13. Response of Activated Sludge System to Metal Dosage.

received in an activated sludge process without having a detectable effect on organic removal efficiency was 1 mg/l. This threshold value decreased to 0.8 mg/l when turbidity was utilized as a control parameter.

McCarty (39) proposed Figure 14 to explain the general effects of salts or other materials on biological reactions. According to the results of his studies, low concentrations of salt can actually stimulate biological activity. As the salt dose is increased above an inhibitory concentration, however, the activity decreases to a point below normal activity, eventually dropping to zero. Sujarittanonta (34) conducted a laboratory, bench-scale investigation to determine the effects of nickel on the completely-mixed activated sludge process. Utilizing θ_c as the operational control parameter, he found that nickel concentrations of 1 mg/l and 5 mg/l, added continuously to a 400 mg/l COD process influent, did not significantly affect the COD removal efficiency of activated sludge at θ_c values greater than 5 days. These nickel doses, however, appeared to have stimulated heterotrophic bacterial growth as indicated by a greater Y_{max} value in the nickel-fed reactors than in the control reactor. This apparent stimulation was attributed to either a shift in the microbial species to a population of nickel-tolerant organisms that naturally maintained a higher yield coefficient, or to the fact that nickel, in itself, may have stimulated the growth of organisms in the reactor. The increased growth was accompanied by a higher maintenance energy requirement, k_d , indicating that the microorganisms were stressed by the nickel and were unable to efficiently stabilize organic matter. The 1 mg/l and 5 mg/l nickel doses inhibited the nitrification process as indicated by the lower effluent nitrate concentrations in the nickel-fed reactors as compared to the control reactor. By increasing the COD of the 1 mg/l nickel-fed reactor to 787 mg/l, Sujarittanonta observed that heterotrophic microbial growth was not stimulated but approached that of the control reactor. In

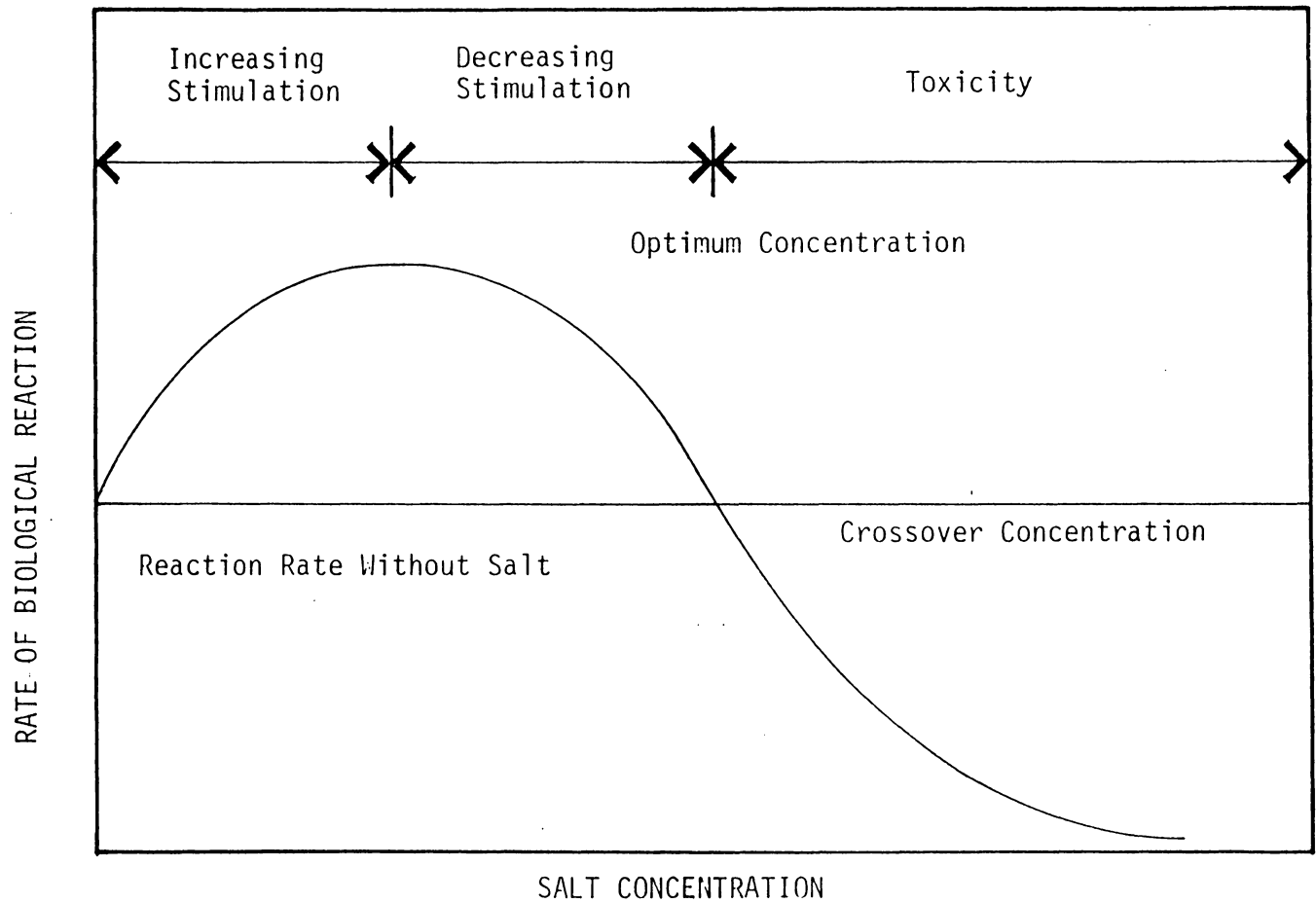


Figure 14. General Effects of Salts or Other Materials on Biological Reactions (40).

addition, the increased COD in the feed solution appeared to reduce any detrimental effects of nickel to the nitrification process.

Disalvo (40) conducted a bench-scale treatability study, similar to that of Sujarittanonta (34), to investigate the effects of an 0.5 mg/l nickel dose on the completely-mixed activated sludge process. His results also showed a stimulation of heterotrophic bacterial growth and an increased maintenance energy requirement by the presence of low nickel concentrations in the activated sludge process. Autotrophic activity was also stimulated in this study as evidenced by an increased rate of nitrification in the reactors. COD removal efficiency was marginally inhibited with the greatest inhibition occurring at low θ_c values.

Adams et al. (31) noted from their investigations of the effects of copper in aerobic treatment that metal toxicity is related to metal equilibrium conditions in solution, which depend upon metal concentration, MLSS concentration, and influent sewage strength. A decrease in metal dosage, an increase in MLSS, or an increase in sewage strength should decrease the proportion of active cellular components tied up as metal-ligand complexes and increase process performance.

Salotto et al. (41) operated three identical activated sludge pilot plants to investigate the effects of organic loading on the toxicity of copper in the activated sludge process. While an increase in organic loading of 2-3:1 did not significantly alter the toxicity of copper to the activated sludge, it did alter the distribution and form of the 5 mg/l copper concentration. The unit receiving a high organic loading was more efficient in removing copper and produced a higher ratio of soluble to total copper in the effluent.

Sujarittanonta (34) noted from his laboratory nickel toxicity studies that increasing COD:Ni ratios in an activated sludge influent are accompanied by increasing COD removal efficiencies. The high organic substrate enhances the

formation of nickel-organic and nickel-amine complexes, subsequently decreasing the toxicity of nickel. Coincident with the increased substrate is an increase in the MLSS of the reactor and a decrease in the proportion of active cellular components bound as nickel-organic complexes, allowing for more substrate utilization. The increased microorganism concentration produces additional extracellular polysaccharides for microbial aggregation which can form organic-nickel complexes and subsequently settle out in the clarifier. Thus, the nickel removal efficiency in the reactors is increased at high COD:Ni ratios. A high operating mean cell residence time, which also leads to larger MLSS concentrations in a biological reactor, was found to reduce metal toxicity to both the organic removal and the nitrification processes.

Disalvo (40) noted the effects of θ_c and the MLSS:Ni ratio on nickel toxicity to the completely mixed activated sludge process. Coincident with higher operating θ_c 's and larger MLSS:Ni ratios in the biological reactor were better COD and ammonia nitrogen removal efficiencies. Nickel removal efficiency was greatest at a θ_c between 9 and 12 days.

Kugelman and McCarty (42) conducted continuous flow daily feed studies to assess cation toxicity and stimulation to biological activity. Results showed that the toxic effects of heavy metals are magnified in units operated at low θ_c , where organisms are required to metabolize at a faster rate, than in units operated at longer θ_c . A decrease in θ_c , then, also reduces the upper limit of cation concentration in a biological process.

Heavy Metal Removal in the Activated Sludge Process

Various investigations have taken place to determine the feasibility of using the activated sludge process for heavy metal removal. Brown et al. (43) investigated six municipal sewage treatment plants, and found that secondary biological treatment has a definite advantage over primary treatment for heavy metals removal which can be attributed to the increased adsorption of heavy metals onto microbial flocs and the increased suspended solids removal in this process. Oliver and Cosgrove (44) conducted a study on heavy metals removal in activated sludge by examining the influent and effluent metal concentrations of a treatment plant over a four-week period. Results showed that metals are removed by activated sludge systems in two stages:

1. Primary settling of insoluble metals or metals adsorbed to particles.
2. Adsorption of dissolved metals or fine particulate metals to biological floc in aeration tanks with subsequent settling out of material in secondary clarifiers.

Pilot plant investigations by Barth et al. (37) showed that considerable portions of metal are removed in primary and secondary sludge. On a percent solids basis, the metals in secondary sludge are concentrated to a much greater extent than in primary sludge. For example, a continuous influent nickel concentration of 10 mg/l to one activated sludge system in the study resulted in nickel concentrations of 62 mg/l in the primary sludge and 89 mg/l in secondary sludge.

McDermott et al. (38) also studied nickel removal by activated sludge pilot plants. Results showed that primary treatment removed only 5 percent of the influent nickel, while secondary biological treatment achieved a 30 percent nickel

removal efficiency. Most nickel passed out with the effluent in a dissolved form. From similar pilot plant studies, McDermott et al. (38) noted a 50 to 79 percent copper removal efficiency in the activated sludge process when influent concentrations ranged from 0.4 to 25 mg/l. Soluble copper in the effluent ranged from 30 to 50 percent of total effluent copper.

Stones (44) studied the removal of nickel by a continuous-flow activated sludge system for influent nickel concentrations of 0.19 mg/l. Data indicated a 21.1 percent reduction of nickel by primary sedimentation, which was unaffected by biological activity, and a 30 percent reduction of nickel by secondary biological treatment.

Influence of Various Factors on the Removal of Heavy Metals in Biological Treatment

According to Brown and Lester [11], total heavy metal removal by the activated sludge process depends upon operating parameters, including sludge age, dissolved oxygen and suspended solids removal; physical/chemical factors, including temperature, pH, metal ion concentration, metal valency, concentration of complexing agent and particle size; and biological factors, including bacterial extracellular polymers. Their summary of previous research on heavy metal removal in activated sludge showed that a wide range of metal removal efficiencies has been obtained by varying the type of metal and operating conditions utilized in an experiment.

Nelson et al. (45) conducted batch reactor experiments to study the factors affecting the fate of heavy metals in the activated sludge process. Results indicated that the equilibrium distribution of metals between bacterial solids and

solution is mediated by physical/chemical factors and is not influenced greatly by active biological transport. The system pH was found to be the most important factor influencing chemical speciation and distribution between bacterial solids and solution. Adsorption of heavy metals was highest at a system pH of 4.0 to 7.5. The mean cell residence time of the system was also found to be an important parameter for control of heavy metal uptake. Metal affinity of bacterial solids increased with a one to five day increase in θ_c .

Neufeld and Herman (35) examined the technical feasibility of using the completely-mixed activated sludge process as a rational alternative for treatment of metal-laden wastewaters. Activated sludge that was acclimated to concentrations of mercury, cadmium and zinc up to 1000 mg/l was effective in removing heavy metals along with organic substrate. Batch, shock-loaded studies for these metals indicated that metal affinity and uptake was greatest for mercury than for cadmium and zinc, and that saturation of the floc surface by mercury did not permit much additional uptake of the other metals by the floc. The authors concluded that heavy metals removal is related to physical/chemical factors of the wastewater along with surface properties of the biological floc.

Oliver and Cosgrove (10) noted from their study of a conventional activated sludge treatment process that metal removal efficiency is related to the dissolved/insoluble metal ratio in raw sewage and that removal efficiency is greatest for lower ratios. Thus, industrial wastewaters containing the more insoluble metals, such as iron and lead, tend to be effectively treated for metal removal by the activated sludge process.

Cheng et al. (15) investigated heavy metals uptake by activated sludge in batch-type activated sludge systems. Results showed the total metal uptake by

sludge floc to increase as the concentration of volatile suspended solids, VSS, increased; however, the nickel uptake per unit weight of VSS decreased with increasing VSS. The total nickel uptake by activated sludge floc was found to be 10^{-5} M Ni/gram VSS for a 30 minute contact time. The uptake was not linear with time but showed a rapid initial uptake followed by a declining rate of uptake. The solution pH influenced the interactions between metal ions and organic functional groups with low pH waters exhibiting a lower uptake of nickel per gram of MLSS.

III. MATERIALS AND METHODS

This research was conducted to investigate the effects of nickel on the completely mixed activated sludge process. Two continuous flow bench scale reactors operated at COD:TKN ratios of 1:03:1 and 0.54:1, respectively, were each fed a synthetic wastewater containing a nickel concentration of 0.77 mg/l. A prior study conducted by a graduate student (34), which utilized similar experimental conditions and feed concentrations, with the exception of nickel, provided the control data. The mean cell residence time, θ_c , was the operational variable employed to compare data for all three systems. Performance indicators utilized to assess the effects of nickel on the activated sludge units included organic removal efficiency, degree of nitrification, and the biokinetic coefficients Y_{max} and k_d .

LABORATORY APPARATUS

A schematic diagram of the laboratory apparatus utilized in this study is depicted in Figure 15. Each reactor was made of 3/8 inch-Plexiglas and held a total volume of 8.5 liters. An adjustable baffle divided the reactor into a 6.0 liter aeration chamber and a 2.5 liter settling basin. A Calgon Co. chemical feed pump (Model TA-8) continually fed a synthetic wastewater from a calibrated 16-liter Nalgon carboy into the aeration chamber through Tygon tubing. A feed rate of approximately 14.5 liters per day was maintained in order to provide each reactor with a hydraulic detention time of 14.0 hours. Effluent was collected daily from each reactor in a 16-liter Nalgene carboy. All feed lines and carboys were disinfected daily with chlorine and rinsed with water to prevent microbial growth.

Air was supplied to each reactor through two porous diffuser stones by a Whisper 800 aquarium air pump (Willinger Brothers, Inc.). The diffuser stones were

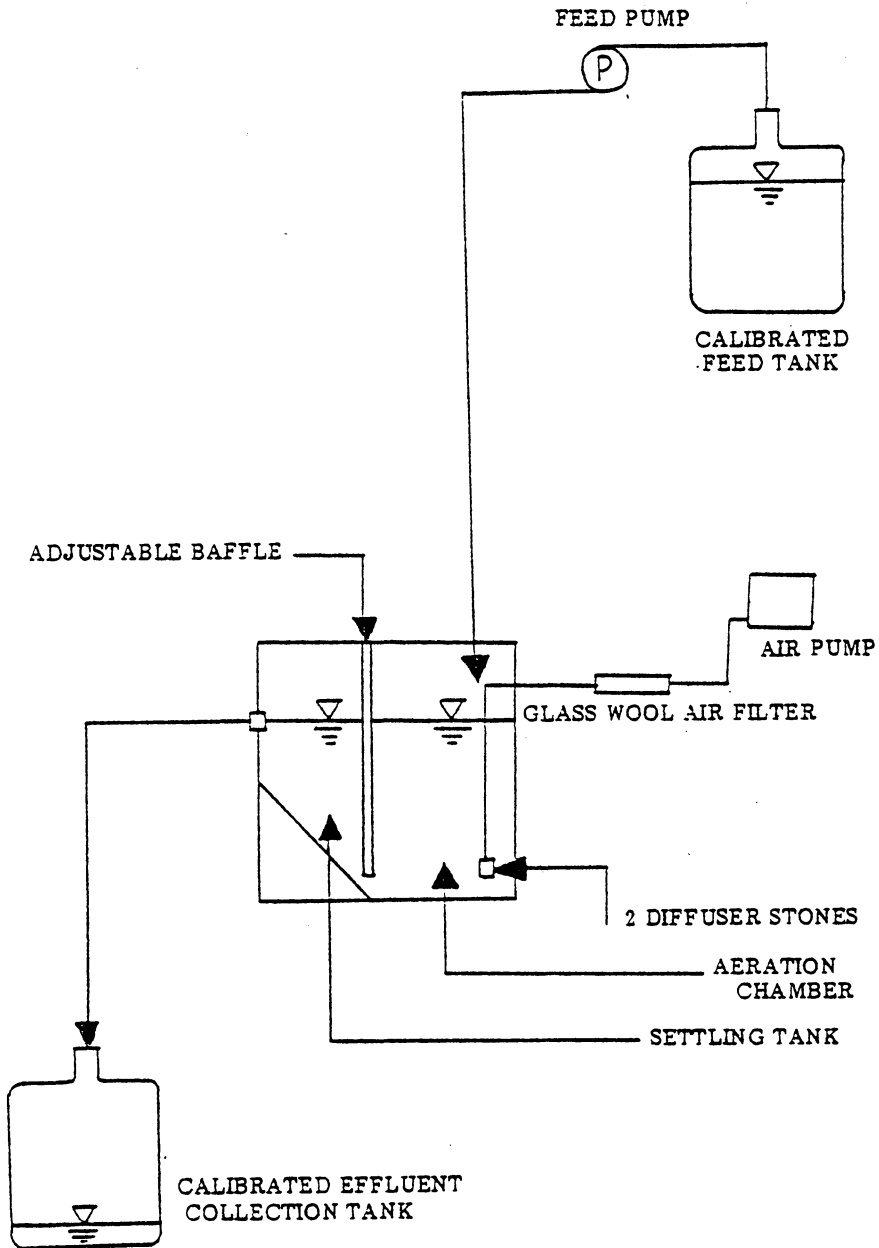


Figure 15. Experimental Activated Sludge Unit With Internal Cell Recycle.

positioned in the aeration chamber so as to provide adequate mixing and sludge recirculation. Glass wool filters were inserted inside the air lines to remove any impurities and to prevent contamination of the reactors.

FEED SOLUTION

A reproducible soluble organic solution containing essential inorganic nutrients for microorganisms served as the wastewater for this study. Table I lists the chemical composition of the feed solution for each reactor. As shown, Bacto-Peptone served as the carbon and energy source for the microorganisms while providing a nominal chemical oxygen demand, COD, of 400 mg/l and an approximate organic nitrogen concentration of 56 mg/l to each reactor. Supplemental nitrogen, in the form of an ammonium sulphate solution, was added to the feed solutions in order to obtain influent COD:TKN ratios of 1.03:1 and 0.54:1; respectively.

A nickel chloride solution served as the source for the 0.77 mg/l dose of nickel (II) to the reactors. A potassium phosphate solution was added to function both as a buffer against a pH change in the systems and as a source of nutrients to the microorganisms.

Each feed solution was prepared daily in the influent carboy by adding the correct chemical constituents from Table I with tap water to make a final volume of 16 liters. The contents of the carboys were thoroughly mixed before being connected to the feed lines.

TABLE I
COMPOSITION OF WASTEWATER FEED SOLUTION

Constituent	Stock Concentration per 2 liters (g)	Quantity Used Per 16 liters (ml)	Final Concentration (mg/l)
Bacto-Peptone (nutrient broth)	64.50*	87.50	352.73
MgSO ₄ · 7H ₂ O	20.00	80.00	50.00
MnSO ₄ · H ₂ O	2.00	80.00	5.00
FeCl ₃ · 6H ₂ O	0.25	80.00	0.63
CaCl ₂	1.50	80.00	3.75
(NH ₄) ₂ SO ₄	600.00	87.50** 175.00***	1640.63 3281.26
KH ₂ PO ₄ ****	104.50	107.00	349.40
K ₂ HPO ₄	214.00	107.00	715.56
NiCl ₂ · 6H ₂ O	8.10	12.00	0.75

- * Prepared in one liter stock solutions (Nominal COD of waste = 400 mg/l,
- ** COD:TKN = 1.03:1
- *** COD:TKN = 0.54:1
- **** Phosphate buffer solution.

SYSTEM START-UP

The initial seed for this study was obtained from an extended aeration activated sludge plant located in Blacksburg, Virginia. The microbial solids concentration of the seed was allowed to increase to a concentration of 2000 mg/l by operating the laboratory-scale units on a batch-flow basis. The units were then converted to a continuous-flow operation and the microorganisms were acclimated to the feed solution. Those unable to acclimate to the synthetic wastewater were lost in the effluent as suspended solids.

Once the effluent cleared, daily measurements of MLSS were taken and wasting from the aeration chamber was begun to obtain a desired mean cell residence time, θ_c . Constancy of MLSS and low effluent suspended solids concentrations were used as performance indicators of steady state conditions.

DAILY PROTOCOL

The laboratory activated sludge units in this study were operated for a period of 12 months. During this time, θ_c was utilized as the operational control parameter to assess system performance. Wasting from the reactors was accomplished daily in order to obtain a desired θ_c . This procedure included plugging the overflow port and removing the baffle from each reactor to allow complete mixing of both suspended and settled solids. A calculated quantity of MLSS was then siphoned from each reactor. After replacing the baffle and unplugging the overflow port, a new feed solution was connected to the feed lines. The influent flow rate was then checked and adjusted to maintain the desired hydraulic detention time in the reactors.

The waste activated sludge was thoroughly mixed by means of a magnetic stirrer and a 10 ml sample was withdrawn for an MLSS determination. Constancy of this value was used as an indicator for equilibrium, or steady-state conditions in a reactor.

SAMPLING PROCEDURE

Once steady-state conditions were reached in a reactor, the parameters listed in Table II were monitored for a seven-day period. Contents of both the influent and effluent carboys were thoroughly mixed prior to withdrawing samples. Alkalinity and pH determinations were performed immediately on a 50-ml sample of the influent and a 50-800 ml sample of the unfiltered effluent. An additional 100 ml of the unfiltered effluent was withdrawn for a suspended solids determination.

Approximately 300 ml each of the influent and the effluent were obtained and preserved for the remainder of the tests listed in Table III. The portions to be analyzed for nickel were acidified with HNO_3 to a pH of 2.0, while the portions to be analyzed for COD and nitrogen were acidified, also to a pH 2.0, with H_2SO_4 . All samples were collected in Nalgene containers and stored at 4°C for later analysis. The effluent samples were filtered through a 0.45 micron glass-fiber filter prior to storage.

TABLE II
PARAMETERS MONITORED DAILY DURING
STEADY STATE PERIODS

INFLUENT FEED

Chemical Oxygen Demand
Ammonia-Nitrogen Concentration
Total Kjeldahl Nitrogen Concentration
Nitrate-Nitrogen Concentration
Nickel Concentration
pH
Alkalinity as CaCO_3

FILTERED EFFLUENT

Chemical Oxygen Demand
Ammonia-Nitrogen Concentration
Total Kjeldahl Nitrogen Concentration
Nitrate-Nitrogen Concentration
Nickel Concentration

UNFILTERED EFFLUENT

Suspended Solids Concentration
Nickel Concentration
pH
Alkalinity as CaCO_3

BIOLOGICAL REACTORS

Mixed-Liquor Suspended-Solids Concentration

ANALYTICAL TECHNIQUES

The laboratory analyses of the parameters listed in Table II were performed on the samples as follows:

Chemical Oxygen Demand. A soluble COD determination was performed on the influent and filtered effluent samples according to the dichromate reflux method as outlined in Standard Methods (46).

Ammonia-Nitrogen. An ammonia nitrogen determination was performed on the influent and filtered effluent samples by distillation and acidimetric titration as described in Standard Methods (46).

Total Kjeldahl Nitrogen. The influent and filtered effluent samples were digested in accordance with Standard Methods (46). The acidimetric titration technique was used to determine the total Kjeldahl nitrogen concentration in the samples.

Nitrate-Nitrogen. Nitrate-nitrogen analyses were performed on the influent and filtered effluent samples according to the Brucine technique as outlined in Standard Methods (46). Nitrate concentrations were determined by using a Bausch and Lomb atomic adsorption spectrophotometer (Model 703).

Nickel. Nickel concentrations were determined in the influent, unfiltered effluent and filtered effluent samples using an Atomic Adsorption Spectrophotometer (Model 403, Perkin-Elmer).

Solids. Mixed liquor suspended solids and effluent solids concentrations were determined according to Standard Methods [46]. The reactor and unfiltered

effluent samples were filtered through 5.5 cm membrane filters (0.45 μ pore size, Millipore Filter Corporation). Dry weight determinations were performed on a Mettler AC 100 digital balance.

pH. Influent and effluent pH measurements were conducted on a Fisher pH meter (Model 120), outlined in Standard Methods (46).

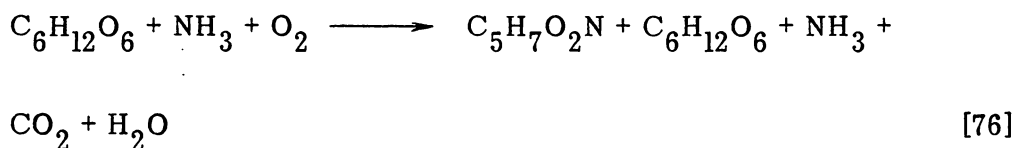
Alkalinity. Influent and effluent alkalinity measurements were performed according to Standard Methods (46). A calibrated Fisher pH meter (model 120) was used to indicated the endpoint of titration at a pH of 4.5.

DATA ANALYSIS

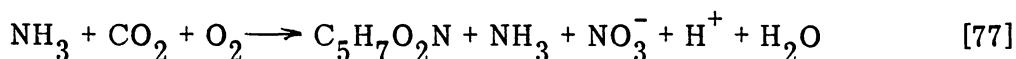
The data from this study have been analyzed utilizing a mathematical procedure based upon the microbial kinetic theory, as introduced by Lawrence and McCarty (18), and the stoichiometric relationships, as presented by Sherrard and Schroeder (19). Each of these microbiological principles has been discussed, in detail, in previous sections of this paper.

The overall equations that describe the carbon-oxidation and nitrification processes, respectively, are as follows:

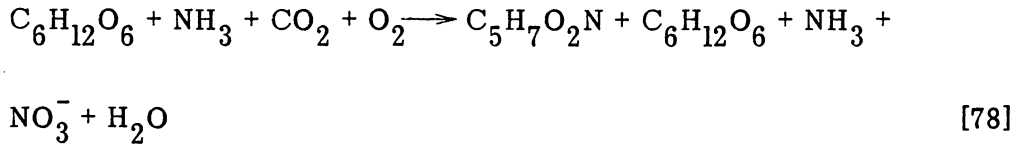
COD Removal



Nitrification



For combined organic removal and nitrification systems, as utilized in this research, the overall stoichiometric equation can be described as:



The microbial growth kinetic equations that describe the heterotrophic and autotrophic microbial systems are:

$$\frac{1}{\theta_c} = Y_{\max_1} U_1 - k_{d_1} \quad [79]$$

$$\frac{1}{\theta_c} = Y_{\max_2} U_2 - k_{d_2} \quad [80]$$

where, $\frac{1}{\theta_c}$ = specific growth rate, days⁻¹,

Y_{\max_1} = maximum growth yield coefficient for heterotrophs, mass of microorganisms/mass of organic substrate utilized,

U_1 = specific utilization rate of heterotrophs, time⁻¹,

k_{d_1} = microbial decay coefficient of heterotrophs, time⁻¹,

Y_{\max_2} = maximum growth yield for autotrophs, mass of nitrogen utilized,

U_2 = specific utilization rate of autotrophs, time⁻¹,

k_{d_1} = microbial decay coefficient of heterotrophs, time⁻¹, and,

k_{d_2} = microbial decay coefficient of autotrophs, time⁻¹.

Mean cell residence time was determined as follows:

$$\theta_c = \frac{VX}{Q_w(X) + (Q - Q_w)X_e} \quad [81]$$

where, θ_c = mean cell residence time or sludge age, days,

V = volume of reactor, volume,

X = biomass concentration in the total reactor, or mixed liquor suspended solids (MLSS), mass/volume,

Q_w = rate of sludge wasting, volume/time,

Q = rate of raw wastewater entering the aeration tank, volume/time,
and

X_e = effluent suspended solids concentration, mg/l.

The specific utilization rates for the heterotrophs, U_1 , and the autotrophs, U_2 , were determined from the following definitions:

$$U_1 = \frac{(S_1^o - S_1)}{\theta X_1} \quad [82]$$

$$U_2 = \frac{(S_2^o - S_2)}{\theta X_2} \quad [83]$$

where, S_1^o = influent COD to the reactor, mg/l

S_1 = steady-state concentration of COD in the reactor, mg/l,

X_1 = heterotrophic microorganism concentration in the reactor, mg/l,

S_2^0 = influent nitrogen concentration available for nitrification, mg/l,

S_2 = steady-state ammonia concentration in the reactor, mg/l, and

X_2 = autotrophic microorganism concentration in the reactor, mg/l.

Because ammonia stripping may occur in a reactor and the combined organic removal-nitrification system does not allow for an accurate prediction of the influent ammonia nitrogen that is available for nitrification, the following relationship will be substituted for equation (83):

$$U_2 = \frac{S_0}{\theta X_2} \quad [84]$$

where, S_0 equals the steady-state nitrate concentration in the reactor, mg/l.

In an activated sludge system which combines organic removal with nitrification, the mixed liquor suspended solids, X , includes both heterotrophic and autotrophic microorganisms. Consequently, an exact evaluation of the microbial growth kinetics for COD removal and nitrogen removal, separately, is difficult to obtain.

In general, however, the nitrifying microorganisms comprise only a small fraction of the total biomass as compared to the heterotrophic microorganisms and the autotrophic microbial yield and decay have an insignificant effect on the total microbial yield and decay. For purposes of this research, a method has been developed to estimate the fraction of autotrophic microorganisms at each θ_c from the amount of nitrate-nitrogen in the process effluent. This method employs the biokinetic equations for microbial growth and is based on the following assumptions:

1. The effluent nitrate concentration equals the concentration of ammonia oxidized. It was assumed that nitrite concentrations were negligible as compared to nitrate concentrations.
2. The yield coefficient of the autotrophic microorganisms per mg/l $\text{NH}_3\text{-N}$ oxidized and the microbial decay coefficient equals 0.04 days^{-1} .

By subtracting the estimated fraction of autotrophs from the measurement of the total biomass in the reactor, X_t , the heterotrophic MLSS can be obtained. In turn, the specific utilization rate for the heterotrophs can be calculated from equation [82]. A plot of the specific growth rate versus the specific utilization rate yields a line from which the slope, Y_{max} , and Y-intercept, k_{d2} , for the heterotrophs can be obtained. Utilizing these biokinetic coefficients, the observed yield, Y_{obs} , can then be calculated at each θ_c according to:

$$Y_{\text{obs}} = \frac{Y_{\text{max}}}{1 + \theta_c k_d} \quad [85]$$

See Appendix E for detailed calculations of the biokinetic coefficients for this research and prior experiments which investigated the effects of various nickel concentrations on the activated sludge process. The microbial yield and decay coefficients reported in the results section of this paper pertain only to the heterotrophs.

In order to investigate the fate of nitrogen in the activated sludge process pertaining to this study, a mass balance was performed on all nitrogen compounds in each system. The sum of the influent ammonia-nitrogen and organic nitrogen concentrations should equal the sum of the effluent ammonia-nitrogen, organic-nitrogen and nitrate-nitrogen concentrations less the nitrogen utilized by waste

sludge and effluent microbial suspended solids. The percent nitrogen unaccounted for is assumed to be in the supernatant of the waste sludge and the effluent.

The percentage of influent nitrogen leaving the activated sludge system can be calculated for each nitrogen species as follows:

$$\%NH_3-N = \frac{100[Q_w(NH_3 - N_f) + (Q_e NH_3 - N_f)]}{Q_o TKN_o} \quad [86]$$

where, $\%NH_3-N$ = percentage of influent nitrogen leaving system as ammonia nitrogen,

NH_3-N_f = ammonia nitrogen concentration of filtered effluent, mg/l, and

TKN_o = total Kjeldahl nitrogen concentration of influent, mg/l.

$$\%Org-N = \frac{100[Q_w(\%N_x)(X) + Q_o(Org-N_f) + Q_e(\%X)(X_e)]}{Q_o TKN_o} \quad [87]$$

where, $\%Org-N$ = percentage of influent nitrogen leaving system as ammonia nitrogen,

$\%N_x$ = percent nitrogen in microbial solids, and

$Org-N_f$ = organic nitrogen concentration of filtered effluent, mg/l.

$$\%NO_3-N = \frac{100[Q_o(NO_3-N_f)]}{Q_o TKN_o} \quad [88]$$

where, $\%NO_3-N$ = percentage of influent nitrogen leaving system as nitrate nitrogen, and

$\text{NO}_3\text{-N}_f$ = nitrate nitrogen concentration of filtered effluent, mg/l.

The soluble COD removal efficiency of each reactor was calculated as follows:

$$E_s = \frac{100(S_o - S_e)}{S_o} \quad [89]$$

where, E_s = soluble COD removal efficiency, percent,

S_o = influent soluble COD, mg/l, and

S_e = effluent soluble COD, mg/l.

The nickel removal efficiency of each reactor was determined from the following expression:

$$E_{\text{Ni(II)}} = \frac{100[\text{Ni(II)}_o - \text{Ni(II)}_f]}{\text{Ni(II)}_o} \quad [90]$$

where, $E_{\text{Ni(II)}}$ = nickel removal efficiency, percent,

Ni(II)_f = nickel concentration in the filtered effluent, mg/l, and

Ni(II)_o = nickel concentration in the influent, mg/l.

IV. RESULTS AND DISCUSSION

The effects of nickel on the completely mixed activated sludge system were determined by conducting a continuous flow laboratory study. The mean cell residence time, θ_c , was utilized as the operational control parameter to assess system performance. Steady-state data taken from the reactor was analyzed to determine the influence of nickel, in relation to low COD:TKN ratios, and high influent ammonia concentrations, on organic removal efficiency, the degree of nitrification and the biokinetic coefficients, Y_{\max} and k_d .

Two bench-scale reactors were operated at COD:TKN ratios of 1.03:1 and 0.54:1, respectively, by varying the nitrogen concentrations in the feed solutions. Each unit received an initial COD of 400 mg/l and were dosed continuously with nickel concentrations of 0.77 mg/l.

The control data for this study were obtained from a study conducted by another student (34) which utilized similar experimental conditions. The control reactor was fed a soluble COD of approximately 400 mg/l but was not dosed with heavy metals. This reactor provided baseline data which could be used to evaluate system performance of the nickel-laden reactors.

Each activated sludge unit was operated for a period of approximately eight months during which data from four, steady-state periods were obtained. Raw data from the control and nickel-fed reactors are shown in Appendix C. A summary of the results from each study is presented in the following sections.

RESULTS

Control

The control reactor was operated at mean cell residence times of 5.8, 11.5, 12.3, and 16.4 days to obtain baseline data. The results are shown in Table III. The soluble COD of the feed solution averaged 396 mg/l and the total nitrogen concentration averaged 106.1 mg/l for the steady-state periods studied. The effluent soluble COD concentration, ranging from 19 to 28 mg/l, was nearly constant for all operating θ_c . The soluble COD removal efficiency was found to be independent of θ_c and the microorganism concentration and exceeded 92 percent for all four runs. Total reactor microorganism concentrations of 1156, 1920, 2120, and 2681 mg/l were obtained in the control reactor at mean cell residence times of 5.8, 11.5, 12.3, and 16.4 days, respectively.

Nitrification proceeded at all mean cell residence times and was found to increase with increasing θ_c . The maximum degree of nitrification for this study, based upon the effluent nitrate data, was observed at a θ_c of 16.4 days, with 42.2 mg/l $\text{NO}_3\text{-N}$, while the minimum degree of nitrification occurred at a θ_c of 5.8 days, with 8.8 mg/l NO_3N . A mean cell residence time of approximately three days is considered the minimum operating sludge age for nitrification. Corresponding to the nitrate production, the total Kjeldahl nitrogen concentration decreased 23.9 percent at a θ_c of 5.8 days and 51.4 percent at a θ_c of 16.4 days. Ammonia nitrogen production was observed at the 5.8 day θ_c due to the mineralization of organic nitrogen and a minimal degree of nitrification, while an ammonia nitrogen removal of 14.4 percent was noted at θ_c equal to or greater than 16.4 days. Soluble organic nitrogen was independent of θ_c , averaging 93.9 percent for the four steady-state runs.

TABLE III

SUMMARY OF STEADY STATE DATA

CONTROL, COD:TKN = 3.71:1 (2)

PARAMETER	θ_c , days			
	5.8	11.5	12.3	16.4
<u>COD</u>				
Feed (mg/l)	386	405	390	396
Effluent, filtered (mg/l)	19	23	28	27
Removal Efficiency (%)	95.2	94.3	92.9	93.2
<u>Biological Solids</u>				
Reactor (mg/l)	1156	1920	2120	2681
Effluent (mg/l)	15	5	30	4
<u>pH</u>				
Feed	7.2	7.2	7.1	7.2
Effluent	7.5	6.6	6.8	6.6
<u>Alkalinity as CaCO₃</u>				
Feed (mg/l)	248	259	228	263
Effluent (mg/l)	297	106	165	102
Removal Efficiency (%)	+19.8	-59.1	-27.6	-61.2
<u>NH₃-N</u>				
Feed (mg/l)	59.2	54.7	51.0	57.7
Effluent, filtered (mg/l)	78.3	48.7	51.2	49.4
Net Change (%)	+32.3	-11.0	0.4	-14.4
<u>Org-N</u>				
Feed (mg/l)	48.7	52.5	51.1	49.6
Effluent, filtered (mg/l)	3.8	2.5	3.0	2.8
Net Change (%)	-92.2	-95.2	-94.1	-94.4
<u>TKN</u>				
Feed (mg/l)	107.9	107.2	102.1	107.3
Effluent, filtered (mg/l)	82.1	51.2	54.2	52.2
Net Change (%)	-23.9	-52.2	-46.9	-51.4
<u>NO₃-N</u>				
Feed (mg/l)	0.5	0.5	0.5	0.5
Effluent, filtered (mg/l)	8.8	41.5	30.3	42.2
<u>COD:TKN</u>	3.58:1	3.78:1	3.82:1	3.69:1

Table III
 Summary of Steady State Data
 Control, COD:TKN = 3.71:1 (2) (continued)
 Page 2 of 2

<u>PARAMETER</u>	θ_c , days			
	5.8	11.5	12.3	16.4
<u>Specific Growth Rate</u> (days ⁻¹)	0.173	0.087	0.082	0.061
<u>Specific Utilization Rate</u> (days ⁻¹)	0.553	0.363	0.306	0.250
<u>Observed Yield Coefficient</u>	0.308	0.263	0.258	0.234
<u>Maximum Yield Coefficient</u>	0.372	0.372	0.372	0.372
<u>Microbial Decay Coefficient</u> (days ⁻¹)	0.036	0.036	0.036	0.036
Q_o (l/day)	14.54	14.54	14.54	14.54
Q_w (l/day)	1.30	0.70	0.50	0.50
θ (days)	0.58	0.59	0.58	0.58

Alkalinity destruction, ranging from 27.6 percent to 61.2 percent, was observed at all operating θ_c except for a θ_c of 5.8 days where a 19.8 percent production occurred. Effluent pH values paralleled the changes in alkalinity. A mean cell residence time of 5.8 days showed an increase in pH from 7.2 to 7.5, while θ_c of 11.5, 12.3, and 16.4 days showed a decrease in pH to 6.6, 6.8, and 6.6, respectively.

Both the observed yield and the specific utilization rate for the control reactor decreased with increasing θ_c . A maximum microbial yield coefficient, Y_{\max} , equal to 0.372, and a microbial maintenance energy coefficient, k_d , equal to 0.036 days⁻¹, were calculated from the steady-state data.

COD:TKN = 1.03:1, COD = 400 mg/l, Ni(II) = 0.77 mg/l

A continuous-flow reactor receiving an average influent COD of 408 mg/l, an average total nitrogen concentration of 394.8 mg/l, and an average nickel concentration of 0.77 mg/l was operated at mean cell residence times of 3.0, 6.5, 13.6, and 20.0 days. A summary of steady-state data for the four runs is shown in Table IV. The soluble COD of the filtered effluent ranged from 16 to 29 mg/l for the operating θ_c . The soluble COD removal efficiency appeared to be independent of sludge age and was greater than 92 percent for all runs. Total reactor microorganism concentrations of 786, 1436, 2214, and 2731 mg/l were obtained in the reactor at θ_c of 3.0, 6.5, 13.6, and 20.0 days, respectively.

Nitrification proceeded in the reactor at all mean cell residence times studied as evidenced by effluent nitrate concentrations of 5.6, 67.1, 72.4, and 71.6 mg/l. Nitrification increased with θ_c and the highest degree was obtained at a θ_c between 13.6 and 20.0 days. Coincident with the nitrate production in the

TABLE IV

SUMMARY OF STEADY STATE DATA

COD:TKN = 1.03:1, Ni = 0.77 mg/l

PARAMETER	θ_c , days			
	3.0	6.5	13.6	20.0
<u>COD</u>				
Feed (mg/l)	405	403	404	419
Effluent, filtered (mg/l)	27	28	29	16
Removal Efficiency (%)	93.3	93.1	92.8	96.2
<u>Biological Solids</u>				
Reactor (mg/l)	786	1436	2214	2731
Effluent (mg/l)	39	34	11	15
<u>pH</u>				
Feed	7.0	7.0	7.0	7.0
Effluent	7.3	5.6	5.3	5.4
<u>Alkalinity as CaCO₃</u>				
Feed (mg/l)	452	461	448	439
Effluent (mg/l)	534	39	19	23
Net Change (%)	+18.2	-91.6	-95.7	-94.8
<u>Ni(II)</u>				
Feed (mg/l)	0.75	0.77	0.77	0.77
Effluent, filtered (mg/l)	0.65	0.66	0.73	0.73
Effluent, total (mg/l)	0.68	0.68	0.77	0.74
Removal Efficiency (%)	13.3	14.3	5.2	5.2
<u>NH₃-N</u>				
Feed (mg/l)	323.9	336.5	343.1	351.2
Effluent, filtered (mg/l)	338.9	264.2	287.7	294.4
Removal Efficiency (%)	+4.6	-21.5	-16.1	-16.2
<u>Org-N</u>				
Feed (mg/l)	58.8	57.2	56.0	54.0
Effluent, filtered (mg/l)	4.2	4.5	5.2	2.2
Net Change (%)	-92.9	-92.1	-90.8	-96.0
<u>TKN</u>				
Feed (mg/l)	382.7	393.7	397.9	405.2
Effluent, filtered (mg/l)	342.7	268.7	292.8	296.5
Net Change (%)	-10.4	-31.7	-22.9	-26.8

Table IV
 Summary of Steady State Data
 COD:TKN = 1.03:1, Ni = 0.77 mg/l (continued)
 Page 2 of 2

<u>PARAMETER</u>	θ_c , days			
	3.0	6.5	13.6	20.0
<u>NO₃-N</u>				
Feed (mg/l)	0.4	0.3	0.4	0.6
Effluent, filtered (mg/l)	5.6	67.1	72.4	71.6
<u>COD:TKN</u>	1.06:1	1.02:1	1.02:1	1.03:1
<u>Specific Growth Rate</u> (days ⁻¹)	0.333	0.154	0.074	0.050
<u>Specific Utilization Rate</u> (days ⁻¹)	0.793	0.473	0.337	0.267
<u>Observed Yield Coefficient</u>	0.418	0.327	0.227	0.178
<u>Maximum Yield Coefficient</u>	0.549	0.549	0.549	0.549
<u>Microbial Maintenance Energy</u> (days ⁻¹) <u>Coefficient</u>	0.104	0.104	0.104	0.104
Q _o (l/day)	13.94	14.18	15.24	14.01
Q _w (l/day)	2.25	1.00	0.55	0.35
θ (days)	0.61	0.60	0.56	0.61

reactor were total Kjeldahl nitrogen removal efficiencies of 10.4, 31.7, 22.9, and 26.8 percent for θ_c of 3.0, 6.5, 13.6, and 20.0 days, respectively. An ammonia nitrogen production of 4.6 percent was observed at a 3-day θ_c while a 16.2 to 21.5 percent ammonia nitrogen destruction occurred at all other θ_c . The mineralization of organic nitrogen was found to be greatest at a 20-day θ_c , 96.0 percent, and to average 92.0 percent for sludge ages between 3.0 and 13.6 days.

Alkalinity destruction, ranging from 91.6 to 95.7 percent, was observed in the reactors operated at θ_c of 6.5, 13.6, and 20.0 days. An 18.2 percent production in alkalinity was noted at a θ_c of 3.0 days due to the minimal degree of nitrification at this low sludge age. The change in system pH for each steady-state period corresponded to the observed change in alkalinity. An increase in pH to a value of 7.3 was noted in the reactor at a three day sludge age, while a decrease in pH was observed at all other operating θ_c .

Nickel removal efficiency was found to be dependent upon the operating mean cell residence time with removals of 13.3 and 14.3 percent at θ_c of 3.0 and 6.5, respectively, as compared to a removal of 5.2 percent for the 13.6 and 20.0 day θ_c . Most of the effluent nickel was in the soluble form.

Both the observed yield and the specific utilization rate for the system decreased with increasing mean cell residence times. A Y_{\max} equal to 0.549 and a k_d equal to 0.104 days⁻¹ were calculated from the steady-state data.

COD:TKN = 0.54:1, COD = 400 mg/l, Ni(II) = 0.77 mg/l

Four steady state runs were conducted at mean cell residence times of 3.0, 6.1, 14.0, and 17.8 days for the reactor operated at a COD:TKN of 0.54:1. A summary of the steady-state data is shown in Table V. The feed solution contained an average COD of 403 mg/l, an average total nitrogen concentration of

TABLE V

SUMMARY OF STEADY STATE DATA

COD:TKN = 0.54:1, Ni = 0.77 mg/l

<u>PARAMETER</u>	θ_c , days			
	3.0	6.1	14.0	17.8
<u>COD</u>				
Feed (mg/l)	403	391	426	392
Effluent, filtered (mg/l)	31	27	28	31
Removal Efficiency (%)	92.3	93.1	93.4	92.1
<u>Biological Solids</u>				
Reactor (mg/l)	776	1400	2451	2477
Effluent (mg/l)	42	45	11	24
<u>pH</u>				
Feed	7.0	7.0	7.0	7.0
Effluent	7.2	5.8	5.2	4.9
<u>Alkalinity as CaCO₃</u>				
Feed (mg/l)	446	452	452	447
Effluent (mg/l)	499	68	18	8
Net Change (%)	+11.9	-85.0	-96.0	-98.2
<u>Ni(II)</u>				
Feed (mg/l)	0.79	0.76	0.73	0.79
Effluent, filtered (mg/l)	0.70	0.68	0.72	0.75
Effluent, total (mg/l)	0.76	0.70	0.73	0.79
Removal Efficiency (%)	11.4	10.5		
<u>NH₃-N</u>				
Feed (mg/l)	673.7	690.5	684.3	687.2
Effluent, filtered (mg/l)	669.0	622.3	606.3	589.8
Removal Efficiency (%)	-0.7	-9.9	-11.4	-14.2
<u>Org-N</u>				
Feed (mg/l)	57.3	55.7	55.4	56.5
Effluent, filtered (mg/l)	7.7	11.9	5.1	2.6
Net Change (%)	-86.6	-78.6	-90.8	-95.4
<u>TKN</u>				
Feed (mg/l)	731.0	746.2	739.8	743.7
Effluent, filtered (mg/l)	676.7	634.3	611.5	592.4
Net Change (%)	-7.4	-15.0	-17.3	-20.3

Table V
 Summary of Steady State Data
 COD:TKN = 0.54:1, Ni = 0.77 mg/l (continued)
 Page 2 of 2

<u>PARAMETER</u>	θ_c , days			
	3.0	6.1	14.0	17.8
<u>NO₃-N</u>				
Feed (mg/l)	0.5	0.6	0.4	0.4
Effluent, filtered (mg/l)	9.9	81.7	70.8	69.2
<u>COD:TKN</u>	0.55:1	0.52:1	0.57:1	0.53:1
<u>Specific Growth Rate</u> (days ⁻¹)	0.333	0.164	0.071	0.056
<u>Specific Utilization Rate</u> (days ⁻¹)	0.782	0.454	0.295	0.259
<u>Observed Yield Coefficient</u>	0.427	0.354	0.247	0.215
<u>Y_{max}</u>	0.533	0.533	0.533	0.533
<u>k_d</u> (days ⁻¹)	0.083	0.083	0.083	0.083
<u>Q_o</u> (l/day)	13.68	13.42	14.14	13.67
<u>Q_w</u> (l/day)	2.25	1.00	0.55	0.35
<u>θ</u> (days)	0.62	0.63	0.60	0.62

740.2 mg/l, and an average nickel concentration of 0.77 mg/l. The effluent soluble COD remained nearly constant for all operating θ_c , ranging from 27 to 31 mg/l. Soluble COD removal efficiency appeared to be independent of sludge age and averaged 92.7 percent for all steady state periods. Total reactor microorganism concentrations of 776, 1400, 2451, and 2577 mg/l were obtained in the reactor for θ_c of 3.0, 6.1, 14.0, and 17.8 days, respectively.

Nitrification proceeded at all operating θ_c as indicated by effluent nitrate concentrations ranging from 9.9 to 81.2 mg/l. The maximum and minimum degrees of nitrification were observed at θ_c of 6.1 and 3.0 days, respectively. The net removal of total Kjeldahl nitrogen was found to be dependent upon the microbial sludge age. The removal efficiency of TKN ranged from 7.4 to 20.3 percent as θ_c , increased from 3.0 to 17.8 days. Paralleling the change in TKN, the ammonia nitrogen removal efficiency increased from 0.7 to 14.2 percent as θ_c increased. A high degree of organic nitrogen mineralization was observed at all operating θ_c with the largest conversion occurring at a θ_c of 17.8 days.

Alkalinity destructions of 85.0, 96.0, and 98.2 percent were noted for sludge ages of 6.1, 14.0, and 17.8 days, respectively. Net alkalinity production, however, occurred at a θ_c of 3.0 days, corresponding to the lack of nitrification at this mean cell residence time. An increase in system pH from 7.0 to 7.2 was noted in the reactor at a 3.0 day θ_c , while a decrease in pH to values of 5.8, 5.2, and 4.9 was noted at all other operating θ_c .

Nickel removal efficiencies ranged from 11.4 to 0 percent with the largest removal being obtained at the lowest sludge age. Most of the effluent nickel was present in the soluble form. Both the observed yield and the specific utilization rate decreased with increasing mean cell residence times. A Y_{max} equal to 0.533 and a k_d equal to 0.083 days⁻¹ were observed in this study.

DISCUSSION

Graphical interpretations of the data tabulated previously are presented and discussed in this section. These graphs allow an easy comparison between the performance indicators of the control and nickel-fed reactors, including COD removal efficiency, nitrification, and the biokinetic coefficients, Y_{\max} and k_d . Where applicable, these parameters are, in turn, related to the low operating COD:TKN ratios in the nickel-fed reactors.

COD Removal

The effect of nickel on the soluble COD removal efficiency at different mean cell residence times is shown in Figure 16. As shown, the soluble COD removal efficiencies of the the control and the reactor receiving nickel were nearly identical and were in the range of 92 to 96 percent, indicating that the nickel dose of 0.77 mg/l did not greatly inhibit the organic removal capacity of the herero-trophic microorganisms. Previous studies on the effects of heavy metals in biological treatment have demonstrated similar results. McDermott et al. (3) found that nickel doses between 1 and 2.5 mg/l had essentially no effect on organic substrate removal in the activated sludge process. Barth et al. (37) found that activated sludge units can tolerate metal doses up to 10 mg/l with only a 5 percent reduction in COD removal efficiency.

Total Reactor Microorganisms Concentration

Figure 17 depicts the heterotrophic mixed liquor suspended solids concentration as a function of mean cell residence time for the control reactor and for the reactors receiving nickel. All three reactors were fed a soluble COD of

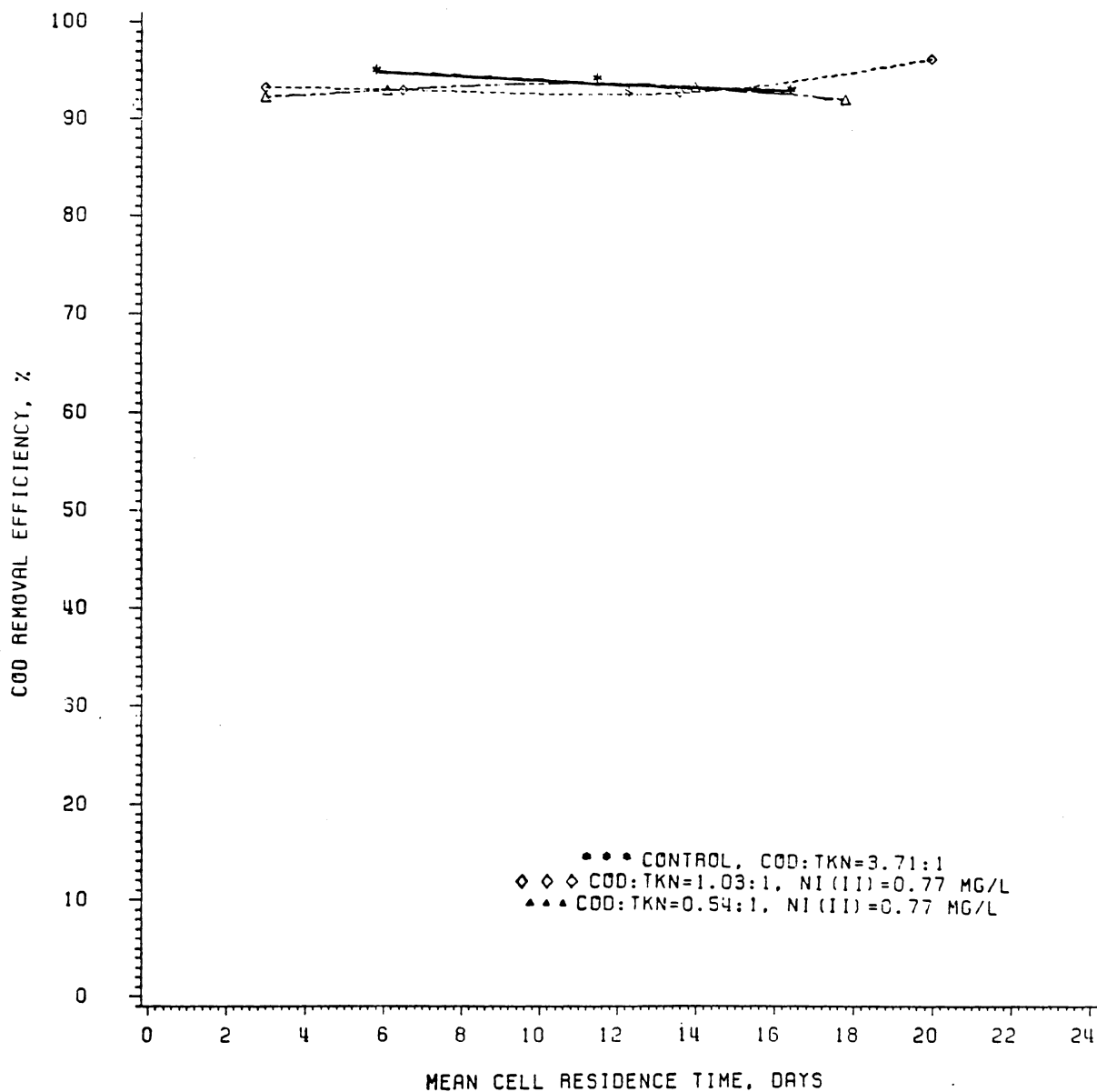


FIGURE 16. EFFECT OF NICKEL ON COD REMOVAL EFFICIENCY AT DIFFERENT MEAN CELL RESIDENCE TIMES

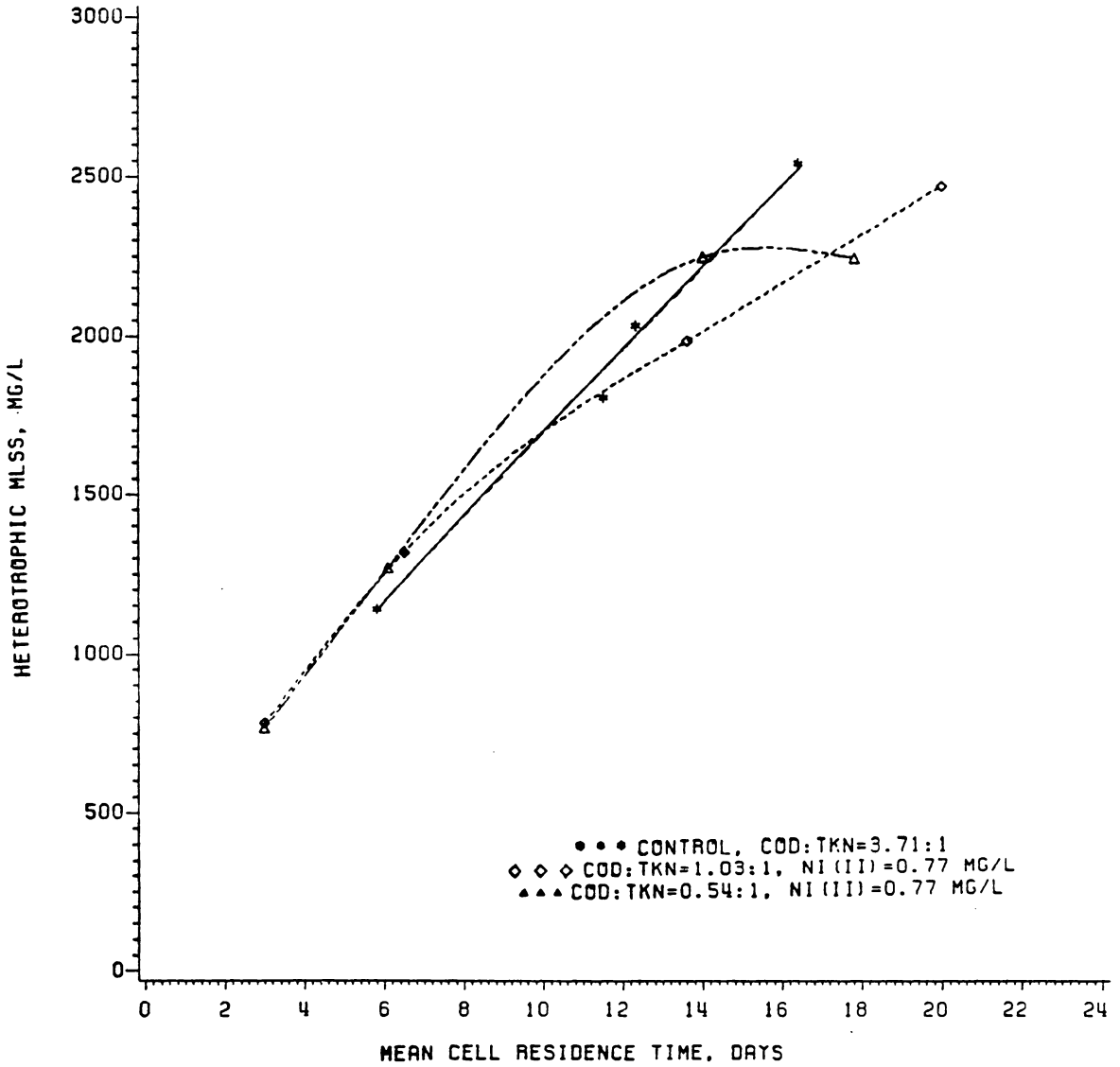


FIGURE 17. EFFECT OF NICKEL ON HETEROTROPHIC MIXED LIQUOR SUSPENDED SOLIDS AT DIFFERENT MEAN CELL RESIDENCE TIMES

approximately 400 mg/l. As shown, both of the nickel-dosed reactors maintained a larger MLSS than the control reactor for mean cell residence times up to approximately 13 days. This indicates an apparent stimulation of heterotrophic microbial growth in the presence of nickel. For mean cell residence times greater than 13 days, however, the MLSS curves for the nickel-fed reactors tend to reach a limiting plateau while the MLSS curve for the control reactor surpasses these with a steadily increasing microorganism concentration. This indicates that while the low concentration of nickel stimulated heterotrophic growth in the activated sludge process, it also stressed the microorganisms. At larger mean cell residence times, the stressed microorganisms required more energy for cell maintenance, leaving less substrate available for cellular synthesis. Sujarittanonta [34] and Disalvo (40) found similar results from their metal toxicity studies using nickel concentrations of 1 and 0.5 mg/l, respectively.

Specific Utilization Rate

The effects of nickel on the specific utilization rate of the heterotrophic microorganisms as a function of θ_c is shown in Figure 18. Values for the specific utilization rate were obtained from the following relationship:

$$U = \frac{S_o - S_e}{\theta_c} \quad [91]$$

where, U is the specific utilization rate, S_o and S_e are the influent and effluent COD concentrations, respectively, θ is the hydraulic detention time in the reactor and X is the heterotrophic mixed liquor suspended solids concentration in the reactor.

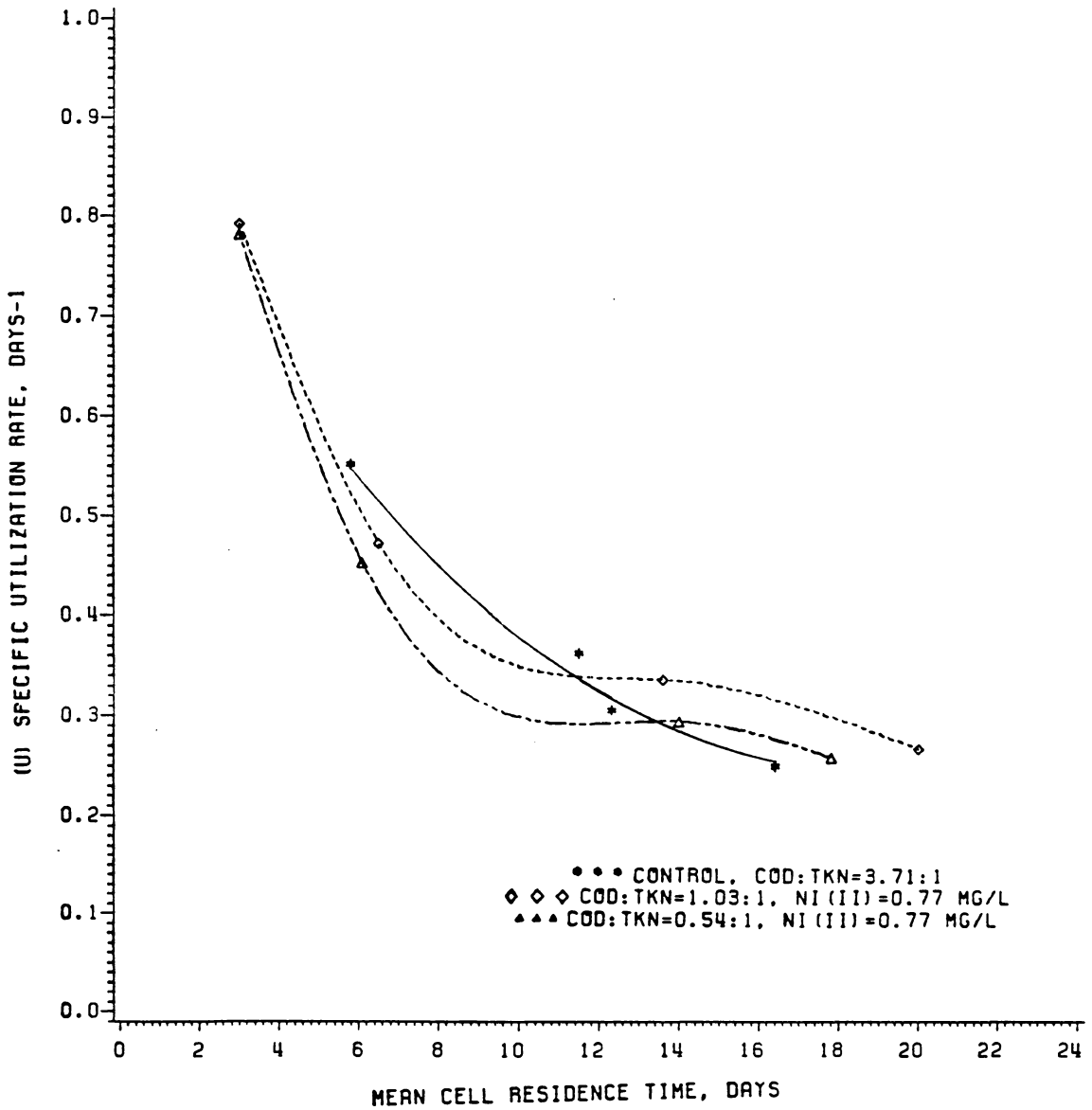


FIGURE 18. EFFECT OF NICKEL ON SPECIFIC UTILIZATION RATE OF HETEROTROPHIC MLSS AS A FUNCTION OF MEAN CELL RESIDENCE TIME

Figure 18 indicates that the specific utilization rate for the control reactor was slightly greater than that for the reactors dosed with nickel for mean cell residence times up to approximately 12 days. For mean cell residence times greater than 12 days, however, the control reactor maintained lower substrate utilization rates than the other two reactors in the study. An interpretation of these results is two-fold. First, it should be noted that equation [91] is sensitive to changes in COD removal efficiency and MLSS concentration. A comparison of these parameters between the control reactor and the nickel-fed reactors as illustrated in Figures 16 and 17, indicates that at each mean cell residence time the COD removal efficiency differs, at a maximum, only four percent. On the other hand, the MLSS concentration in the control reactor differs up to 500 mg/l from the MLSS concentrations in the nickel fed reactors. For mean cell residence times less than 12 days, a lower MLSS concentration in the control is coincident with a larger specific utilization rate. At each mean cell residence time greater than 12 days, a higher MLSS concentration in the control is coincident with a smaller specific utilization rate.

A second explanation for the results as illustrated in Figure 18 includes the effects of nickel on the activated sludge process as noted from previous figures presented in this section. The smaller substrate utilization rates that are evident in the nickel-fed reactors up to a 12 day θ_c can be attributed to the stimulation of microbial growth and the subsequent higher MLSS concentrations. For mean cell residence times greater than 12 days, the increased maintenance energy requirement of the nickel-stressed microorganisms caused a decrease in the amount of substrate utilized for cellular growth. In turn, the MLSS concentration was lower in these reactors than in the control, resulting in an increase in the specific utilization rate.

Biokinetic Coefficients

The microbial growth yield and maintenance energy coefficients can be obtained from the linear relationship between the specific utilization rate and the specific growth rate, expressed as:

$$\frac{1}{\theta_c} = Y_{\max} U - k_d \quad [92]$$

where, $1/\theta_c$ is the specific growth rate, Y_{\max} is the microbial yield coefficient, U is the specific utilization rate, and k_d is the microbial decay coefficient.

Figure 19 depicts the linear plots for the microbial yield data obtained from the control and the nickel-fed reactors. The slope of these lines represents the microbial growth yield, Y_{\max} , while the intercept represents the maintenance energy coefficient, k_d . As shown, the biokinetic coefficients for the reactors receiving nickel were considerably larger. This result indicates an apparent stimulation of microbial growth by the 0.77 mg/l nickel concentration. At the same time, however, the nickel caused an increased demand for microbial maintenance energy. Sujarttanonta (34) and Disalvo (40) found similar results in their treatability studies utilizing low concentrations of nickel. These authors attributed the apparent stimulation of microbial growth to a shift in the microbial species to a population of nickel tolerant organisms that naturally maintained a higher yield coefficient. On the other hand, nickel, in itself, may have stimulated heterotrophic growth. Sujarittanonta (34) and Disalvo (40) attributed the increased maintenance energy requirement of the microorganisms to the fact that these organisms were stressed by the nickel and were unable to efficiently stabilize organic matter.

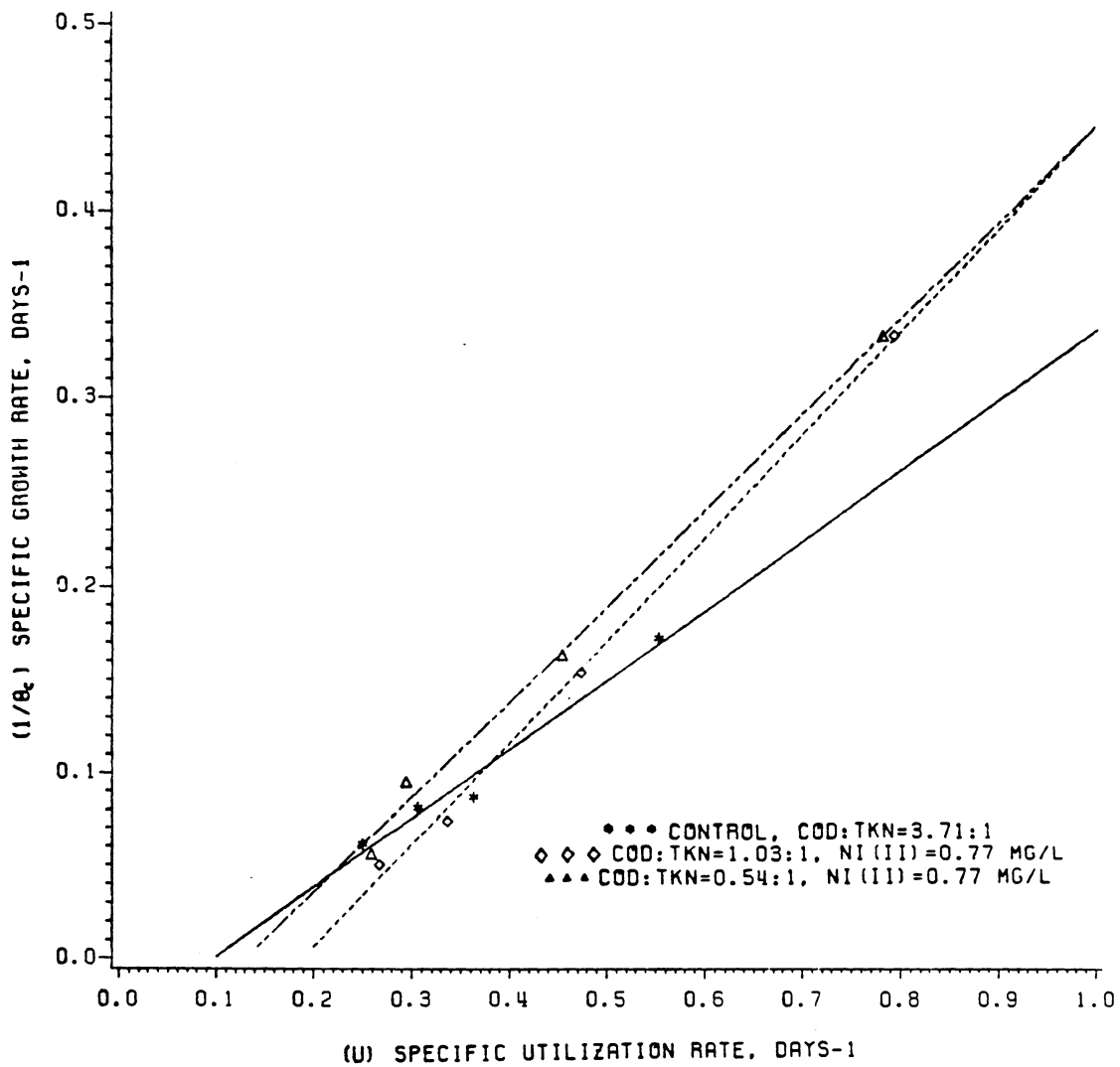


FIGURE 19. EFFECT OF NICKEL ON THE BIOKINETIC COEFFICIENTS OF HETEROTROPHIC MLSS

Figures 20 and 21 illustrate the trend in the microbial yield coefficient, Y_{\max} , and microbial maintenance coefficient, k_d , coefficients for a bench-scale activated sludge process receiving nickel concentrations ranging from 0.5 to 1.0 mg/l. Data for these figures was obtained from laboratory studies which were conducted in a manner similar to the present study (34, 40, 47). As shown, a strong correlation existed between the influent nickel concentration and the microbial yield and maintenance energy coefficients for the range of nickel concentrations studied. As the nickel concentration was increased from 0 to 1 mg/l, the Y_{\max} coefficient nearly doubled, while the k_d coefficient increased approximately five-fold. McCarty (39) found similar results in his study of the effects of salt on certain microorganisms and proposed that low concentrations of salt can actually stimulate biological activity. As the salt dose is increased above an inhibitory concentration, however activity decreases to a point below normal activity, eventually dropping to zero. Apparently, as shown in Figures 20 and 21 the threshold or inhibitory nickel concentration lies above 1 mg/l.

Observed Yield

The effects of nickel on the observed yield coefficient as a function of θ_c is depicted in Figure 22. The values for the observed yield were obtained from the following relationship:

$$Y_{\text{obs}} = \frac{Y_{\max}}{1 + k_d \theta_c} \quad [93]$$

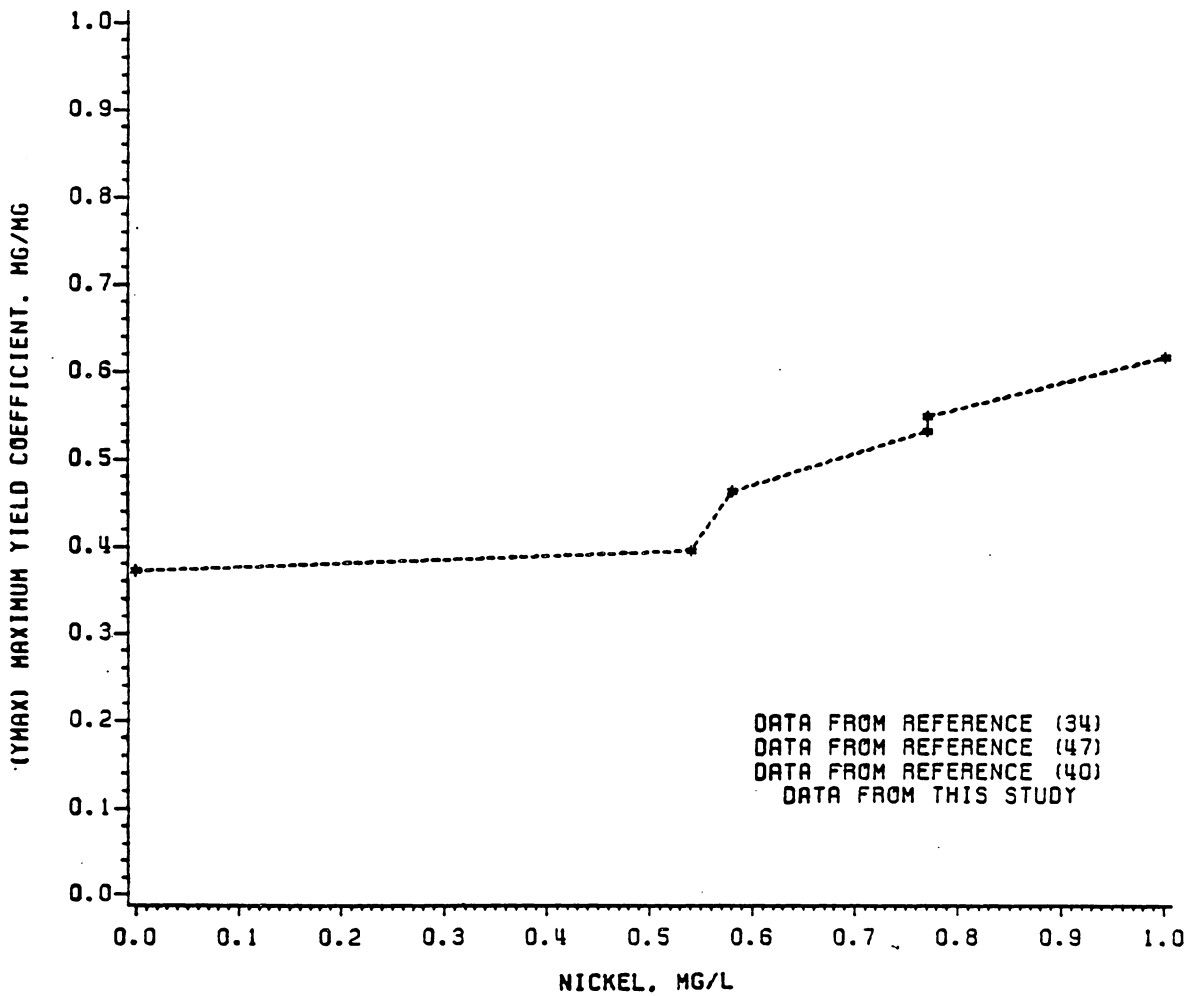


FIGURE 20. EFFECT OF NICKEL ON MAXIMUM YIELD COEFFICIENT OF HETEROTROPHIC MLSS

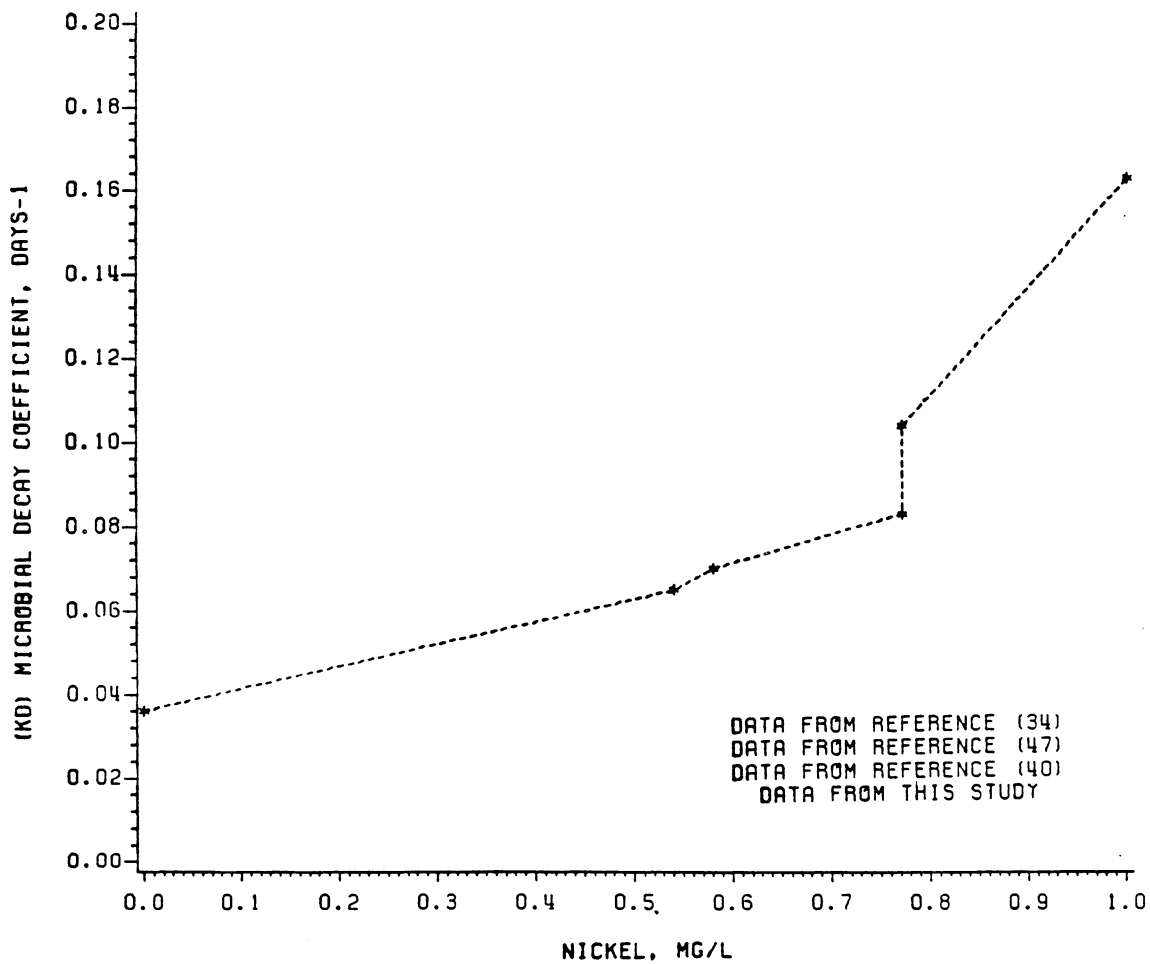


FIGURE 21. EFFECT OF NICKEL ON THE MICROBIAL DECAY COEFFICIENT HETEROTROPHIC MLSS

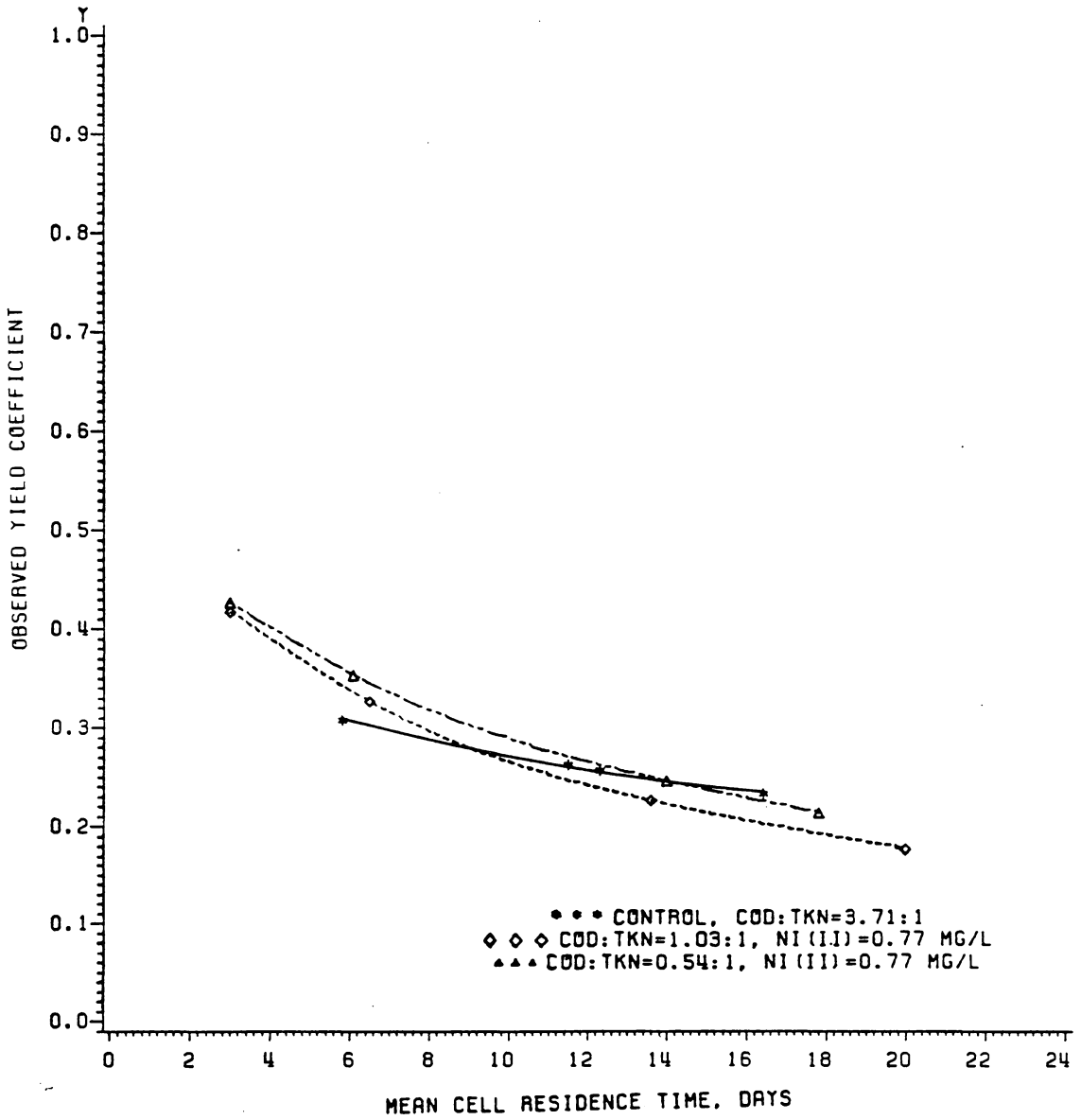


FIGURE 22. EFFECT OF NICKEL ON THE OBSERVED YIELD COEFFICIENT OF HETEROTROPHIC MLSS AS A FUNCTION OF MEAN CELL RESIDENCE TIME

where, Y_{obs} is the observed yield coefficient, Y_{max} is the microbial yield coefficient, k_d is the microbial maintenance coefficient, and θ_c is the mean cell residence time.

As equation (93) illustrates, the microbial maintenance energy coefficient has a definite influence on the observed yield. Large k_d coefficients can significantly reduce the Y_{obs} value and offset a large Y_{max} . Figure 22 illustrates this concept. As shown, the Y_{obs} values for both nickel-fed reactors were higher than those for the control reactor at mean cell residence times less than 12 days. At each operating θ_c beyond 12 days, however, the large maintenance energy requirement of the nickel-stressed microorganisms significantly reduced the Y_{obs} value, indicating that less substrate was available for cellular synthesis.

A comparison of the observed yield values for the nickel-fed reactors shows that the reactor operated at a COD:TKN of 0.54:1 maintained a slightly higher yield than the reactor operated a a COD:TKN of 1.03:1. This phenomena can be attributed to the increased amount of ammonia in the 0.54:1 reactor which was available to complex with the nickel species. The complexation of the nickel ion subsequently reduced the toxicity of the metal to the activated sludge process.

Nickel Removal Efficiency

Figure 23 depicts the nickel removal efficiency of the reactors utilized in this study as a function of mean cell residence time. As shown, both reactors achieved the greatest nickel removal efficiency at mean cell residence times between 3 and 8 days. This observation supports the general belief that most of the reduction of the dissolved metal species occurs in the aeration tank by adsorption onto biological floc. Reactors operated at mean cell residence times

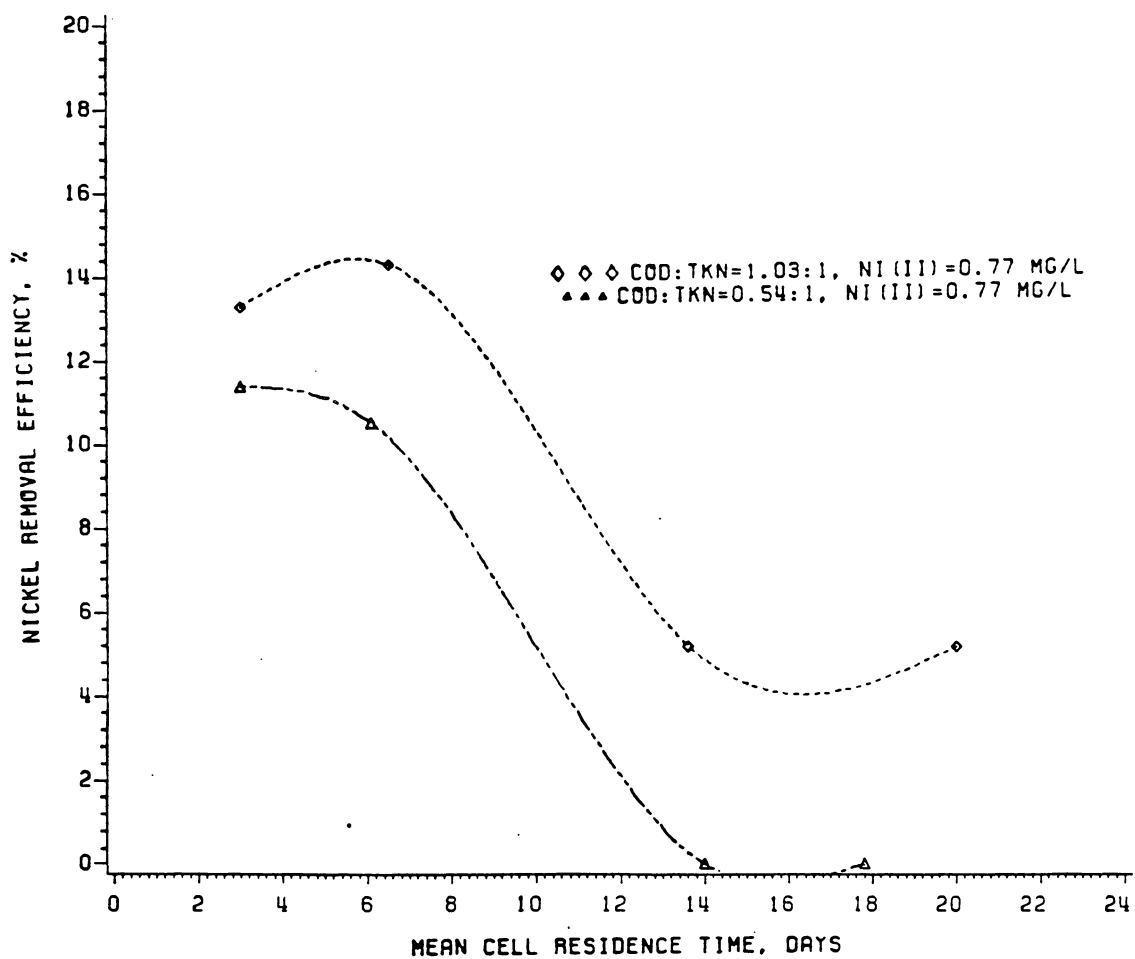


FIGURE 23. NICKEL REMOVAL EFFICIENCY AT DIFFERENT MEAN CELL RESIDENCE TIMES

less than 8-10 days are generally characteristic of larger microbial growth rates and increased sludge production. Adsorption of nickel onto the biological floc and the subsequent wasting of MLSS removes the nickel from the secondary biological process. Friedman and Dugan (13) found metal removal to vary with the physiological state of the microorganisms and to be greatest at high growth rates. The uptake of the metal ions was attributed to the combined influence of the cell and its surrounding matrix.

The reactor operated at a COD:TKN of 1.03:1 was more efficient in removing nickel from the wastewater than the reactor operated at a COD:TKN of 0.54:1, for all θ_c studied. This could be attributed to the formation of nickel-amine complexes in the reactor receiving the higher ammonia concentrations, which were not as readily adsorbed by the biological floc as the free metal ion. Brown and Lester (11) concluded that microorganisms produce large quantities of extracellular polysaccharides which are organized in well-defined capsules around the cells. Most of the polysaccharides are negatively charged and thus attract positively charged ions. The complexation of the ion may reduce the affinity of the cell floc for the metals.

Effluent Nitrate Concentration

The effluent nitrate concentrations from the activated sludge systems in this study are depicted, at different mean cell residence times, in Figure 24. It should be noted that an evaluation of system performance cannot be made by directly comparing the effluent nitrate concentrations for all three systems because the influent total Kjeldahl nitrogen concentrations to these reactors were not identical. The graph, however, can be utilized to illustrate the inhibitory effect of nickel on the nitrification process by examining the shape of the curves for each

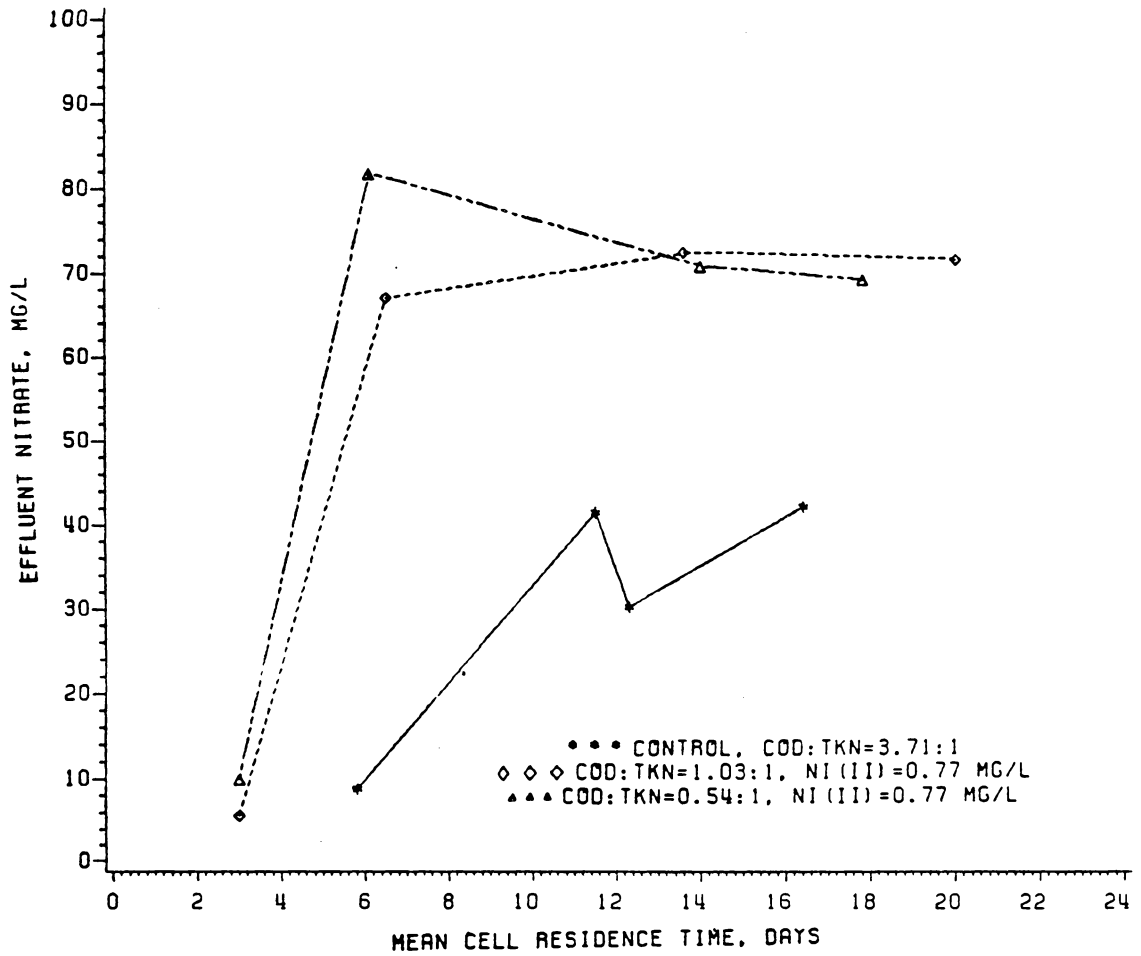


FIGURE 24. EFFECT OF NICKEL ON NITRIFICATION AT DIFFERENT MEAN CELL RESIDENCE TIMES

reactor. The effluent nitrate concentrations from the control reactor appear to increase with increasing mean cell residence times, while the effluent nitrate concentrations from the nickel-fed reactors were nearly identical and reached a limit at a θ_c of approximately 6 days. The plateau-type response in the nickel-fed reactors indicates an apparent inhibition of the nitrifying activity by the presence of the 0.77 mg/l nickel concentration. Operating the nickel-fed reactors at lower COD:TKN ratios did not overcome the toxicity of nickel to the nitrifiers.

Percent Distribution of Effluent and Wasted Nitrogen

Figures 25, 26, and 27 illustrate the influence that mean cell residence time, nickel concentration, and the COD:TKN ratio have on the degree of nitrification in the activated sludge process, and, in turn, on the percent distribution of effluent and wasted nitrogen. These plots were generated according to the method outlined in Chapter III. The organic nitrogen that was incorporated into microbial cell tissue was assumed to be 14 percent of the total microbial mass concentration.

The distribution of nitrogen forms throughout an activated sludge process is mainly a function of the degree of nitrification obtained by the system. The influent ammonia nitrogen and the influent organic nitrogen that is deaminized to ammonia nitrogen are, under optimum environmental conditions for nitrifying organisms, oxidized to nitrate. Thus, a system with a large degree of nitrification would show a shift in the organic and ammonia nitrogen concentrations to nitrate nitrogen.

Figures 25, 26, and 27 show a definite correlation between the mean cell residence time and the degree of nitrification in a reactor. As θ_c increased to approximately 6 days, the percent effluent nitrate also increased in all

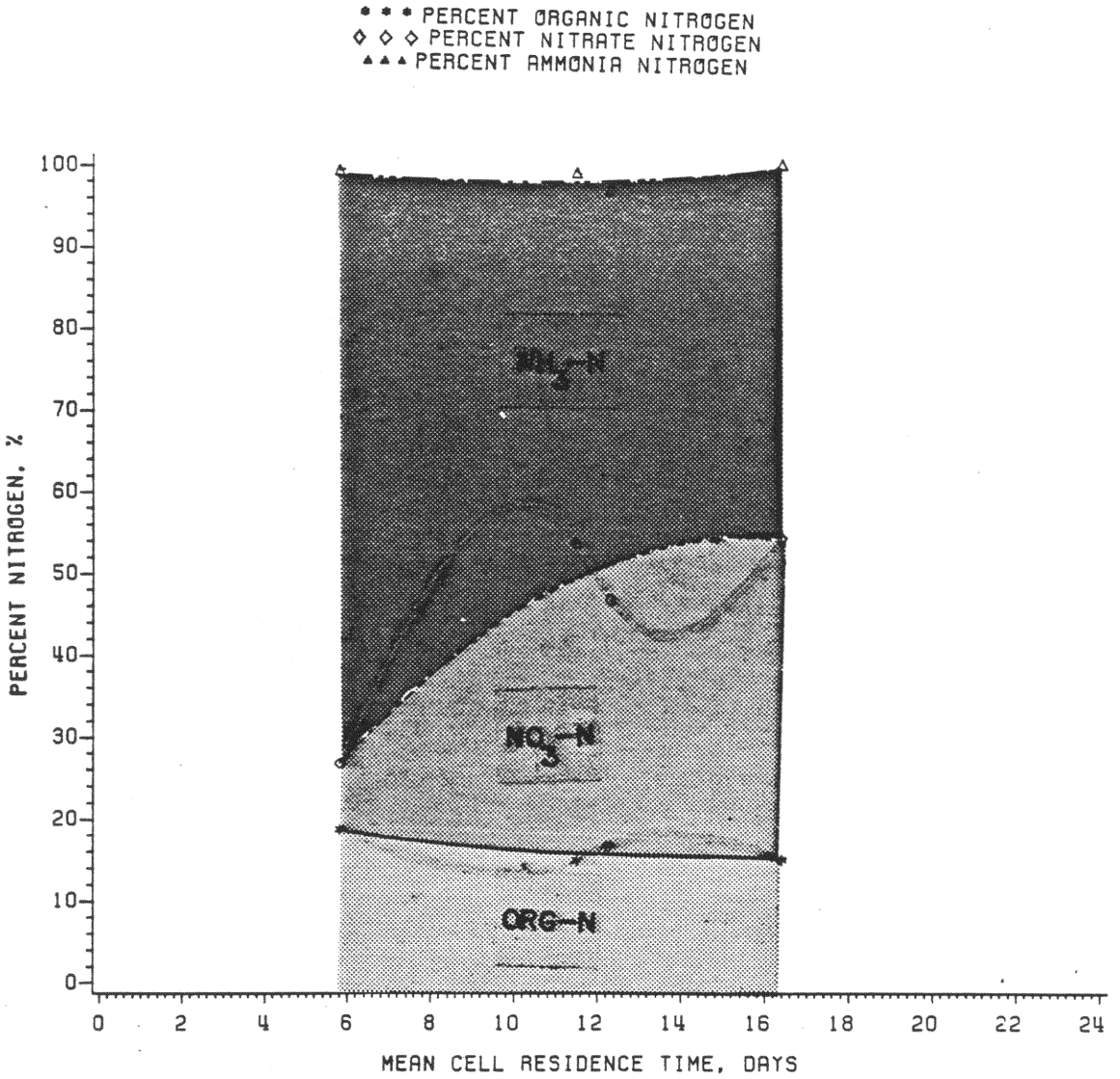


FIGURE 25. PERCENT DISTRIBUTION OF EFFLUENT AND WASTED NITROGEN
 AS A FUNCTION OF MEAN CELL RESIDENCE TIME
 CONTROL, COD:TKN=3.71:1

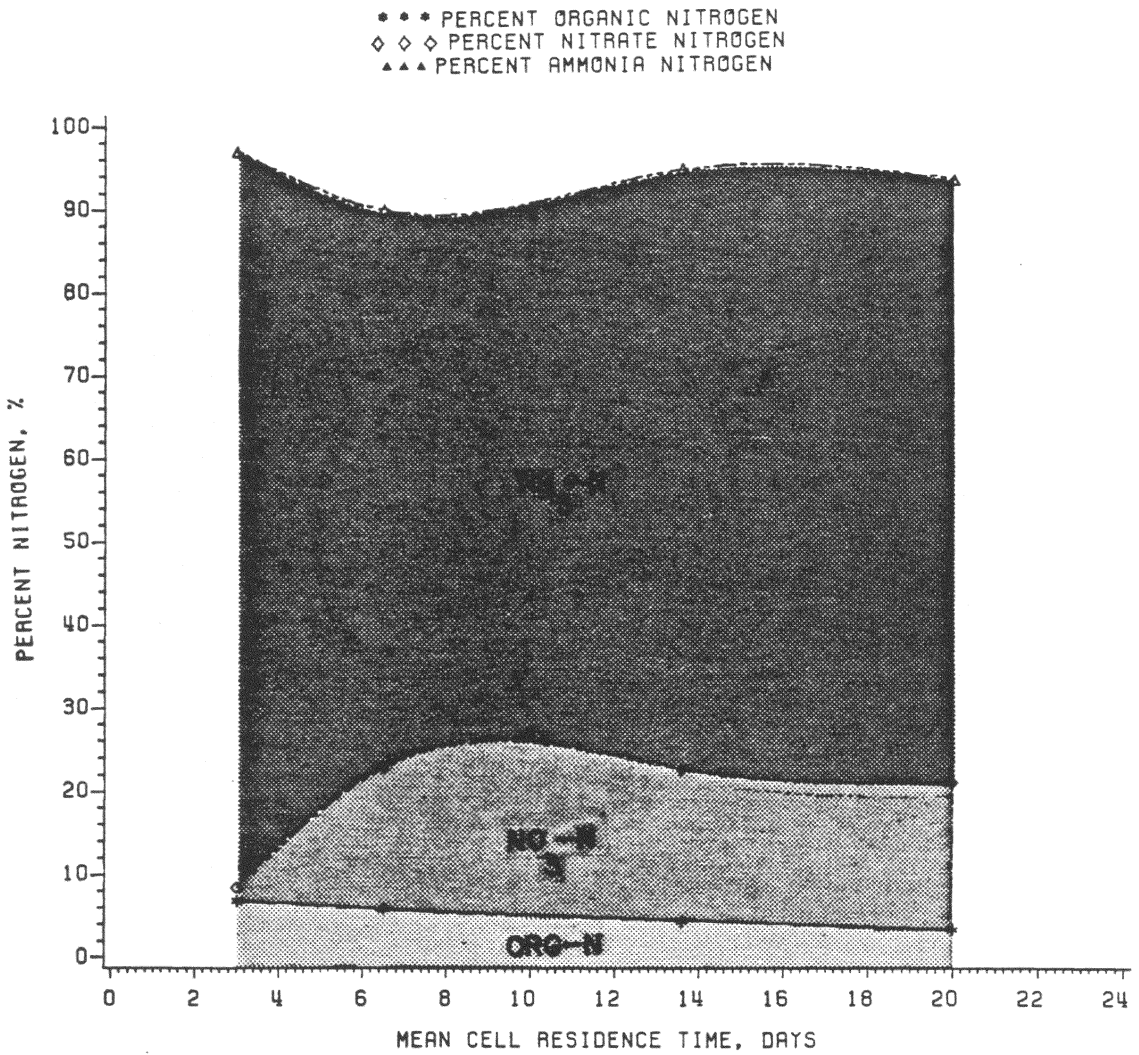


FIGURE 26. PERCENT DISTRIBUTION OF EFFLUENT AND WASTED NITROGEN
 AS A FUNCTION OF MEAN CELL RESIDENCE TIME
 COD:TKN=1.03:1, NI (II)=0.77 MG/L

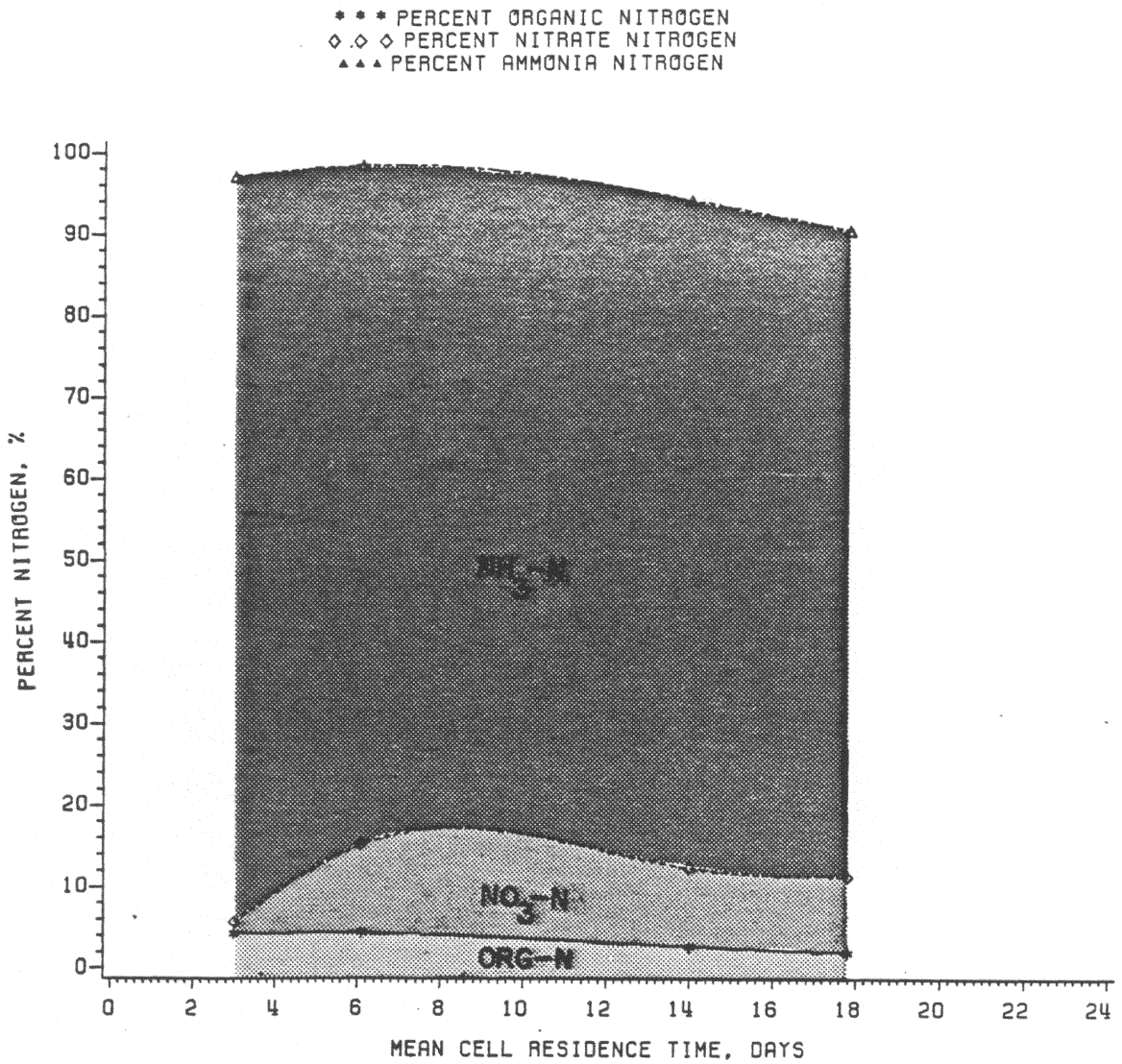


FIGURE 27. PERCENT DISTRIBUTION OF EFFLUENT AND WASTED NITROGEN
 AS A FUNCTION OF MEAN CELL RESIDENCE TIME
 COD:TKN=0.54:1, NI (II)=0.77 MG/L

three reactors. This can be attributed to the development of the nitrifying population at higher θ_c which exhibits a much slower growth rate than the heterotrophic biomass.

At the mean cell residence times beyond 6 days, the control reactor obtained a steady increase in nitrification while the reactors receiving low concentrations of nickel reached a limiting plateau for nitrate production. In addition, while the nickel-fed reactors were fed influent ammonia concentrations 4 to 8 times that of the control reactor, the graphs depict a larger percent effluent nitrate concentration in the control. Apparently, the oxidation of ammonia to nitrate was inhibited by the presence of nickel.

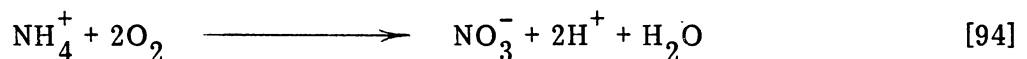
The inhibition to the nitrification process by nickel can also be substantiated by comparing the percent organic nitrogen and percent ammonia nitrogen curves for the three reactors. As θ_c increased, the percent organic nitrogen decreased in all three systems due to the deaminization of organic compounds containing nitrogen. At the same time, the ammonia concentration decreased in the control reactor and in the reactor operated at a COD:TKN of 0.54:1 due to the oxidation of ammonia to nitrate in these systems. On the other hand, the reactor operated at a COD:TKN of 1.03:1, shows an increase in the ammonia nitrogen concentration as θ_c increased. Apparently, nickel prevented the nitrifiers from oxidizing a significant percentage of the influent ammonia nitrogen in this reactor to nitrate. Any organic nitrogen in this reactor that was deaminized, then, only served to increase the ammonia concentration in the effluent.

Other studies on nitrification have found that high influent free ammonia concentrations to a reactor can be inhibitory to the oxidation process. An examination of the equilibrium relationship between the free ammonia species and the

ammonium ion species for this study (Appendix A) shows that the free ammonia species comprises only a fraction of the total ammonia in a reactor. Therefore, any inhibition to the nitrification process as noted in this study is attributed to the toxicity of nickel.

Effluent pH

The change in effluent pH as a function of mean cell residence time is shown in Figure 28. All reactors in this study showed a decrease in pH at mean cell residence times greater than 6 days which can be attributed to the onset of nitrification at higher mean cell residence times. During the nitrification process, hydrogen ions are released into solution as indicated in the following oxidation reaction:



The nickel-fed reactors were operated at COD:TKN ratios of 1.03:1 and 0.54:1 as compared to the control reactor which was operated at a COD:TKN of 3.71:1. Consequently, these reactors contained more nitrogen available for nitrification than the control. As shown in Figure 29, the effluent nitrate concentrations from the reactors dosed with nickel ranged from 67.1 to 81.7 mg/l as compared to effluent nitrate concentrations ranging from 30.3 to 42.2 mg/l in the control reactor. Coincident with the larger effluent nitrate concentrations in these reactors was a larger pH depression than in the control.

A comparison of Figures 23 and 28 illustrates that nitrification proceeded in the reactors receiving nickel at pH values below 6.0. Sujarittanonta (34) and Trahern (47) found from their studies that a significant amount of nitrification can

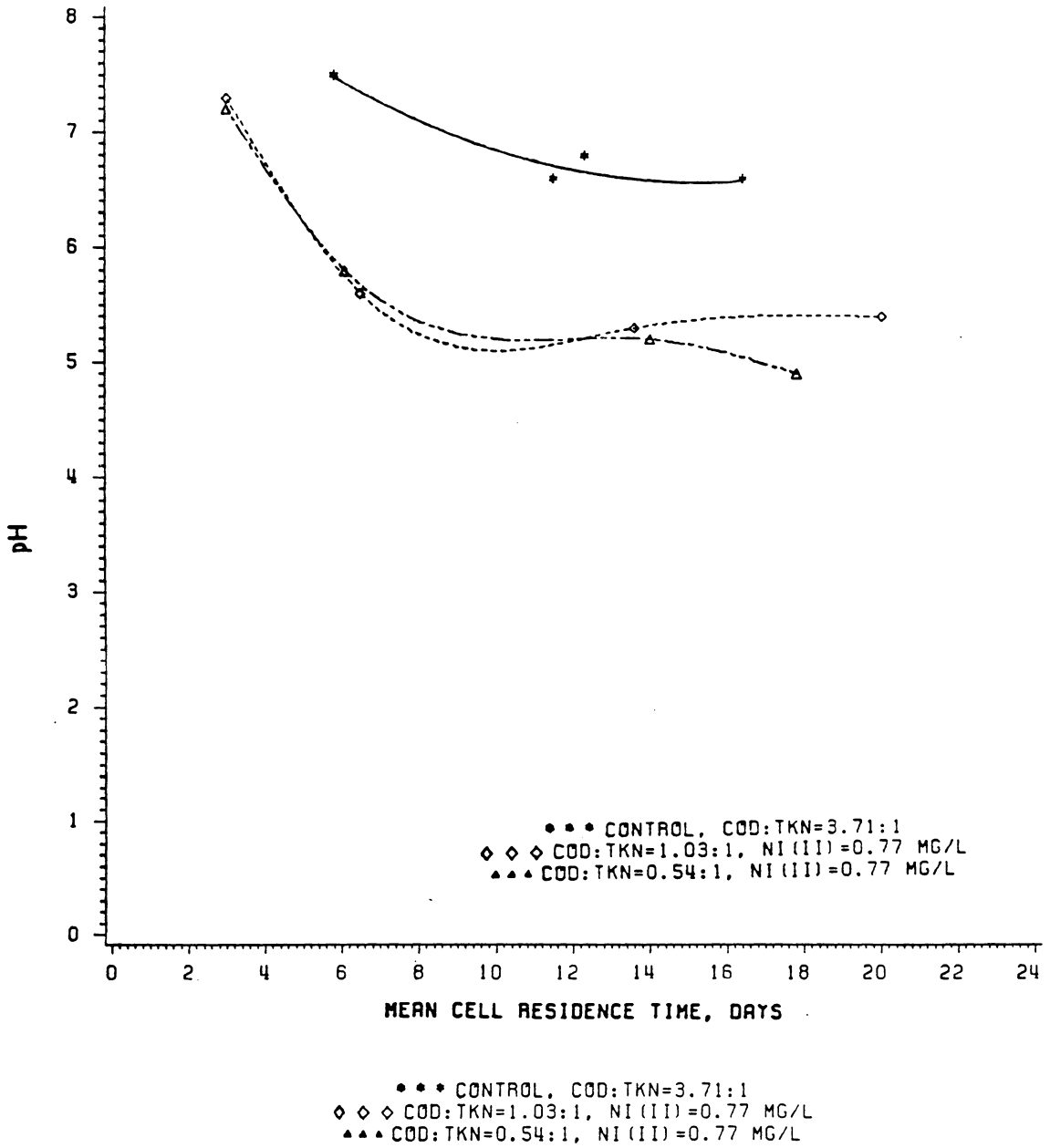


FIGURE 28. CHANGE IN EFFLUENT PH AS A FUNCTION OF MEAN CELL RESIDENCE TIME

occur in reactors at pH values as low as 4.9. These findings differ from the presently held concept (21) that nitrification can only occur, to any extent, at pH values between 7.0 and 9.8.

Nitrification in Relation to MLSS:Ni(II)

The effect of the MLSS:Ni(II) ratio on nitrification is illustrated in Figure 29. This graph shows a definite correlation between the MLSS:Ni(II) ratio and the toxicity of nickel to the nitrifying microorganisms. Coincident with an increase in the MLSS:Ni(II) ratio up to a value of 2000:1, in both nickel-fed reactors, was an increase in the effluent nitrate concentration. Adams et al. (31) noted that metal toxicity was related to the metal-enzyme equilibrium conditions. A decrease in metal dosage, an increase in MLSS, or an increase in sewage strength should decrease the proportion of active cellular components tied up as metal-enzyme complexes and increase process performance.

As shown in Figure 29, both reactors reached a limiting plateau for percent nitrification at the 2000:1 MLSS to soluble nickel ratio. Figure 24, which depicts effluent nitrate concentrations as a function of θ_c , indicates that this plateau for the reactors is reached at a θ_c of 6 days. Further increases in mean cell residence time, accompanied by larger MLSS concentrations, do not overcome the inhibitory effects of nickel on the microorganisms.

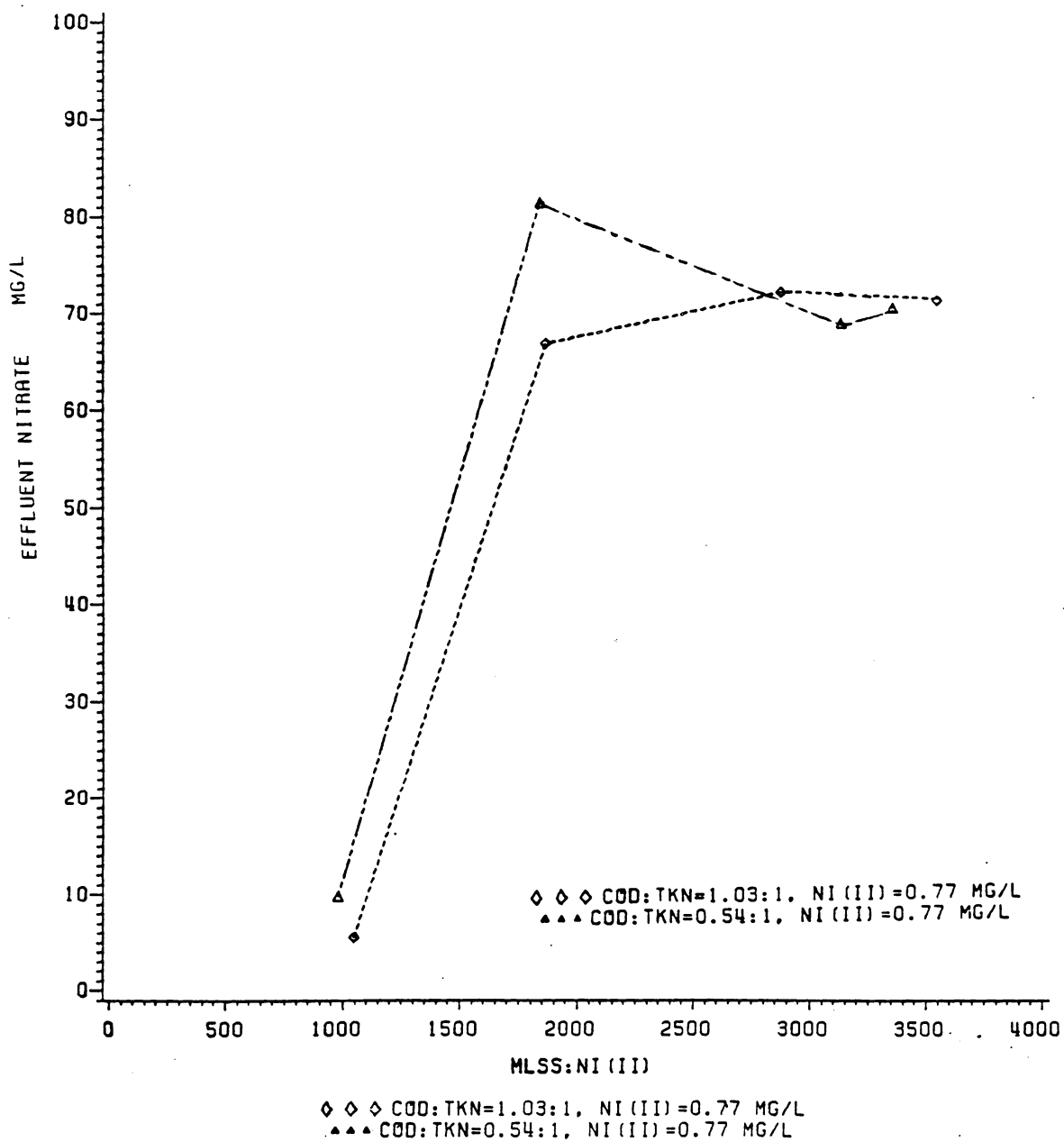


FIGURE 29. EFFECT OF THE MLSS:NI (II) RATIO ON EFFLUENT NITRATE CONCENTRATION

V. CONCLUSIONS

The data obtained from laboratory bench-scale continuous-flow reactors was analyzed to determine the effects of a low concentration of nickel, in relation to the COD:TKN ratio, on the operation of the activated sludge process. The conclusions drawn from this study are as follows:

1. The soluble COD removal efficiency of the heterotrophic microorganisms was not inhibited by a nickel concentration of 0.77 mg/l.
2. The low continuous nickel dose to the activated sludge units appeared to stimulate the growth of the heterotrophic microorganisms or to cause a replacement of the organisms with a species of nickel-tolerant organisms as indicated by the Y_{\max} value.
3. Coincident with the high Y_{\max} in the nickel-fed reactors was a higher k_d value, indicating that nickel also stressed the microorganisms causing an increase in their maintenance energy requirement.
4. The observed yield coefficients for the nickel-fed reactors were higher than those for the control at operating θ_c less than 12 days, indicating an apparent stimulation of microbial growth by the low nickel concentration. For operating θ_c greater than 12 days, however, the observed yield of the nickel-fed reactors below that of the control due to the large maintenance requirement of the organisms stressed by nickel.
5. The reactor operated at a COD:TKN of 0.54:1 maintained a slightly higher observed yield than the reactor operated at a COD:TKN of 1.03:1.

This phenomenon can be attributed to the larger percentage of nickel-amine complexation in the reactor receiving higher concentrations of ammonia and a reduced toxicity of the metal species.

Autotrophic Effects

1. The 0.77 mg/l nickel concentration inhibited nitrification as illustrated by the plateau-type response of the nitrifiers which was obtained in the nickel-fed reactors as compared to that in the control reactor.
2. Operating the nickel-fed reactors at lower COD:TKN ratios and greater TKN:Ni(II) concentrations did not appear to reduce the toxicity of nickel to the nitrification process. Both nickel-fed reactors in this study reached the same limit for nitrification.
3. The degree of nitrification increased with increasing mean cell residence times in the three reactors studied.
4. Increasing MLSS:Ni ratios in the reactors of this study were accompanied by increased degrees of nitrification.
5. Nitrification proceeded at pH values as low as 4.9.

Nickel Removal

1. Nickel is accumulated into or adsorbed onto microbial cells as shown by higher nickel removal efficiencies at lower mean cell residence times and corresponding higher waste sludge productions.

2. The reactor operated at the COD:TKN of 1.03:1 was more efficient in removing nickel from the wastewater than the reactor operated at a COD:TKN of 0.54:1. This result is attributed to the formation of nickel-amine complexes in solutions with large TKN concentrations which are not as readily adsorbed by the biological floc as the free metal ion.

RECOMMENDATION FOR FUTURE STUDY

Based on the experimental results, the following topic is suggested for future study:

An investigation to determine the effects of nickel on the microbial growth rate, in the completely-mixed activated sludge process, utilizing the Monod equation for data analysis.

REFERENCES

1. United States Environmental Protection Agency, Ambient Water Quality Criteria for Nickel, EPA 440/5-80-060, October (1980).
2. Jenkins, S. H., Keight, D. G., and Edwins, Auril, "The Solubility of Heavy Metal Hydroxides in Water, Sewage and Sewage Sludge - II: The Precipitation of Metal by Sewage." Int. J. Air Water Pollution, 8, 679 (1964).
3. McDermott, Gerald N., Post, Mildred A., Jackson, Burney, N., and Ettinger, Morris B., "Nickel in Relation to Activated Sludge and Anaerobic Digestion Processes." Journal Water Pollution Control Federation, 37, 163 (1965).
4. United States Department of Health, Education and Welfare, "Interaction of Heavy Metals and Biological Treatment Processes." Public Health Service No. 999-WP-22 (1965).
5. Rubin, A. J., Aqueous Environment Chemistry of Metals, Ann Arbor Science, Ann Arbor (1974).
6. Manahan, S. E., and Smith, M. J., "The Importance of Chelating Agents." Water and Sewage Works, 9, 102 (1973).
7. Snoyenk, Vernon L., and Jenkins, David, Water Chemistry, John Wiley and Sons, Inc., New York, NY (1980).
8. Sawyer, C. N. and McCarty, P. L., Chemistry for Environmental Engineering. McGraw Hill Book Company, New York, NY (1978).
9. Patterson, J. W., Scala, J. J. and Allen, H. E., "Heavy Metal Treatment by Carbonate Precipitation." Proc. 31st Industrial Waste Conference, Purdue University, 132 (1976).
10. Oliver, Barry G. and Cosgrove, Ernest G., "The Efficiency of Heavy Metal Removal by a Conventional Activated Sludge Treatment Plant." Water Research, 8, 869 (1974).
11. Brown, Melanie J. and Lester, J. N., "Metal Removal in Activated Sludge." The Role of Bacterial Extracellular Polymers." Water Research, 13, 817 (1979).
12. Bitton, G. and Freihofer, V., "Influence of Extracellular Polysaccharides on the Toxicity of Copper and Cadmium Towards Klebsiella aerogenes." Microbial Ecology, 4, 119 (1978).
13. Friedman, B. A. and Dugan, P. R., "Concentration and Accumulation of Metallic Ions by the Bacterium Zoogloea." Devs ind. Microbiol, 9, 381 (1968).

References (continued)

Page 2 of 4

14. Parsons A., and Dugan P., "Production of Extracellular Polysaccharide Matrix by Zoogloea Ramigera", Applied Microbiology, 21, 4, 657 (1971).
15. Cheng, M. H., Patterson, J. W., and Minear, R. A., "Heavy Metals Uptake by Activated Sludge." Journal Water Pollution Control Federation, 47, 362 (1975).
16. Metcalf and Eddy, Inc., Wastewater Engineering Treatment, Disposal and Reuse. Second Edition, McGraw-Hill Book Company, New York 1979.
17. Randall, Clifford W.
18. Lawrence, Alonze W., and McCarty, Perry L., "Unified Basis for Biological Treatment Design and Operation." Journal of the Sanitary Engineering Discussion, ASCE, Vol. 96. No. SA3, Proc. Paper 7365, 757 (1970).
19. Sherrard, Joseph H., and Schroeder, Edward D., "Cell Yield and Growth Rate in Activated Sludge." Journal Water Pollution Control Federation, 45, No. 9, 1889 (1973).
20. Sherrard, Joseph H., "Activated Sludge Wastewater Treatment - Stoichiometric Relationships." J. Chem. Tech. Biotechnol, 30, 447 (1980).
21. Wild, Harry E., Jr., Sawyer, Clair N., and McMahan, Thomas C., "Factors Affecting Nitrification Kinetics."
22. Searce, Steven N., Benninger, Robert W., Weber, A. Scott, and Sherrard, Joseph H., "Prediction of Alkalinity Changes in the Activated Sludge Process." Journal Water Pollution Control Federation, February, 399 (1980).
23. Sherrard, Joseph H., Searce, Steven N., Benninger, Robert W., and Weber, A. Scott, "Influence of the COD:TKN:NH₄-N Ratio on Nitrification and Alkalinity in the Activated Sludge Process." J. Civil Eng. Design, 2(1), 31 (1980).
24. Stover, E. L. and Kincannon, D. F., "Effets of COD:NH₃-N Ratio on a One Stage Nitrification Activated Sludge System," Water and Sewage Works, 119, 9, 120 (1976).
25. Jenkins, D. and Garrison, W. E., "Control Activated Sludge by Mean Cell Residence Time," Journal Water Pollution Control Federation, 40, 11, 905 (1968).
26. Sherrard, Joseph H., and Schroeder, Edward D., "Stoichiometry of Industrial Biological Wastewater Treatment." Journal Water Pollution Control Federation, 48, 742 (1976).

References (continued)
Page 3 of 4

27. Neufeld, R. D., Hill, A. J., and Adekoya, D. O., "Phenol and Free Ammonia Inhibition to Nitrosomonas Activity." Water Research, 14, 1695 (1980).
28. Ford, D. L., Churchwell, J. W., and Kachtick, J. W., "Comprehensive Analysis of Nitrification of Chemical Processing Wastewaters." Journal Water Pollution Control Federation, 52, 2726 (1980).
29. Anthonisen, A. C., Loehr, R. C., Prakasam, T. B., and Srinath, Journal Water Pollution Control Federation, 48, 835 (1976).
30. Benninger, R. W. and Sherrard, J. H., "Nitrification and Alkalinity Relationships in Activated Sludge." Journal Water Pollution Control Federation, 50, 2132 (1978).
31. Adams, C. E., Eckenfelder, W. W. and Goodman, B. L., "The Effects and Removal of Heavy Metals in Biological Treatment." Heavy Metals in the Aquatic Environment, Krenkel, P. A. (ed.), Pergamon Press, Oxford (1975).
32. Barth, E. F., "The Effects and Removal of Heavy Metals in Biological Treatment." Heavy Metals in the Aquatic Environment, Krenkel, P. A. (ed.), Pergamon Press, Oxford (1975).
33. Tomlinson, T. G., Boon, A. G., and Trotman, C. N. A., "Inhibition of Nitrification in the Activated Sludge Process of Sewage Disposal," Journal Applied Bacteriology, 29, No. 2, 266 (1966).
34. Sujarittanonta, Suthirak, "The Effects of Nickel on the Completely Mixed Activated Sludge Process." Doctor of Philosophy Dissertation, Civil Engineering Department, Virginia Polytechnic Institute and State University (1979).
35. Nuefeld, Ronald D. and Hermann, Edward R., "Heavy Metals Removal by Acclimated Activated Sludge." Journal Water Pollution Control Federation, 47, 310 (1975).
36. Poon, Calvin P. C., and Bhayani, Kiran H., "Metal Toxicity to Sewage Organisms." Journal of the Sanitary Engineering Division, ASCE, Vol. 97, No. SA2, Proc. Paper 8020, 161 (1971).
37. Barth, E. F., Ehinger, M. B., Salotto, B. V., McDermott, G. N., "Summary Report on the Effects of Heavy Metals on the Biological Treatment Process." Journal Water Pollution Control Federation, 37, 86 (1965).
38. McDermott, Gerald, N., Moore, W. Allen, Post, Mildred A., and Ettinger, M. B., "Effects of Copper on Aerobic Biological Sewage Treatment." Journal Water Pollution Control Federation, 35, 227 (1963).

References (continued)

Page 4 of 4

39. McCarty, Perry L., "Anaerobic Waste Treatment Fundamentals, Part III: Toxic Materials and Their Control." Public Works, 11, 91 (1964).
40. Disalvo, Richard M., "The Response of Completely Mixed Activated Sludge to Nickel." Master of Science Thesis, Sanitary Engineering Department, Virginia Polytechnic Institute and State University, 1982.
41. Salotto, B. V., Barth, E. F., Tolliver, W. E., and Ettinger, M. B., "Organic Load and the Toxicity of Copper in the Activated Sludge Process," Proc. 19th Industrial Waste Conference, Purdue University, 1025 (1964).
42. Kugelman, I. J. and McCarty, P. L., "Cation Toxicity and Stimulation in Anaerobic Waste Treatment II: Daily Feed Studies," Proc. 19th Industrial Waste Conference, Purdue University, 667 (1964).
43. Brown, H. G., Hensley, C. P. McKinney, G. L., and Robinson, J. L., "Efficiency of Heavy Metals Removal in Municipal Sewage Treatment Plants." Environmental Letters, 5, 103 (1973).
44. Stones, T., "The Fate of Nickel During the Treatment of Sewage." Journal Institute of Sewage Purification, Part 2, 252 (1959).
45. Nelson, P. O., Chung, A. K., and Hudson, M. C., "Factors Affecting the Fate of Heavy Metals in the Activated Sludge Process." Journal Water Pollution Control Federation, 53, 1323 (1981).
46. Standard Methods for the Examination of Water and Wastewater, 14th Edition, American Public Health Association, Washington, D.C. (1976).
47. Trahern, Patti G., "The Effect of Nickel in the Nitrification Process." Master of Science Thesis, Virginia Polytechnic Institute and State University, (In Press).

APPENDIX A

Calculations for Log Concentration Diagram of Nickel-Amine Complexes

Appendix (A)

Calculations for Log Concentration Diagram of
Nickel-Amine Complexes

Given:

$$\begin{aligned}
 [\text{Ni}^{2+}] &= 0.77 \text{ mg/l} \\
 &= 0.77 \frac{\text{mg}}{\text{l}} \times \frac{1 \text{ mole}}{58,700 \text{ mg}} = 1.31 \times 10^{-5} \text{ M} = 10^{-4.89} \text{ M}
 \end{aligned}$$

Equilibrium Relationships:

$$\frac{[\text{Ni}(\text{NH}_3)^{2+}]}{[\text{Ni}^{2+}][\text{NH}_3]} = \beta_1 = 10^{3.00} \quad [1]$$

$$\frac{[\text{Ni}(\text{NH}_3)_2^{2+}]}{[\text{Ni}^{2+}][\text{NH}_3]^2} = \beta_2 = 10^{5.18} \quad [2]$$

$$\frac{[\text{Ni}(\text{NH}_3)_3^{2+}]}{[\text{Ni}^{2+}][\text{NH}_3]^3} = \beta_3 = 10^{6.82} \quad [3]$$

$$\frac{[\text{Ni}(\text{NH}_3)_4^{2+}]}{[\text{Ni}^{2+}][\text{NH}_3]^4} = \beta_4 = 10^{7.98} \quad [4]$$

Logarithmically Expressing the Equilibrium Relationships:

$$\log[\text{Ni}(\text{NH}_3)^{2+}] = \log\beta_1 + \log[\text{Ni}^{2+}] + \log[\text{NH}_3] \quad [5]$$

$$\log[\text{Ni}(\text{NH}_3)_2^{2+}] = \log\beta_2 + \log[\text{Ni}^{2+}] + 2\log[\text{NH}_3] \quad [6]$$

$$\log[\text{Ni}(\text{NH}_3)_3^{2+}] = \log\beta_3 + \log[\text{Ni}^{2+}] + 3\log[\text{NH}_3] \quad [7]$$

$$\log[\text{Ni}(\text{NH}_3)_4^{2+}] = \log\beta_4 + \log[\text{Ni}^{2+}] + 4\log[\text{NH}_3] \quad [8]$$

The following table lists the log of each nickel-amine species for various ammonia concentrations.

$[\text{NH}_3]$	$\log[\text{NH}_3]$	$\log[\text{Ni}^{2+}]$	$\log[\text{Ni}(\text{NH}_3)^{2+}]$	$\log[\text{Ni}(\text{NH}_3)_2^{2+}]$	$\log[\text{Ni}(\text{NH}_3)_3^{2+}]$	$\log[\text{Ni}(\text{NH}_3)_4^{2+}]$
1.0	0	-4.89	-1.89	+0.29	+1.93	+3.09
3.2×10^{-1}	-0.5	-4.89	-2.39	-0.71	+0.43	+1.09
1.0×10^{-1}	-1.0	-4.89	-2.89	-1.71	-1.07	-0.91
3.2×10^{-2}	-1.5	-4.89	-3.39	-2.71	-2.57	-2.91
1.0×10^{-2}	-2.0	-4.89	-3.89	-3.71	-4.07	-4.91
3.2×10^{-3}	-2.5	-4.89	-4.39	-4.71	-5.57	-6.91
1.0×10^{-3}	-3.0	-4.89	-4.89	-5.71	-7.07	-8.91
3.2×10^{-4}	-3.5	-4.89	-5.39	-6.71	-8.57	-10.91
1.0×10^{-4}	-4.0	-4.89	-5.89	-7.71	-10.07	-12.91
3.2×10^{-5}	-4.5	-4.89	-6.39	-8.71	-11.57	-14.91
1.0×10^{-5}	-5.0	-4.89	-6.89	-9.71	-13.07	-16.91

Figure 1 depicts the log of each nickel species as a function of ammonia concentration.

APPENDIX B

Calculation for Distribution Diagram of Nickel-Amine Complexes

Appendix (B)

Calculation for Distribution Diagram of
Nickel-Amine Complexes

Given:

$$\begin{aligned}
 [\text{Ni}^{2+}] &= 0.77 \text{ mg/l} \\
 &= 0.77 \frac{\text{mg}}{\text{l}} \times \frac{1 \text{ mole}}{58,700 \text{ mg}} = 1.28 \times 10^{-5} \text{ M} = 10^{-4.89} \text{ M}
 \end{aligned}$$

Fraction of Nickel-Amine Species:

$$\alpha_0 = \frac{[\text{Ni}^{2+}]}{[\text{Ni}^{2+}] + [\text{Ni}(\text{NH}_3)^{2+}] + [\text{Ni}(\text{NH}_3)_2^{2+}] + [\text{Ni}(\text{NH}_3)_3^{2+}] + [\text{Ni}(\text{NH}_3)_4^{2+}]} \quad [1]$$

$$= \frac{1}{1 + \beta_1(\text{NH}_3) + \beta_2(\text{NH}_3)^2 + \beta_3(\text{NH}_3)^3 + \beta_4(\text{NH}_3)^4}$$

$$\alpha_1 = [\text{Ni}(\text{NH}_3)^{2+}] = \beta_1[\text{NH}_3]\alpha_0 \quad [2]$$

$$\alpha_2 = [\text{Ni}(\text{NH}_3)_2^{2+}] = \beta_2[\text{NH}_3]^2\alpha_0 \quad [3]$$

$$\alpha_3 = [\text{Ni}(\text{NH}_3)_3^{2+}] = \beta_3[\text{NH}_3]^3\alpha_0 \quad [4]$$

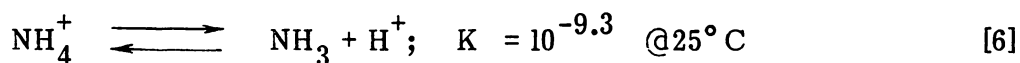
$$\alpha_4 = [\text{Ni}(\text{NH}_3)_4^{2+}] = \beta_4[\text{NH}_3]^4\alpha_0 \quad [5]$$

The fraction of each nickel species at various ammonia concentrations is tabulated below.

$[\text{NH}_3]$	α_0	α_1	α_2	α_3	α_4
1.0	\approx	\approx	0.001	0.065	0.934
3.2×10^{-1}	\approx	\approx	0.013	0.177	0.810
1.0×10^{-1}	\approx	0.006	0.085	0.372	0.537
3.2×10^{-2}	0.002	0.065	0.310	0.428	0.196
1.0×10^{-2}	0.030	0.297	0.449	0.196	0.028
3.2×10^{-3}	0.170	0.536	0.257	0.035	0.002
1.0×10^{-3}	0.463	0.463	0.070	0.003	\approx
3.2×10^{-4}	0.751	0.237	0.011	\approx	\approx
1.0×10^{-4}	0.908	0.091	0.001	\approx	\approx
3.2×10^{-5}	0.970	0.031	\approx	\approx	\approx
1.0×10^{-5}	0.990	0.010	\approx	\approx	\approx

Figure 2 depicts the α_n values plotted as a function of pNH_3 , or $-\log[\text{NH}_3]$. For a given concentration of free ammonia in a solution containing 0.77 mg/l Ni(II), the extent of nickel-amine complexation can be obtained from this graph. The following paragraphs detail the exact procedure for determining the percent of complexed nickel in the feed solutions pertinent to this research.

The concentration of free ammonia in a solution, in relation to the total ammonia concentration depends upon the equilibrium of the following relationship:



where,

$$K = \frac{[\text{NH}_3][\text{H}^+]}{[\text{NH}_4^+]} \quad [7]$$

For a given pH value, the ratio of $[\text{NH}_4^+]$ to $[\text{NH}_3]$ can be expressed as:

$$[\text{NH}_4^+] = 10^{-\text{pH}+9.3} [\text{NH}_3] \quad [8]$$

The mass balance of nitrogen, including the uncomplexed and complexed forms, can be expressed as:

$$[\text{N}_t] = [\text{NH}_3] + [\text{NH}_4^+] + [\text{Ni}(\text{NH}_3)^{2+}] + 2[\text{Ni}(\text{NH}_3)_2^{2+}] + 3[\text{Ni}(\text{NH}_3)_3^{2+}] + 4[\text{Ni}(\text{NH}_3)_4^{2+}] \quad [9]$$

Substituting equations [2] through [5]:

$$[\text{N}_t] = [\text{NH}_3](1 + 10^{-\text{pH}+9.3}) + \beta_1[\text{NH}_3][\text{Ni}^{2+}] + 2\beta_2[\text{NH}_3]^2[\text{Ni}^{2+}] + 3\beta_3[\text{NH}_3]^3[\text{Ni}^{2+}] + 4\beta_4[\text{NH}_3]^4[\text{Ni}^{2+}] \quad [10]$$

For a total ammonia concentration, $[\text{N}_t]$, the free ammonia concentration, $[\text{NH}_3]$, can be obtained from equation [10] by trial and error. (The equilibrium expression for the ammonia species, equation [8], can be used to estimate an initial $[\text{NH}_3]$). From Figure 2, the fraction of each nickel-amine species in the feed solution can be obtained at the calculated pHN_3 .

The percent complexation of the influent nickel can then be determined by:

$$\% \text{Complexation} = \frac{[\text{Ni}(\text{NH}_3)_N^{2+}]}{[\text{Ni}]_T} \quad [11]$$

where, $[\text{Ni}]_T = [\text{Ni}^{2+}] + [\text{Ni}(\text{NH}_3)^{2+}] + [\text{Ni}(\text{NH}_3)_2^{2+}] + [\text{Ni}(\text{NH}_3)_3^{2+}] + [\text{Ni}(\text{NH}_3)_4^{2+}]$

The free ammonia concentrations and percent nickel-amine complexation of the feed solution for the steady state runs of this study are tabulated below.

INFLUENT PARAMETER	COD:TKN = 1.03:1			
	θ_c , days			
	3.0	6.5	13.6	20.0
pH	7.0	7.0	7.0	7.0
* $[N_T]$ (moles/l)	$10^{-1.64}$	$10^{-1.62}$	$10^{-1.61}$	$10^{-1.60}$
$[NH_3]$ (moles/l)	$10^{-3.94}$	$10^{-3.92}$	$10^{-3.91}$	$10^{-3.90}$
** $[Ni^{2+}]$	$10^{-4.89}$	$10^{-4.89}$	$10^{-4.89}$	$10^{-4.89}$
%Ni(II)Complexation	10.3	10.7	10.9	11.1

INFLUENT PARAMETER	COD:TKN = 0.54:1			
	θ_c , days			
	3.0	6.1	14.0	17.8
pH	7.0	7.0	7.0	7.0
$[N_T]$ (moles/l)	$10^{-1.32}$	$10^{-1.31}$	$10^{-1.31}$	$10^{-1.31}$
$[NH_3]$ (moles/l)	$10^{-3.62}$	$10^{-3.61}$	$10^{-3.61}$	$10^{-3.61}$
$[Ni^{2+}]$	$10^{-4.87}$	$10^{-4.89}$	$10^{-4.91}$	$10^{-4.87}$
%Ni(II)Complexation	19.9	20.0	20.0	20.0

$$* X \frac{\text{mg}}{1} \times \frac{1 \text{ mole}}{14,000 \text{ mg}} = X \frac{\text{mole}}{1}$$

$$** X \frac{\text{mg}}{1} \times \frac{1 \text{ mole}}{58,700 \text{ mg}} = X \frac{\text{mole}}{1}$$

In both systems, then, the majority of the influent nickel remains in the uncomplexed state. Thus, an effect of the nickel noted from this experiment will be attributed to the free ion species of the metal.

APPENDIX C

Calculations for Distribution Diagram of Nickel-Hydroxide Complexes

Appendix (C)

Calculations for Distribution Diagram of
Nickel-Hydroxide Complexes

Given:

$$\begin{aligned}
 [\text{Ni}^{2+}] &= 0.77 \text{ mg/l} \\
 &= 0.77 \frac{\text{mg}}{\text{l}} \times \frac{1 \text{ mole}}{58,700 \text{ mg}} = 1.28 \times 10^{-5} \text{ M} = 10^{-4.89} \text{ M}
 \end{aligned}$$

Fraction of Nickel-Hydroxide Species:

$$\alpha_0 = \frac{[\text{Ni}^{2+}]}{[\text{Ni}^{2+}] + [\text{NiOH}^+] + [\text{Ni}(\text{OH})_2] + [\text{HNiO}_2^-]} \quad [1]$$

$$= \frac{1}{1 + \beta_1(\text{OH}^-) + \beta_2(\text{OH}^-)^2 + \beta_3(\text{OH}^-)^3}$$

$$\alpha_1 = [\text{NiOH}^+] = \beta_1[\text{OH}^-] \alpha_0 \quad [2]$$

$$\alpha_2 = [\text{Ni}(\text{OH})_2] = \beta_2[\text{OH}^-]^2 \alpha_0 \quad [3]$$

$$\alpha_3 = [\text{HNiO}_2^-] = \beta_3[\text{OH}^-]^3 \alpha_0 \quad [4]$$

The fraction of each nickel species at various pH values is tabulated below and depicted in Figure 3.

pH	$[\text{OH}^-]^*$	α_0	α_1	α_2	α_3
7	10^{-7}	0.999	\approx	\approx	\approx
8	10^{-6}	0.982	0.002	0.016	\approx
9	10^{-5}	0.382	0.010	0.605	0.004
10	10^{-4}	0.006	0.002	0.951	0.060
11	10^{-3}	\approx	\approx	0.613	0.387
12	10^{-2}	\approx	\approx	0.137	0.863
13	10^{-1}	\approx	\approx	0.017	0.984
14	10^0	\approx	\approx	\approx	0.998

$\text{pOH} = 14 - \text{pH}$

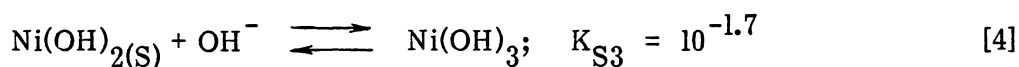
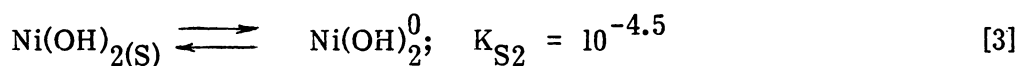
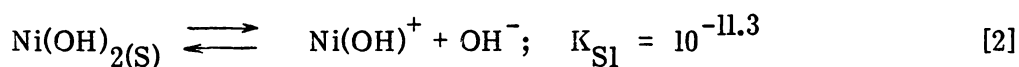
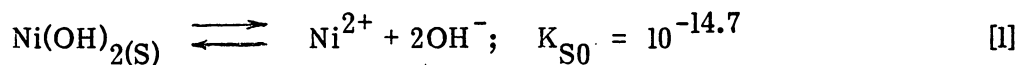
APPENDIX D

Calculations for Theoretical Nickel Hydroxide Solubility Diagram

Appendix (D)

Calculations for Theoretical Nickel Hydroxide Solubility Diagram

Equations utilized to generate solubility data:



where:

$$K_{\text{S0}} = [\text{Ni}^{2+}][\text{OH}^-]^2 \quad [5]$$

$$K_{\text{S1}} = [\text{Ni(OH)}^+][\text{OH}^-] \quad [6]$$

$$K_{\text{S2}} = [\text{Ni(OH)}_2^0] \quad [7]$$

$$K_{\text{S3}} = \frac{[\text{Ni(OH)}_3^-]}{[\text{OH}^-]} \quad [8]$$

Rearranging equations [5] through [8] and putting in logarithmic form:

$$\log[\text{Ni}^{2+}] = \log K_{\text{S0}} - 2\text{pH} + 28 \quad [9]$$

$$\log[\text{Ni(OH)}^+] = \log K_{\text{S1}} - \text{pH} + 14 \quad [10]$$

$$\log[\text{Ni(OH)}_2^0] = \log K_{\text{S2}} \quad [11]$$

$$\log[\text{Ni(OH)}_3^-] = \log K_{\text{S3}} + \text{pH} - 14 \quad [12]$$

Results of the above equations at various pH values are tabulated below and depicted in Figure 6.

pH	$\log[\text{Ni}^{2+}]$	$\log[\text{Ni}(\text{OH})^+]$	$\log[\text{Ni}(\text{OH})_2^0]$	$\log[\text{Ni}(\text{OH})_3^-]$
4	5.3	-1.3	-4.5	-11.7
6	1.3	3.3	-4.5	-9.7
8	-2.7	-5.3	-4.5	-7.7
10	-6.7	-7.3	-4.5	-5.7
12	-10.7	-9.3	-4.5	-3.7
14	-14.7	-11.3	-4.5	-1.7

APPENDIX E

Calculations for the Biokinetic Coefficients Pertaining to Other Nickel Toxicity Studies

Appendix (E)

Calculations for the Biokinetic Coefficients Y_{\max} and k_d for the heterotrophic microorganisms at various nickel concentrations.

Procedure

1. Assume $Y_{\max_1} = 0.20$ and $k_{d_1} = 0.04 \text{ days}^{-1}$ for nitrification.
2. At each θ_c , calculate the specific utilization rate, U_1 , from the following equation:

$$\frac{1}{\theta_c} = Y_{\max_1} N_1 - k_{d_1} \quad [1]$$

3. Calculate the autotrophic MLSS, X_1 , from the following equation:

$$U_1 = \frac{S_o - S_e}{\theta X_1} \quad [2]$$

4. Subtract X_1 from the total MLSS, X_t , to obtain the heterotrophic MLSS, X_2 .
5. Obtain U_2 for the heterotrophs from:

$$U_2 = \frac{S_o - S_e}{\theta X_2} \quad [3]$$

6. Plot $1/\theta_c$ versus U_2 , or specific growth rate versus specific utilization rate, and obtain the Y_{\max_2} and k_{d_2} for the heterotrophic microorganisms.

7. Calculate Y_{obs} at each θ_c from:

$$Y_{obs_2} = \frac{Y_{max_2}}{1 + K_{d_2} \theta_c} \quad [4]$$

Results of the calculations for the biokinetic coefficients Y_{max_2} and k_{d_2} of the heterotrophic microorganisms at various nickel concentrations are tabulated below.

θ_c days	Y_1	K_{d_1} days ⁻¹	U_1 mg/l	X_1 mg/l	X_T mg/l	X_2 days ⁻¹	U_2 days ⁻¹	Y_2	k_{d_2} days ⁻¹	Y_{obs}
CONTROL REACTOR COD:TKN = 3.71:1										
5.8	0.20	0.04	1.062	14	1156	1142	0.553	0.372	0.036	0.308
11.5	0.20	0.04	0.635	111	1920	1809	0.363	0.372	0.036	0.263
12.3	0.20	0.04	0.607	85	2120	2035	0.306	0.372	0.036	0.258
16.4	0.20	0.04	0.505	142	2681	2539	0.250	0.372	0.036	0.234
Ni(II) = 0.54 mg/l (49) COD:TKN = 7.3:1										
5.0	0.20	0.04	1.200	2	994	992	0.626	0.396	0.065	0.300
7.1	0.20	0.04	0.900	32	1086	2054	0.562	0.396	0.065	0.271
13.2	0.20	0.04	0.580	157	1942	1785	0.379	0.396	0.065	0.213
14.8	0.20	0.04	0.535	170	2363	2193	0.305	0.396	0.065	0.202
Ni(II) = 0.58 mg/l (41) COD:TKN = 3.71:1										
6.0	0.20	0.04	1.035	60	1258	1198	0.510	0.464	0.070	0.327
8.9	0.20	0.04	0.760	130	1721	1591	0.395	0.464	0.070	0.286
12.0	0.20	0.04	0.615	170	2158	1988	0.330	0.464	0.070	0.252
Ni(II) = 0.77 mg/l COD:TKN = 1.03:1										
3.0	0.20	0.04	1.867	5	786	781	0.793	0.549	0.104	0.418
6.5	0.20	0.04	0.969	115	1436	1321	0.473	0.549	0.104	0.327
13.6	0.20	0.04	0.567	227	2214	1987	0.337	0.549	0.104	0.227
20.0	0.20	0.04	0.450	261	2731	2470	0.267	0.549	0.104	0.178
Ni(II) = 0.77 mg/l COD:TKN = 0.54:1										
3.0	0.20	0.04	1.867	9	776	767	0.782	0.533	0.083	0.427
6.1	0.20	0.04	1.020	127	1400	1273	0.454	0.533	0.083	0.354
14.0	0.20	0.04	0.557	202	2451	2249	0.295	0.533	0.083	0.247
17.8	0.20	0.04	0.481	232	2477	2245	0.259	0.533	0.083	0.215
Ni(II) = 1.00 mg/l (34) COD:TKN = 3.71:1										
5.2	0.20	0.04	1.170	2	1106	1104	0.575	0.617	0.163	0.334
10.6	0.20	0.04	0.675	4	1475	1471	0.429	0.617	0.163	0.226
14.5	0.20	0.04	0.545	5	1716	1711	0.368	0.617	0.163	0.183

APPENDIX F

Raw Data for the Steady State Runs of the
Completely-Mixed Activated Sludge Units

F-1

Raw Data for Control Reactor, COD = 386 mg/l, $\theta_c = 5.8$ Days

Date (1978)	MLSS		θ_c (days)	pH		Alkalinity as CaCO ₃			COD		
	Reactor Solids (mg/l)	Effluent Solids (mg/l)		Feed (mg/l)	Effluent Unfiltered (mg/l)	Feed (mg/l)	Effluent Unfiltered (mg/l)	Net Change (%)	Feed (mg/l)	Effluent Filtered (mg/l)	Removal Efficiency (%)
3-29	1212	18	5.7	7.1	7.5	228	305	33.8	375	20	94.7
3-30	1128	14	5.8	7.2	7.5	241	288	19.5	382	16	95.8
3-31	1132	12	5.9	7.2	7.5	250	293	17.2	390	24	93.9
4-1	1204	18	5.7	7.1	7.5	255	294	15.3	378	20	94.7
4-2	1012	9	6.1	7.2	7.6	264	304	15.2	398	16	96.0
4-3	1248	19	5.7	7.2	7.5	249	298	19.7	392	16	95.9
AVG	1156	15	5.8	7.2	7.5	248	297	20.1	386	19	95.2

Date (1978)	NH ₃ -N Concentration			Org-N Concentration			TKN Concentration			NO ₃ ⁻ -N		COD:TKN	
	Feed (mg/l)	Effluent Filtered (mg/l)	Net Change (%)	Feed (mg/l)	Effluent Filtered (mg/l)	Net Change (%)	Feed (mg/l)	Effluent Filtered (mg/l)	Net Change (%)	Feed (mg/l)	Effluent (mg/l)	(mg/l)	(mg/l)
3-29	62.7	79.5	26.8	45.9	3.9	-91.5	108.6	83.4	23.2	0.5	7.5	1:3.45	
3-30	58.2	78.4	33.6	51.0	4.5	-91.2	109.2	82.9	24.1	0.5	7.0	1:3.40	
3-31	56.0	78.4	40.0	50.4	1.1	-97.8	106.4	79.5	25.3	0.5	8.5	1:3.67	
4-1	59.4	78.4	32.0	50.4	3.9	-92.3	109.8	82.3	25.0	0.5	12.5	1:3.44	
4-2	60.5	77.8	28.6	48.1	5.1	-85.4	108.6	82.9	23.7	0.5	10.5	1:3.66	
4-3	58.2	77.3	32.8	46.5	4.5	-90.3	107.9	82.1	23.9	0.5	7.0	1:3.74	
AVG	59.2	78.3	32.3	48.7	3.8	-91.4	107.9	82.1	23.9	0.5	8.8	1:3.58	

F-II

Raw Data for Control Reactor, COD = 405 mg/l, $\theta_c = 11.5$ Days

Date (1978)	MLSS		θ_c (days)	pH		Alkalinity as CaCO ₃			COD		
	Reactor Solids (mg/l)	Effluent Solids (mg/l)		Feed (mg/l)	Effluent Unfiltered (mg/l)	Feed (mg/l)	Effluent Unfiltered (mg/l)	Net Change (%)	Feed (mg/l)	Effluent Filtered (mg/l)	Removal Efficiency (%)
6-4	1952	2	11.9	7.3	6.5	269	88	-67.3	427	32	92.5
6-5	1956	2	11.9	7.2	6.6	258	107	-58.5	399	30	92.5
6-6	1956	2	11.9	7.3	6.7	257	117	-54.4	383	18	95.3
6-7	1952	8	11.2	7.2	6.6	259	106	-59.1	403	24	94.0
6-8	1852	14	10.6	7.3	6.7	254	111	-56.3	427	22	94.9
6-9	1896	2	11.9	7.3	6.6	251	107	-57.4	399	18	95.5
6-10	1876	7	11.3	7.2	6.6	268	107	-60.1	395	18	95.4
AVG	1920	5	11.5	7.2	6.6	259	106	-59.0	405	23	94.3

Date (1978)	NH ₃ -N Concentration			Org-N Concentration			TKN Concentration			NO ₃ ⁻ -N		COD:TKN	
	Feed (mg/l)	Effluent Filtered (mg/l)	Net Change (%)	Feed (mg/l)	Effluent Filtered (mg/l)	Net Change (%)	Feed (mg/l)	Effluent Filtered (mg/l)	Net Change (%)	Feed (mg/l)	Effluent (mg/l)	(mg/l)	(mg/l)
6-4	53.8	49.3	-8.4	56.0	1.1	-98.0	109.8	50.4	54.0	0.5	46.5		1:3.89
6-5	54.8	48.2	-12.0	52.2	2.2	-95.8	107.0	50.4	53.0	0.5	40.5		1:3.73
6-6	53.8	48.2	-10.4	49.8	3.3	-93.4	103.6	51.5	51.0	0.5	40.5		1:3.70
6-7	56.0	49.3	-12.0	52.6	2.2	-95.8	108.6	51.5	53.0	0.5	41.5		1:3.71
6-8	56.0	50.4	-10.0	54.9	3.4	-93.8	110.9	53.8	52.0	0.5	38.0		1:3.85
6-9	54.9	49.3	-10.2	50.4	1.1	-97.8	105.3	50.4	53.0	0.5	41.5		1:3.79
6-10	53.8	46.5	-13.6	51.5	4.5	-91.3	105.3	51.0	52.0	0.5	42.0		1:3.76
AVG	54.7	48.7	-10.9	52.5	2.5	-95.1	107.2	51.2	53.0	0.5	41.5		1:3.78

F-III

Raw Data for Control Reactor, COD = 390 mg/l, $\theta_c = 12.3$ Days

Date (1978)	MLSS		θ_c (days)	pH		Alkalinity as CaCO ₃			COD		
	Reactor Solids (mg/l)	Effluent Solids (mg/l)		Feed (mg/l)	Effluent Unfiltered (mg/l)	Feed (mg/l)	Effluent Unfiltered (mg/l)	Net Change (%)	Feed (mg/l)	Effluent Filtered (mg/l)	Removal Efficiency (%)
3-9	2164	28	12.5	7.1	7.0	218	132	-16.5	391	31	92.1
3-10	2144	25	12.8	7.0	6.9	221	172	-22.2	385	27	93.0
3-11	2056	24	12.8	7.1	6.8	232	156	-32.8	372	27	92.7
3-12	2152	15	14.2	7.1	6.8	243	155	-36.2	391	28	92.8
3-13	2072	36	11.4	7.1	6.7	232	141	-39.2	387	23	94.1
3-14	2104	44	10.7	7.1	6.7	232	132	-43.1	400	35	91.3
3-15	2148	36	11.6	6.9	6.8	220	218	-0.9	402	23	94.3
AVG	2120	30	12.3	7.1	6.8	228	165	-27.3	390	28	92.9

Date (1978)	NH ₃ -N Concentration			Org-N Concentration			TKN Concentration			NO ₃ ⁻ -N		COD:TKN	
	Feed (mg/l)	Effluent Filtered (mg/l)	Net Change (%)	Feed (mg/l)	Effluent Filtered (mg/l)	Net Change (%)	Feed (mg/l)	Effluent Filtered (mg/l)	Net Change (%)	Feed (mg/l)	Effluent (mg/l)	(mg/l)	(mg/l)
3-9	44.8	51.5	15.0	50.4	1.7	-96.6	95.2	53.2	44.1	0.5	13.3		1:4.11
3-10	47.0	55.3	17.7	52.6	2.2	-95.8	99.6	57.5	42.3	0.5	26.6		1:3.87
3-11	49.3	52.6	6.7	51.5	3.9	-93.4	100.8	56.5	43.9	0.5	26.6		1:3.69
3-12	55.4	57.1	3.1	51.0	2.2	-95.7	106.4	59.3	44.3	0.5	55.8		1:3.67
3-13	59.9	57.1	-4.7	48.7	3.4	-93.0	108.6	60.5	44.3	0.5	28.3		1:3.56
3-14	49.8	54.9	10.2	52.1	3.4	-93.5	101.9	58.3	42.8	0.5	37.5		1:3.93
3-15	51.0	30.2	-40.8	51.1	4.5	-85.3	102.1	34.7	66.1	0.5	24.2		1:3.94
AVG	51.0	51.2	-1.0	51.1	3.0	-93.3	102.1	54.2	46.9	0.5	30.3		1:3.82

F-IV

Raw Data for Control Reactor, COD = 396 mg/l, $\theta_c = 16.4$ Days

Date (1978)	MLSS		θ_c (days)	pH		Alkalinity as CaCO ₃			COD		
	Reactor Solids (mg/l)	Effluent Solids (mg/l)		Feed (mg/l)	Effluent Unfiltered (mg/l)	Feed (mg/l)	Effluent Unfiltered (mg/l)	Net Change (%)	Feed (mg/l)	Effluent Filtered (mg/l)	Removal Efficiency (%)
7-26	2620	6	16.0	7.2	6.7	264	136	-48.5	399	12	97.0
7-27	2644	2	16.7	7.3	6.7	276	128	-53.6	413	35	91.5
7-28	2668	2	16.7	7.3	6.6	264	108	-59.1	396	29	92.7
7-29	2724	2	16.7	7.2	6.6	261	102	-60.9	393	29	92.6
7-30	2692	1	16.8	7.2	6.5	263	88	-66.5	403	27	93.3
7-31	2772	4	16.3	7.2	6.5	254	101	-60.2	396	26	93.4
8-1	2776	0	17.0	7.2	6.5	260	99	-61.9	374	35	90.6
8-2	2656	4	16.3	7.2	6.6	256	96	-62.5	395	26	93.4
8-3	2636	10	15.4	7.2	6.5	264	84	-68.2	401	37	90.8
8-4	2620	6	16.0	7.2	6.5	264	82	-68.9	387	12	96.9
AVG	2681	4	16.4	7.2	6.6	263	102	-61.0	396	27	93.2

Date (1978)	NH ₃ -N Concentration			Org-N Concentration			TKN Concentration			NO ₃ ⁻ -N		COD:TKN (mg/l) (mg/l)
	Feed (mg/l)	Effluent Filtered (mg/l)	Net Change (%)	Feed (mg/l)	Effluent Filtered (mg/l)	Net Change (%)	Feed (mg/l)	Effluent Filtered (mg/l)	Net Change (%)	Feed (mg/l)	Effluent (mg/l)	
7-26	55.4	50.4	-9.0	51.6	2.8	-94.6	107.0	53.2	50.3	0.5	38.4	1:3.73
7-27	66.1	50.4	-23.8	47.6	2.8	-94.1	113.7	53.2	53.2	0.5	31.5	1:3.63
7-28	57.7	49.0	-15.1	49.6	2.8	-94.4	107.3	51.8	51.7	0.5	40.0	1:3.69
7-29	54.9	50.4	-8.2	51.5	2.8	-94.6	106.4	53.2	50.0	0.5	37.0	1:3.69
7-30	52.5	49.0	-6.7	50.5	2.8	-94.5	103.0	51.8	49.7	0.5	40.0	1:3.91
7-31	57.7	49.3	-14.6	49.6	2.8	-94.4	107.3	52.1	51.4	0.5	42.2	1:3.69
8-1	57.1	50.4	-11.7	47.1	2.8	-94.1	104.2	53.2	48.9	0.5	53.0	1:3.59
8-2	58.2	49.3	-15.3	51.6	2.8	-94.6	109.8	52.1	52.6	0.5	42.2	1:3.60
8-3	58.2	46.5	-20.1	48.7	4.5	-90.8	106.9	51.0	52.3	0.5	45.9	1:3.75
8-4	59.4	49.3	-17.0	47.0	1.1	-97.7	106.4	50.4	52.6	0.5	51.5	1:3.64
AVG	57.7	49.4	-14.2	49.6	2.8	-94.4	107.3	52.2	52.6	0.5	42.2	

F-V

RAW DATA FOR COD:TKN = 1.06:1, $\theta_c = 3.0$ days
 Ni(II) = 0.75 mg/l

Date	MLSS		θ_c (days)	Ni(II) Concentration			pH		Alkalinity as CaCO ₃			COD		
	Reactor Solids (mg/l)	Effluent Solids (mg/l)		Feed (mg/l)	Effluent Unfiltered (mg/l)	Effluent Filtered (mg/l)	Feed	Effluent Unfiltered	Feed (mg/l)	Effluent Unfiltered (mg/l)	Net Change (%)	Feed (mg/l)	Effluent Filtered (mg/l)	Removal Efficiency (%)
11-15	800	24	3.2	0.77	0.68	0.64	7.0	7.2	453	514	+13.5	403	28	93.1
11-16	820	30	3.2	0.74	0.68	0.64	7.0	7.3	453	530	+17.0	423	24	94.3
11-17	820	39	3.0	0.75	0.69	0.65	7.0	7.3	455	528	+16.0	413	24	94.2
11-18	790	51	2.9	0.74	0.69	0.70	7.0	7.2	450	537	+19.3	381	28	92.7
11-19	690	40	2.9	0.76	0.70	0.63	7.0	7.2	455	540	+18.7	395	30	92.4
11-20	850	57	2.8	0.78	0.64	0.64	7.0	7.3	448	544	+21.4	399	20	95.0
11-21	730	35	3.1	0.73	0.71	0.66	7.0	7.3	449	544	+21.2	423	32	92.4
AVG	786	39	3.0	0.75	0.68	0.65	7.0	7.3	452	534	+18.2	405	27	93.3

Date	NH ₃ -N Concentration			ORG-N Concentration			TKN Concentration			NO ₃ -N Concentration			COD:TKN (mg/l)/(mg/l)
	Feed (mg/l)	Effluent Filtered (mg/l)	Net Change (%)	Feed (mg/l)	Effluent Filtered (mg/l)	Net Change (%)	Feed (mg/l)	Effluent Filtered (mg/l)	Net Change (%)	Feed (mg/l)	Effluent Filtered (mg/l)	Net Change (mg/l)	
11-15	331.7	334.6	+0.9	56.3	5.9	-89.5	388.0	340.5	12.2	0.6	8.7	+8.1	1.04:1
11-16	306.5	337.6	+10.1	65.2	--	-100.0	371.7	337.6	9.2	0.6	7.4	+6.8	1.14:1
11-17	313.9	330.2	+5.2	59.2	5.9	-90.0	373.1	336.1	9.9	0.6	8.3	+7.7	1.11:1
11-18	325.8	345.0	+5.9	62.2	3.0	-95.2	388.0	348.0	10.3	0.5	5.3	+4.8	0.98:1
11-19	328.7	349.4	+6.3	51.8	5.9	-88.6	380.5	355.3	6.6	0.2	4.2	+4.0	1.04:1
11-20	328.7	340.6	+3.6	59.2	5.9	-90.0	387.9	346.5	10.7	0.2	2.8	+2.6	1.03:1
11-21	331.7	334.6	+0.9	57.8	3.0	-94.8	389.5	334.9	14.0	0.2	2.7	+2.5	1.09:1
AVG	323.9	338.9	+4.6	58.8	4.2	-92.9	382.7	342.7	10.4	0.4	5.6	+5.2	1.06:1

F-VI

RAW DATA FOR COD:TKN = 1.02:1, $\theta_c = 6.5$ days
 NI = 0.77 mg/l

Date	MLSS		θ_c (days)	Ni(II) Concentration			pH		Alkalinity as CaCO ₃			COD		
	Reactor Solids (mg/l)	Effluent Solids (mg/l)		Feed (mg/l)	Effluent Unfiltered (mg/l)	Effluent Filtered (mg/l)	Feed	Effluent Unfiltered	Feed (mg/l)	Effluent Unfiltered (mg/l)	Net Change (%)	Feed (mg/l)	Effluent Filtered (mg/l)	Removal Efficiency (%)
10-24	1510	42	6.2	0.80	0.71	0.67	7.0	5.6	459	39	-91.5	400	34	91.6
10-25	1540	31	6.7	0.77	0.69	0.69	7.0	5.6	457	39	-91.5	406	32	92.1
10-26	1410	42	6.1	0.77	0.68	0.66	7.0	5.6	459	35	-92.4	400	32	92.0
10-27	1390	25	6.9	0.78	0.67	0.64	7.0	5.7	463	41	-91.1	408	26	93.6
10-28	1390	16	7.4	0.76	0.68	0.64	7.0	5.7	463	47	-89.8	398	24	94.0
10-29	1420	48	5.9	0.75	0.65	0.67	7.0	5.6	465	35	-92.5	404	22	94.6
10-30	1390	33	6.5	0.76	0.67	0.65	7.0	5.6	461	35	-92.4	406	24	94.1
AVG	1436	34	6.5	0.77	0.68	0.66	7.0	5.6	461	39	-91.6	403	28	93.1

Date	NH ₃ -N Concentration			ORG-N Concentration			TKN Concentration			NO ₃ -N Concentration			COD:TKN (mg/l)/(mg/l)
	Feed (mg/l)	Effluent Filtered (mg/l)	Net Change (%)	Feed (mg/l)	Effluent Filtered (mg/l)	Net Change (%)	Feed (mg/l)	Effluent Filtered (mg/l)	Net Change (%)	Feed (mg/l)	Effluent Filtered (mg/l)	Net Change (mg/l)	
10-24	336.5	263.5	-21.7	53.6	4.5	-91.6	390.1	268.0	-31.3	0.6	66.0	+65.4	1.03:1
10-25	333.5	268.8	-19.4	56.6	4.5	-92.0	390.1	273.3	-29.9	0.2	64.4	+64.2	1.04:1
10-26	335.0	270.2	-19.3	59.6	4.5	-92.4	394.6	274.7	-30.4	0.4	65.0	+64.6	1.01:1
10-27	336.5	257.6	-23.4	56.6	4.5	-92.0	393.1	262.1	-33.3	0.3	47.0	+46.7	1.04:1
10-28	343.9	263.5	-23.4	56.6	4.5	-92.0	400.5	268.0	-33.1	0.4	71.5	+71.1	0.99:1
10-29	336.5	265.0	-21.2	62.5	6.0	-90.4	399.0	271.0	-32.1	0.3	77.0	+76.7	1.01:1
10-30	333.5	260.6	-21.9	55.1	3.0	-94.6	388.5	263.6	-32.1	0.1	79.0	+78.9	1.05:1
AVG	336.5	264.2	-21.5	57.2	4.5	-92.1	393.7	268.7	-31.7	0.3	67.1	+66.8	1.02:1

F-VII

RAW DATA FOR COD:TKN = 1.02:1, $\theta_c = 13.6$ days
 Ni(II) = 0.77 mg/l

Date	MLSS		θ_c (days)	Ni(II) Concentration			pH		Alkalinity as CaCO ₃			COD		
	Reactor Solids (mg/l)	Effluent Solids (mg/l)		Feed (mg/l)	Effluent Unfiltered (mg/l)	Effluent Filtered (mg/l)	Feed	Effluent Unfiltered	Feed (mg/l)	Effluent Unfiltered (mg/l)	Net Change (%)	Feed (mg/l)	Effluent Filtered (mg/l)	Removal Efficiency (%)
8-18	2010	15	12.8	0.83	0.80	0.75	7.0	5.3	453	21	-95.4	385	28	92.7
8-19	2340	12	13.5	0.78	0.76	0.73	7.0	5.3	437	21	-95.2	404	37	90.8
8-20	2140	8	14.1	0.75	0.81	0.71	7.0	5.3	450	21	-95.3	404	28	93.1
8-21	2190	7	14.2	0.75	0.73	0.71	7.0	5.4	448	22	-95.1	430	28	93.5
8-22	2170	9	14.0	0.77	0.75	0.73	7.0	5.3	448	20	-95.5	398	29	92.7
8-23	2290	15	13.3	0.74	0.80	0.79	7.0	5.2	448	13	-97.1	398	28	93.0
8-24	2360	12	13.6	0.74	0.72	0.71	7.0	5.2	450	16	-96.4	412	26	93.7
AVG	2214	11	13.6	0.77	0.77	0.73	7.0	5.3	448	19	-95.7	404	29	92.8

Date	NH ₃ -N Concentration			ORG-N Concentration			TKN Concentration			NO ₃ -N Concentration			COD:TKN (mg/l)/(mg/l)
	Feed (mg/l)	Effluent Filtered (mg/l)	Net Change (%)	Feed (mg/l)	Effluent Filtered (mg/l)	Net Change (%)	Feed (mg/l)	Effluent Filtered (mg/l)	Net Change (%)	Feed (mg/l)	Effluent Filtered (mg/l)	Net Change (mg/l)	
8-18	339.4	288.4	-15.0	53.1	5.8	-89.1	392.5	294.2	-25.0	0.3	76.8	+76.5	0.98:1
8-19	347.3	301.3	-13.2	54.7	6.5	-88.1	402.0	307.8	-23.4	0.5	70.7	+70.2	1.00:1
8-20	335.8	290.5	-13.5	59.2	4.3	-92.7	395.0	294.8	-25.4	0.3	66.5	+66.2	1.02:1
8-21	345.7	289.5	-16.3	57.6	5.1	-91.2	403.3	294.6	-27.0	0.4	67.6	+67.2	1.07:1
8-22	345.7	271.7	-21.4	55.9	4.3	-92.3	401.6	276.0	-31.3	0.4	76.2	+75.8	0.99:1
8-23	345.7	282.8	-18.2	55.9	5.8	-89.6	401.6	288.6	-28.1	0.5	78.4	+77.9	0.99:1
8-24	342.4	289.6	-15.4	55.9	4.3	-92.3	389.3	293.9	-24.5	0.5	70.7	+70.2	1.06:1
AVG	343.1	287.7	-16.1	56.0	5.2	-90.8	397.9	292.8	-22.9	0.4	72.4	+72.0	1.02:1

F-VIII

RAW DATA FOR COD:TKN = 1.03:1, $\theta_c = 20.0$ days
 Ni(II) = 0.77 mg/l

Date	MLSS		θ_c (days)	Ni(II) Concentration			pH		Alkalinity as CaCO ₃			COD		
	Reactor Solids (mg/l)	Effluent Solids (mg/l)		Feed (mg/l)	Effluent Unfiltered (mg/l)	Effluent Filtered (mg/l)	Feed	Effluent Unfiltered	Feed (mg/l)	Effluent Unfiltered (mg/l)	Net Change (%)	Feed (mg/l)	Effluent Filtered (mg/l)	Removal Efficiency (%)
6-21	2500	15	19.4	0.79	0.77	0.77	7.0	5.4	452	25	-94.5	446	20	95.5
6-22	2610	15	19.7	0.78	0.75	0.75	7.0	5.4	449	23	-94.9	446	16	96.4
6-23	2680	12	20.7	0.77	0.73	0.72	7.0	5.3	443	19	-95.7	422	16	96.2
6-24	2870	12	21.2	0.75	0.76	0.74	6.9	5.3	435	16	-96.3	406	16	96.1
6-25	2800	16	20.1	0.76	0.70	0.70	7.0	5.5	435	27	-93.8	402	16	96.0
6-26	2840	16	20.0	0.80	0.73	0.74	7.0	5.4	433	24	-94.4	402	12	97.0
6-27	2820	20	18.8	0.75	0.73	0.69	7.0	5.4	429	25	-94.2	406	16	96.1
AVG	2731	15	20.0	0.77	0.74	0.73	7.0	5.4	439	23	-94.8	419	16	96.2

Date	NH ₃ -N Concentration			ORG-N Concentration			TKN Concentration			NO ₃ -N Concentration			COD:TKN (mg/l)/(mg/l)
	Feed (mg/l)	Effluent Filtered (mg/l)	Net Change (%)	Feed (mg/l)	Effluent Filtered (mg/l)	Net Change (%)	Feed (mg/l)	Effluent Filtered (mg/l)	Net Change (%)	Feed (mg/l)	Effluent Filtered (mg/l)	Net Change (mg/l)	
6-21	356.4	316.4	-11.2	54.6	3.3	-94.0	411.0	319.7	-22.2	0.7	72.0	+71.3	1.09:1
6-22	349.1	289.5	-17.1	52.7	3.3	-93.7	401.8	292.8	-27.1	0.6	74.0	+73.4	1.11:1
6-23	356.4	298.2	-16.3	54.6	1.8	-96.7	411.0	300.0	-27.0	0.6	76.5	+75.9	1.03:1
6-24	360.0	287.3	-20.2	56.4	1.1	-98.0	416.4	288.4	-30.7	0.7	70.0	+69.3	0.98:1
6-25	334.6	287.3	-14.1	54.6	3.3	-94.0	389.2	290.6	-25.3	0.6	66.5	+65.9	1.03:1
6-26	349.1	290.9	-16.7	52.7	0.7	-98.7	401.8	291.6	-27.4	0.7	67.5	+66.8	1.00:1
6-27	352.7	290.9	-17.5	52.7	1.8	-96.6	405.4	292.7	-27.8	0.6	75.0	+74.4	1.00:1
AVG	351.2	294.4	-16.2	54.0	2.2	-96.0	405.2	296.5	-26.8	0.6	71.6	+71.0	1.03:1

F-IX

RAW DATA FOR COD:TKN = 1:1.81, $\theta_c = 3.0$ days
 Ni(II) = 0.79 mg/l

Date	MLSS		θ_c (days)	Ni(II) Concentration			pH		Alkalinity as CaCO ₃			COD		
	Reactor Solids (mg/l)	Effluent Solids (mg/l)		Feed (mg/l)	Effluent Unfiltered (mg/l)	Effluent Filtered (mg/l)	Feed	Effluent Unfiltered	Feed (mg/l)	Effluent Unfiltered (mg/l)	Net Change (%)	Feed (mg/l)	Effluent Filtered (mg/l)	Removal Efficiency (%)
12-9	940	32	3.2	0.80	0.75	0.70	7.0	7.1	451	458	+1.6	399	23	94.2
12-10	830	55	2.8	0.78	0.76	0.68	7.0	7.1	446	501	+12.3	414	30	92.8
12-11	820	54	2.9	0.78	0.76	0.68	7.0	7.2	456	505	+10.7	388	30	92.3
12-12	720	59	2.7	0.81	0.76	0.72	7.0	7.1	444	510	+14.9	414	34	91.8
12-13	790	53	2.8	0.81	0.77	0.75	7.0	7.2	442	510	+15.4	403	34	91.6
12-14	670	20	3.3	0.80	0.75	0.68	7.0	7.2	446	504	+13.0	399	34	91.5
12-15	660	20	3.3	0.77	0.76	0.71	7.0	7.2	434	504	+16.1	407	30	92.6
AVG	776	42	3.0	0.79	0.76	0.70	7.0	7.2	446	499	+11.9	403	31	92.3

Date	NH ₃ -N Concentration			ORG-N Concentration			TKN Concentration			NO ₃ -N Concentration			COD:TKN (mg/l)/(mg/l)
	Feed (mg/l)	Effluent Filtered (mg/l)	Net Change (%)	Feed (mg/l)	Effluent Filtered (mg/l)	Net Change (%)	Feed (mg/l)	Effluent Filtered (mg/l)	Net Change (%)	Feed (mg/l)	Effluent Filtered (mg/l)	Net Change (mg/l)	
12-9	688.0	681.9	-0.9	52.2	9.2	-82.4	740.2	691.1	-6.6	0.4	19.3	18.9	1:1.86 0.54:1
12-10	665.0	660.4	-0.7	58.4	9.2	-84.2	723.4	669.6	-7.4	0.5	10.5	10.0	1:1.75 0.57:1
12-11	688.0	665.0	-3.3	61.4	6.1	-90.1	749.4	671.1	-10.4	0.3	9.4	9.1	1:1.93 0.52:1
12-12	654.2	651.2	-0.5	55.3	4.6	-91.7	709.5	655.8	-7.6	0.5	10.3	9.8	1:1.71 0.58:1
12-13	684.9	669.6	-2.2	52.2	3.1	-94.1	737.1	672.7	-8.7	0.6	9.1	8.5	1:1.83 0.55:1
12-14	669.6	672.7	+0.5	56.8	12.3	-78.3	726.4	685.0	-5.7	0.4	6.3	5.9	1:1.82 0.55:1
12-15	666.5	681.9	+2.3	64.5	9.2	-85.7	731.0	691.1	-5.5	0.5	4.6	4.1	1:1.80 0.56:1
AVG	673.7	669.0	-0.7	57.3	7.7	-86.6	731.0	676.7	-7.4	0.5	9.9	9.4	1:1.81 0.55:1

RAW DATA FOR COD:TKN = 1:1.92, $\theta_c = 6.1$ days
 Ni(II) = 0.76 mg/l

Date	MLSS		θ_c (days)	Ni(II) Concentration			pH		Alkalinity as CaCO ₃			COD		
	Reactor Solids (mg/l)	Effluent Solids (mg/l)		Feed (mg/l)	Effluent Unfiltered (mg/l)	Effluent Filtered (mg/l)	Feed	Effluent Unfiltered	Feed (mg/l)	Effluent Unfiltered (mg/l)	Net Change (%)	Feed (mg/l)	Effluent Filtered (mg/l)	Removal Efficiency (%)
11-13	1380	32	6.4	0.77	0.71	0.70	7.0	5.8	454	66	-85.5	391	24	93.9
11-14	1460	33	6.7	0.73	0.70	0.69	7.0	5.8	454	70	-84.6	395	24	93.9
11-15	1360	71	5.3	0.78	0.68	0.64	7.0	5.8	447	69	-84.6	387	34	91.2
11-16	1380	42	6.2	0.77	0.64	0.62	7.0	5.9	455	95	-79.1	387	34	91.2
11-17	1380	67	5.2	0.76	0.59	0.57	7.0	6.0	455	106	-76.7	383	34	91.1
11-18	1480	30	6.7	0.80	0.54	0.61	7.0	6.1	462	123	-73.4	399	65	83.7
11-19	1350	33	6.6	0.72	0.58	0.55	7.0	6.2	455	141	-69.0	367	30	91.8
AVG	1400	45	6.1	0.76	0.70	0.68	7.0	5.8	452	68	-85.0	391	27	93.1

Date	NH ₃ -N Concentration			ORG-N Concentration			TKN Concentration			NO ₃ -N Concentration			COD:TKN (mg/l)/(mg/l)
	Feed (mg/l)	Effluent Filtered (mg/l)	Net Change (%)	Feed (mg/l)	Effluent Filtered (mg/l)	Net Change (%)	Feed (mg/l)	Effluent Filtered (mg/l)	Net Change (%)	Feed (mg/l)	Effluent Filtered (mg/l)	Net Change (mg/l)	
11-13	692.5	629.8	-9.1	56.7	11.9	-79.0	749.2	641.7	14.3	0.7	72.7	72.0	1:1.92 0.52:1
11-14	692.5	613.4	-11.4	53.7	13.4	-75.0	746.2	626.8	16.0	0.5	86.0	85.5	1:1.89 0.53:1
11-15	686.5		-9.1	56.7	10.5	-81.5	743.2	634.3	14.7	0.7	86.5	85.8	1:1.92 0.52:1
11-16	679.6	626.8	-7.8	62.2	13.4	-78.5	741.8	640.2	13.7	0.8	82.2	81.4	1:1.92
11-17	684.1	626.8	-8.4	59.2	14.9	-74.8	743.3	641.7	13.7	0.3	83.6	83.3	1:1.94
11-18	685.6	665.6	-2.9	56.3	13.4	-76.2	741.9	679.0	8.5	0.3	81.0	80.7	1:1.86
11-19	681.1	635.8	-6.7	56.3	10.5	-81.3	737.4	646.3	12.4	0.3	75.5	75.2	1:2.01
AVG	690.5	622.3	-9.9	55.7	11.9	-78.6	746.2	634.3	-15.0	0.6	81.7	81.1	1:1.91

F-XI

RAW DATA FOR COD:TKN = 1:1.74, $\theta_c = 14.1$ days

Ni(II) = 0.73 mg/l

Date	MLSS		θ_c (days)	Ni(II) Concentration			pH		Alkalinity as CaCO ₃			COD		
	Reactor Solids (mg/l)	Effluent Solids (mg/l)		Feed (mg/l)	Effluent Unfiltered (mg/l)	Effluent Filtered (mg/l)	Feed	Effluent Unfiltered	Feed (mg/l)	Effluent Unfiltered (mg/l)	Net Change (%)	Feed (mg/l)	Effluent Filtered (mg/l)	Removal Efficiency (%)
10-7	2450	18	13.1	0.73	0.73	0.72	7.0	5.2	454	18	-96.0	446	28	-93.7
10-8	2530	9	14.2	0.73	0.73	0.71	7.0	5.2	452	18	-96.0	450	28	-93.8
10-9	2390	20	12.7	0.73	0.71	0.71	7.0	5.2	452	18	-96.0	398	28	-93.0
10-10	2500	9	14.2	0.72	0.72	0.71	7.0	5.2	456	19	-95.8	398	31	-92.2
10-11	2460	3	15.0	0.73	0.73	0.73	7.0	5.2	445	17	-96.2	429	24	-94.4
10-12	2390	7	14.4	0.72	0.74	0.72	7.0	5.2	452	16	-96.5	429	28	-93.5
10-13	2440	10	14.1	0.75	0.76	0.74	7.0	5.2	452	17	-96.2	433	28	-93.5
AVG	2451	11	14.0	0.73	0.73	0.72	7.0	5.2	452	18	-96.0	426	28	-93.4

Date	NH ₃ -N Concentration			ORG-N Concentration			TKN Concentration			NO ₃ -N Concentration			COD:TKN (mg/l)/(mg/l)
	Feed (mg/l)	Effluent Filtered (mg/l)	Net Change (%)	Feed (mg/l)	Effluent Filtered (mg/l)	Net Change (%)	Feed (mg/l)	Effluent Filtered (mg/l)	Net Change (%)	Feed (mg/l)	Effluent Filtered (mg/l)	Net Change (mg/l)	
10-7	688.6	607.0	-11.9	56.4	--	-100.0	745.0	607.0	18.5	0.3	68.6	68.3	1:1.67
10-8	679.7	587.7	-13.5	59.4	--	-100.0	739.1	587.7	20.5	0.3	68.6	68.3	1:1.64
10-9	679.7	615.5	-9.4	53.4	4.5	-91.6	733.1	620.0	15.4	0.4	76.6	76.2	1:1.84
10-10	688.6	596.0	-13.4	56.4	7.5	-86.7	745.0	603.5	19.0	0.3	70.0	69.7	1:1.87
10-11	691.5	616.9	-10.8	56.4	7.5	-86.7	747.9	634.4	16.5	0.6	71.0	70.4	1:1.74
10-12	679.7	610.2	-10.2	52.3	9.0	-82.8	732.0	619.2	15.4	0.3	74.0	73.7	1:1.71
10-13	682.6	611.0	-10.5	53.8	7.5	-86.1	736.4	618.5	16.0	0.4	67.0	66.6	1:1.70
AVG	684.3	606.3	-11.4	55.4	5.1	-90.8	739.8	611.5	17.3	0.4	70.8	70.5	1:1.74

F-XII

RAW DATA FOR COD:TKN = 1:1.90, $\theta_c = 17.8$ days
 Ni(II) = 0.79 mg/l

Date	MLSS			Ni(II) Concentration			pH		Alkalinity as CaCO ₃			COD		
	Reactor Solids (mg/l)	Effluent Solids (mg/l)	θ_c (days)	Feed (mg/l)	Effluent Unfiltered (mg/l)	Effluent Filtered (mg/l)	Feed	Effluent Unfiltered	Feed (mg/l)	Effluent Unfiltered (mg/l)	Net Change (%)	Feed (mg/l)	Effluent Filtered (mg/l)	Removal Efficiency (%)
8-18	2510	24	17.9	0.97	0.99	0.81	7.0	5.1	448	10	97.8	395	32	91.9
8-19	2460	20	18.2	0.75	0.73	0.72	7.0	5.0	437	10	97.7	398	20	95.0
8-20	2410	30	16.5	0.77	0.77	0.76	7.0	5.0	453	9	98.0	385	42	89.1
8-21	2480	31	16.9	0.79	0.77	0.77	7.0	4.8	453	6	98.7	378	30	92.1
8-22	2430	20	18.4	0.75	0.75	0.73	7.0	4.9	453	8	98.2	404	32	92.1
8-23	2500	24	18.0	0.76	0.76	0.73	7.0	4.8	442	7	98.4	384	32	91.7
8-24	2550	20	18.6	0.74	0.74	0.73	7.0	4.9	445	7	98.4	398	28	93.0
AVG	2477	24	17.8	0.79	0.79	0.75	7.0	4.9	447	8	98.2	392	31	92.1

Date	NH ₃ -N Concentration			ORG-N Concentration			TKN Concentration			NO ₃ -N Concentration			COD:TKN (mg/l)/(mg/l)
	Feed (mg/l)	Effluent Filtered (mg/l)	Net Change (%)	Feed (mg/l)	Effluent Filtered (mg/l)	Net Change (%)	Feed (mg/l)	Effluent Filtered (mg/l)	Net Change (%)	Feed (mg/l)	Effluent Filtered (mg/l)	Net Change (mg/l)	
8-18	706.7	607.4	-14.1	58.0	5.4	-90.7	764.7	612.8	-19.9	0.3	67.0	+66.7	1:1.94
8-19	648.5	512.3	-21.0	52.7	1.8	-96.6	701.2	514.1	-26.7	0.3	58.8	+58.5	1:1.76
8-20	678.1	604.4	-10.9	55.9	5.4	-90.3	734.0	609.8	-16.9	0.3	65.0	+64.7	1:1.91
8-21	681.4	626.6	-8.0	59.2	--	-100.0	740.6	626.6	-15.4	0.5	87.5	+87.0	1:1.96
8-22	681.4	611.7	-10.2	59.2	--	-100.0	740.6	611.7	-17.4	0.5	73.8	+73.3	1:1.83
8-23	709.8	644.4	-9.2	54.7	3.6	-93.4	764.5	648.0	-15.2	0.4	71.3	+70.9	1:1.99
8-24	704.5	522.1	-25.9	55.9	1.8	-96.8	760.4	523.9	-31.1	0.4	60.8	+60.4	1:1.91
AVG	687.2	589.8	-14.2	56.5	2.6	-95.4	743.7	592.4	-20.3	0.4	69.2	+68.8	1:1.90

**The vita has been removed from
the scanned document**

THE EFFECTS OF NICKEL ON ORGANIC REMOVAL AND
NITRIFICATION IN THE COMPLETELY-MIXED
ACTIVATED SLUDGE PROCESS

by

Debra Ann Smith

ABSTRACT

The purpose of this research was to conduct a laboratory study to determine the effects of nickel on the completely-mixed activated sludge process.

Continuous-flow bench-scale reactors were operated at COD:TKN ratios of approximately 1.0:1 and 0.5:1 by varying the nitrogen concentrations in the feed solutions. Each unit received a COD concentration of 400 mg/l and was dosed continuously with a nickel concentration of 0.77 mg/l. The mean cell residence time was utilized as the operational control parameter to assess the influence of nickel on organic removal efficiency, on the degree of nitrification, and on the maximum yield and the microbial maintenance energy coefficients, Y_{\max} and k_d .

The results obtained in this study indicated that the soluble COD removal efficiency of the heterotrophic microorganisms was not affected by the 0.77 mg/l nickel concentration. The low continuous nickel dose to the reactor, however, appeared to stimulate the heterotrophic growth or to cause a replacement of the bacteria with a species of nickel-tolerant microorganisms. At the same time, the nickel appeared to stress the heterotrophs and to cause an increase in their maintenance energy requirement. Nitrification was found to be inhibited by the low nickel concentration, and this inhibition was not reduced by operating the reactors at lower COD:TKN ratios.